ISSN: 2764-5886
e-ISSN: 2764-622X

Volume 8· Nº 1 · March 2025

Journal of Bioengineering, Technologies and Health

An Official Publication of
SENAI CIMATEC

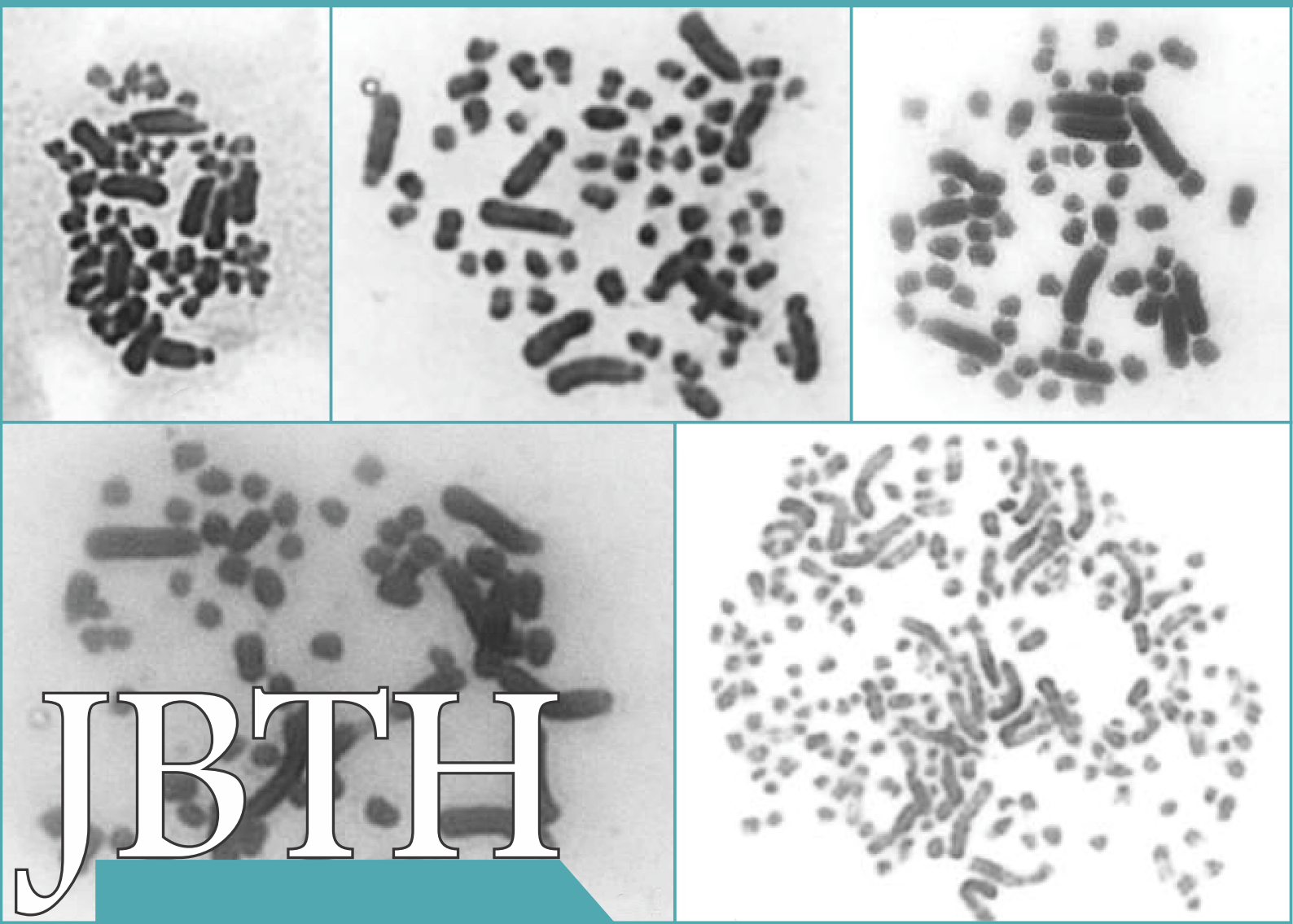

ISSN: 2764-5886 / e-ISSN 2764-622X

Volume 8 • Number 1 • February 2025

JOURNAL OF BIOENGINEERING TECHNOLOGIES AND HEALTH

An Official Publication of SENAI CIMATEC

PUBLISHED BY SENAI CIMATEC

Sistema FIEB | SENAI CIMATEC
PELO FUTURO DA INOVAÇÃO

February 2025
Printed in Brazil

JOURNAL OF BIOENGINEERING TECHNOLOGIES AND HEALTH

An Official Publication of SENAI CIMATEC

JOURNAL OF BIOENGINEERING TECHNOLOGIES AND HEALTH

Volume 8 • Number 1 **SUMMARY** *February 2025*

Original Articles

Project: Low-Cost Articulated Bath Chair 1
Mariane de Jesus Batista, Marlon Coelho Pita, Lucas Santos Reis, Renata de Sousa Mota, Nilmar de Souza

Comparative Prospection of Bioethanol Production from *Musa* spp. Residues 7
Amanda Santos, Emilly Anjos, Félix Santos, Luan Lucas Brito, Tatiana do Vale

Determination of Chromosome Number and Ploidy Level in Five Species of *Agave* from Mexico ...11
José Manuel Rodríguez Domínguez, Vanessa Nataly Magaña Avalos, Sofia Anahí Real Covarrubias

Comparative Assessment for Forage Palm and *Agave sisalana* Biomass for Sustainable Biofuel Production 15
Valdeci Machado, Evily Ribeiro Moura, Gabrielly de Moura Bezerra, Luciano Sergio Hocevar, Carine Tondo Alves, Marcos Machado da Rocha

Analysis of the Main Production Routes of Biomethane and Dimethyl Ether (DME) from Biomass 20
Rozenilton de Jesus Rodrigues, Carine Tondo Alves, Felipe Andrade Torres, Ednildo Andrade Torres

Biomethane Production from Cassava Juice: The Usage of Manipueira as Biomass..... 26
Anderson Freitas Sales, Rubens Pereira Martins, Calisto José da Silva Neto, Adley Diego Ferreira de Almeida, Carine Tondo Alves, Leandro Freitas Sales

Study of the Applicability of pH Mediators in Bioplastic Formulations for Use in Food Packaging..... 32
Camille Victória Carvalho, Gabrielle Honorata Barbosa, Joaquim Dantas, Wendel Costa, Ingrid Lessa Leal, Paulo Romano, Tatiana Vale

Carbon Credit Market: A Comparative Analysis of Consolidation in Brazil and the World..... 42
Natália Fernanda Santos Silva, Victor Menezes Vieira

Image-Based Underwater Liquid Leak Detection and Transfer Learning 50
Eric Oliveira, João Paulo Barros, Misael Alves, Taniel S. Franklin

Enhancing Neural Network Performance for Water Quality Forecasting with Principal Component Analysis in Intensive Aquaculture 56
Guilherme Freire de Almeida, Lucas Cruz da Silva, Valéria Loureiro da Silva

Neural Networks for Classification and Regression Applied to Public Lighting Project 62
Matheus O.C. Cerqueira, Wild F.S. Santos

Panda Manipulator Control with Obstacle Avoidance Through Reinforcement Learning in a Simulated Environment 68
Marcelo Albergaria Paulino Fernandes Ferreira, Taniel Silva Franklin,Oberdan Rocha Pinheiro

Systematic Reviews / Literature Reviews

Bibliometric Review on Planters and Transplanters 74
Vinícius Guimarães Rosa, Alexandre Diogo Poltronieri, Danilo Jefferson Romero, Saulo Queiroz Figliuolo, Valter Estevão Beal

The Role of Enzymes in an Efficient Ethanol Production: A Review and Technological Prospection 81

Leandro Freitas Sales, Douglas José Faria, Lilian Lefol Nani Guarieiro, Ana Lucia Barbosa de Souza, Sabrina Teixeira Martinez, Tatiana Oliveira do Vale

Review of Techniques for Measuring and Monitoring Seabed Subsidence 89
Matheus Anselmo da Silva, Miguel Barbosa de Argolo, Rodrigo Fonseca Carneiro

Detection Methods in CV-QKD System: A Systematic Literature Review 94
Maria Heloísa Fraga da Silva, William Emanuel Viana, Seyed Saman Mahjour, Valéria Loureiro da Silva

Instructions for Authors

Statement of Editorial Policy

Checklist for Submitted Manuscripts

The Journal of Bioengineering, Technologies and Health (JBTH) is an official publication of the SENAI CIMATEC (Serviço Nacional de Aprendizagem Industrial - Centro Integrado de Manufatura e Tecnologia). It is published quarterly (March - June - September - December) in English by SENAI CIMATEC – Avenida Orlando Gomes, 1845, Piatã, Zip Code: 41650-010, Salvador-Bahia-Brazil; phone: (55 71) 3879-5501. The editorial offices are at SENAI CIMATEC.

Editorial Office

Correspondence concerning subscriptions, advertisements, claims for missing issues, changes of address, and communications to the editors should be addressed to the Deputy Editor, Dr. Roberto Badaró, SENAI CIMATEC (Journal of Bioengineering, Technologies and Health – JBTH) – Avenida Orlando Gomes, 1845, Piatã, Zip code: 41650-010, Salvador-Bahia-Brazil; phone: (55 71) 3879-5501; or sent by e-mail: jbth@fieb.org.br / jbth.cimatec@gmail.com.

Permissions

COVER: Figure 1. Chromosome number observed in mitotic metaphase of five different species of *Agave*. Determination of Chromosome Number and Ploidy Level in Five Species of Agave from Mexico by José Manuel Rodríguez Domínguez et al. J Bioeng. Tech. Health 2024;8(1):12.

Postmaster

Send address changes to JBTH, Avenida Orlando Gomes, 1845, Piatã, Zip Code: 41650-010, Salvador-Bahia-Brazil.

Information by JBTH-SENAI CIMATEC

Address: Avenida Orlando Gomes, 1845, Piatã, Zip Code: 41650-010, Salvador-Bahia-Brazil
Home-page: www.jbth.com.br
E-mail: jbth@fieb.org.br / jbth.cimatec@gmail.com
Phone: (55 71) 3879-5501 / 3879-5500 / 3879-9500

DOI:10.34178
ISSN: 2764-5886 / e-ISSN 2764-622X

Copyright

Project: Low-Cost Articulated Bath Chair

Mariane de Jesus Batista[1*], Marlon Coelho Pita[1], Lucas Santos Reis[1], Renata de Sousa Mota[1], Nilmar de Souza[1]
[1]Center for Science and Technology in Energy and Sustainability, Federal University of Recôncavo of Bahia; Feira de Santana, Bahia, Brazil

The project developed a prototype of an articulated bath chair using PVC pipes and 3D-printed components, aiming to meet the accessibility needs of older people. The applied methodology included market research, document analysis of accessibility standards (ABNT NBR 9050/2021), and three-dimensional modeling in Fusion 360 software. The use of additive manufacturing was essential for creating customized components, such as locks, which ensured the prototype's safety and functionality. The result was a low-cost, adaptable, and safe product, ready to be tested in a real environment, with the potential to improve the quality of life for older people and contribute to innovative practices in assistive technology.
Keywords: Accessibility. Articulated Bath Chair. Assistive Technology. 3D Printing. Elderly Care.

The aging of the Brazilian population has resulted from several factors, including the decrease in fertility rates and the increase in life expectancy, driven by improvements in healthcare and socioeconomic conditions. Although this trend is global, the demographic transition in Brazil is happening at a significantly accelerated pace.

According to the latest data from the 2022 Census, there has been a significant increase in Brazil's elderly population, which includes people aged 60 and over, representing 10.9% of the total population, a growth of 57.4% compared to 2010, when this age group made up 7.4% [1]. Additionally, the proportion of older people increased from 11.3% to 14.7% [2]. In contrast, the proportion of young people (0-14 years) has decreased, reflecting a drop in birth rates. Life expectancy at birth has also increased, reaching approximately 77 years, contributing to population aging.

This demographic shift has implications for various aspects of Brazilian society. On the one hand, increased life expectancy and decreased birth rates represent significant health and quality of life achievements. However, this scenario also brings specific challenges regarding accessibility and infrastructure adaptation when considering the elderly population. One of the critical issues that arise is the need for adequate facilities to ensure their safety and autonomy, particularly in the home environment, which increases the need to make spaces more accessible [3].

Accessibility in the home environment is a fundamental concern to ensure the quality of life and autonomy of people with reduced mobility and older people. Among the critical spaces that require adaptations, the bathroom stands out as a potentially risky area where a lack of accessibility can result in falls, injuries, and limitations in performing daily personal hygiene activities [3]. Thus, the articulated bath chair emerges as one response to this demand, offering a practical, economical, and adaptable alternative to make bathing more accessible and safer.

This article proposes to explore the feasibility and benefits of this solution, focusing on using PVC pipes as the primary material due to its low cost. This work aims to present a prototype of an articulated bath chair through a detailed project using PVC pipes, covering everything from design planning to prototype construction. The idea arose from a technical visit during the Gerontechnology course to a long-term care institution for older people in Feira de Santana/Bahia, where the feasibility of installing a bath chair to meet the needs previously assessed by students of the Assistive Technology and Accessibility Engineering course at the Federal

Received on 20 December 2024; revised 28 Jnauary 2025.
Address for correspondence: Mariane de Jesus Batista. Av. Centenário, 697 - Sim. Zipcode: 44042-280. Feira de Santana, Bahia, Brazil. E-mail: marianebatista@aluno.ufrb.edu.br.

J Bioeng. Tech. Health 2025;8(1):1-6

University of Recôncavo da Bahia was observed. This article is relevant as, besides promoting quality of life for this population, it offers an innovative proposal for contributing to knowledge and practices of accessibility in the home environment.

Materials and Methods

The method used in this article consists of action research, where researchers and participants cooperate or participate to solve a situation or problem [4]. This methodology was designed to bridge the gap between theory and practice, uniting both fields and developing knowledge guided by practical experience. One of the characteristics of this type of research is that it allows us to interfere in reality, occurring as part of the research process and not just as a consequence of the final work. Therefore, action research aims to produce knowledge and solve a practical problem [5,6]. The development of the articulated bath chair prototype followed these steps:

1. Benchmarking;
2. Documentary research on accessibility standards;
3. Development in Fusion 360 software;
4. Prototype construction.

The modeling process was carried out using the "Fusion 360" modeling software in the free student license version from Autodesk. Based on ABNT 9050/2021 standards, the normative specifications for product sizing were used to ensure that all measurements and structural characteristics met accessibility and safety requirements. These standards recommend that the bath seat be 70 cm long, 45 cm wide, and 46 cm from the floor [7].

The prototype was built using PVC pipes, a material chosen for its durability, water resistance, and ease of handling. In addition to these characteristics, PVC pipes are low-cost, lightweight, moisture-resistant, easy to handle, and readily available, making them ideal for constructing assistive devices in bathrooms. The prototype construction process included cutting the pipes, modeling and printing the parts with a 3D printer, assembling and fixing the parts, and strictly following the modeled design.

The list of construction materials was: i) 32mm PVC pipes; ii) pipe glue; iii) elbow and "T" type connectors of 32 and 40 inches, respectively; iv) reduction for the "T" type connections made in 3D printing; V) university chair seat (donation).

Results and Discussion

The market model found at the "PHD Support Bars" establishment has the following characteristics: stainless steel 304 finish, 1.¼ inch outer diameter, 1.5mm thickness (polished, brushed, or with white epoxy paint), and is priced at R$ 1,454.00.

Based on the existing market product (Figure 1), a sketch was made, incorporating fundamental technical drawing approaches to ensure the project's functionality. This sketch was the starting point for developing the articulated bath chair (Figure 2). Additionally, the manual sketch allowed for a

Figure 1. A market model of the articulated bath chair.

Figure 2. Initial sketches of the chair.

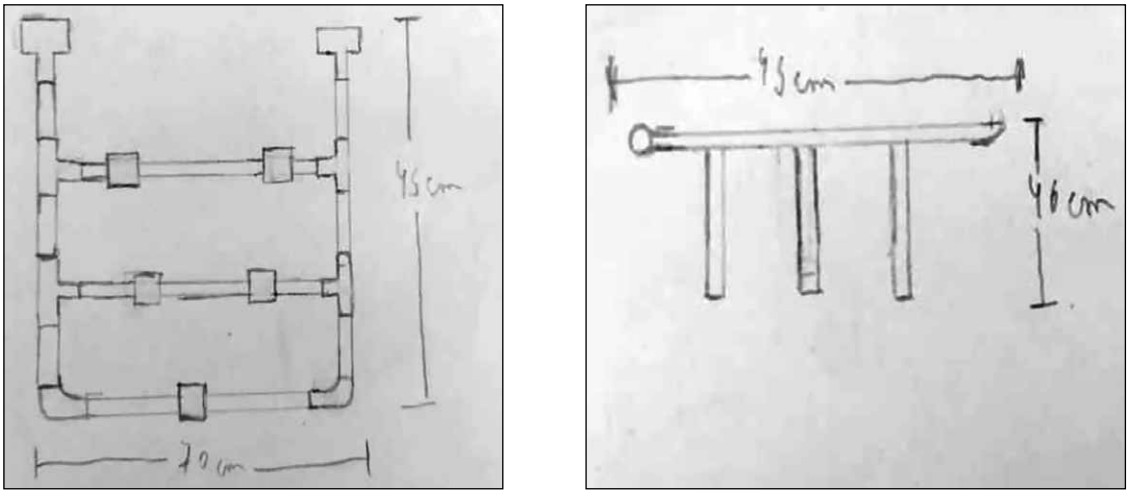

preliminary visualization of the design, facilitating the identification of possible improvements and necessary adjustments before the prototype construction in the software. Analyzing the existing market product also enabled the identification of essential features, such as fixation mechanisms, materials used, and innovative solutions that could be adapted or improved in the new project.

Furthermore, adopting a systematic approach to the design ensured compliance with current safety and accessibility standards, such as those specified by ABNT NBR 9050/2021. This standard provides guidelines for constructing accessible products, ensuring that all prototype measurements and structural characteristics are compatible with accessibility and safety requirements.

With the aid of Fusion 360 software, a 3D prototype was developed to provide a more realistic and detailed visualization of the project (Figure 3). Using this three-dimensional modeling software allowed for the creation of a virtual model that accurately reflects all the technical and structural specifications planned for the bath chair. Through Fusion 360, it was possible to simulate the prototype's dimensions, shapes, and mechanisms, facilitating the identification of potential flaws and making the necessary adjustments before the physical construction phase. Additionally, the software allows for structural and material strength analyses, ensuring that the final prototype meets the safety and durability criteria required for daily use by older people. Moreover, the three-dimensional visualization of the prototype aided communication among the development team members to enable a clear and shared understanding of the proposed design. The precision and detail obtained with Fusion 360 were crucial for fabricating customized parts and efficiently integrating the prototype's components.

The fourth stage of the process consisted of constructing the prototype according to the specifications developed in the previous phases. The prototype construction used PVC pipes, chosen for their durability, water resistance, and ease of handling, which are essential for application in humid environments such as bathrooms. The use of PVC is also justified by its cost-effectiveness and the possibility of customization and adaptation according to the project's specific needs. The construction process began with cutting the PVC pipes according to the detailed measurements in the three-dimensional model developed in Fusion 360 software. This stage required precision and care to ensure that all parts fit together perfectly, guaranteeing the prototype's stability and safety. Next, the parts were assembled and joined using appropriate fixation techniques, such as gluing and mechanical fittings, ensuring a robust and stable structure (Figure 4).

Figure 3. 3D design of the articulated bath chair.

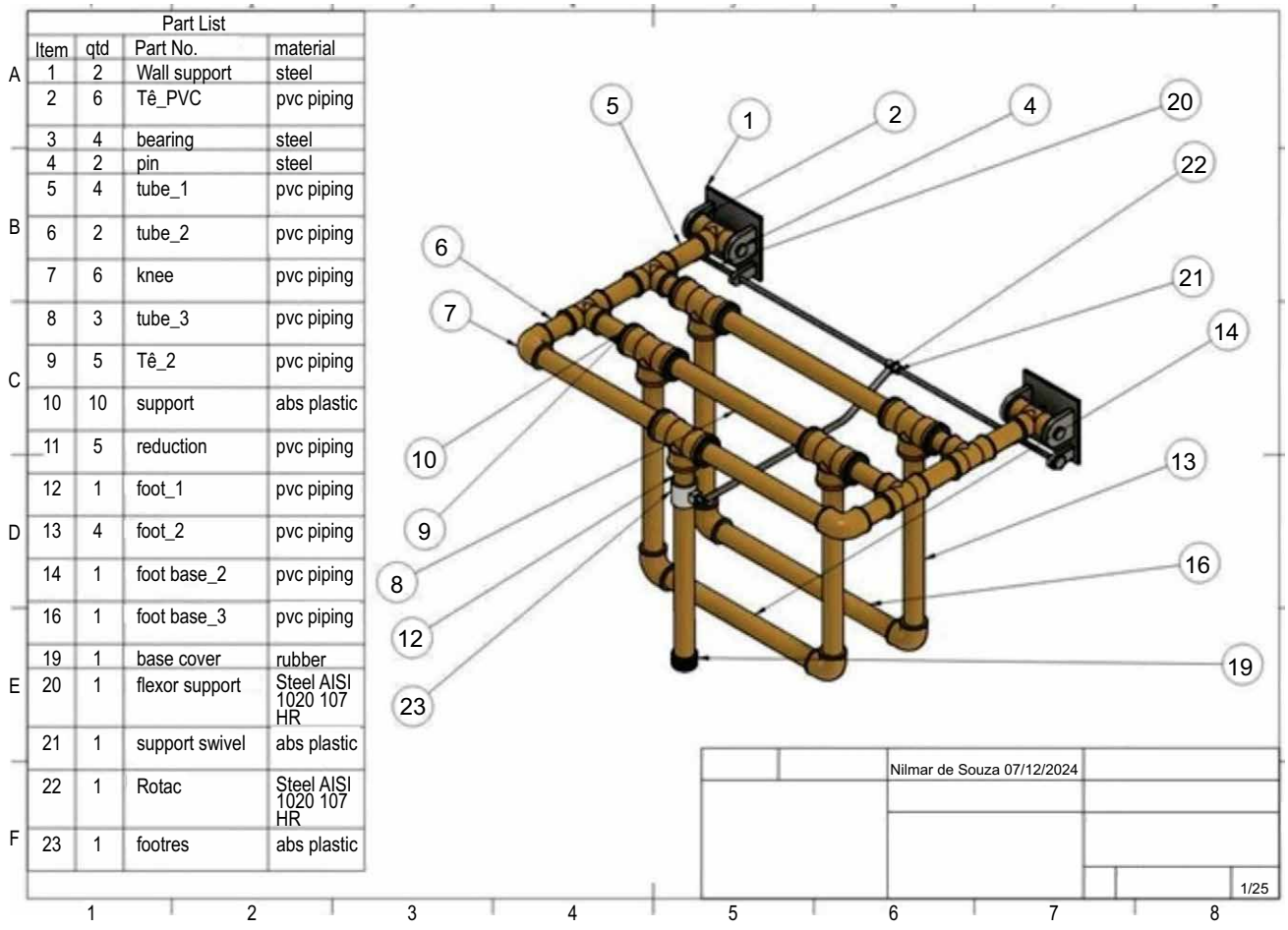

In addition to the PVC parts, the prototype incorporated components produced through additive manufacturing and was designed using Fusion 360 software. 3D printing created customized components that would be unfeasible to produce using conventional manufacturing methods. Among the developed parts, the "locks" stand out—critical elements that limit the joints' movement, ensuring the bath chair's functionality and safety (Figure 5).

One of the difficulties encountered in the prototype construction was defining the seat, as the material needed to be waterproof, resistant to the user's weight, and compliant with ABNT NBR 9050/2021 standards. There were two alternatives: the first was to develop this material in the university's materials laboratory using fiberglass and resin, which, after a heating process, becomes highly resistant. The second alternative was to use one of the university chair seats that were no longer in use but in good condition. Due to the difficulty of developing the first option and the high cost, the second alternative was chosen for its feasibility in terms of time and available material. It is worth noting that the first option will be used for the final project, going through the proper process to ensure user safety (Figure 6).

Each construction phase was documented and reviewed to ensure compliance with the accessibility and safety standards established by ABNT NBR 9050/2021. This phase represented the project's materialization, transforming the drawings and virtual models into a prototype that would be fabricated into a functional and safe product ready

to be used and evaluated in a real environment. This process highlighted the importance of each development stage, from planning and modeling to practical execution, culminating in a prototype that provides accessibility and safety for the end users (Figure 7).

According to the market value attributed to this product, it was R$1,454.00, making it unfeasible for a non-profit institution to purchase in a quantity that would meet all the bathrooms in the location. The chair replicated with low-cost materials offers an average cost of R$123.50, and the 3D printing would cost R$176.00, totaling R$299.50. It is worth noting that this is a prototype of a shower chair. Therefore, its cost may vary according to the availability of materials and the modifications that may be made to the project.

Conclusion

Developing an articulated shower chair using PVC pipes is a practical, economical, and adaptable

Figure 4. PVC pipes.

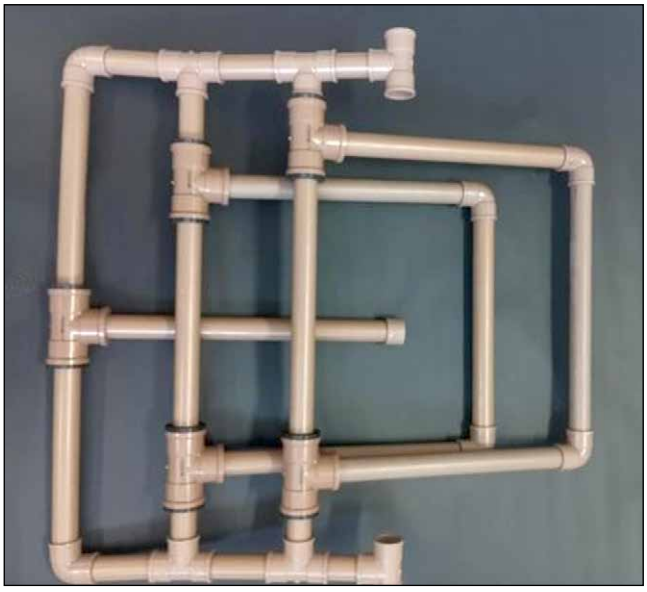

Figure 5. Lock in 3D modeling.

Figure 6. Reused university chair seat.

Figure 7. Final prototype.

solution to meet the needs of long-term care facilities. The method applied in this work involves detailed planning of the development stages (market research, document analysis of accessibility standards, and software modeling), resulting in creating a functional prototype and achieving the proposed objective.

In future work, the product's effectiveness will be evaluated based on feedback from users and healthcare professionals at the institution. This feedback will address aspects such as the suitability of the design to the needs of older people, ease of use, and durability of the material.

The results of this evaluation will be used to make possible improvements to the product and develop a construction manual that will be made available. Therefore, this project not only has the potential to promote the quality of life of older people but also contributes to knowledge and practices of accessibility, highlighting the importance of innovative and personalized solutions. By enabling the safe and independent execution of everyday tasks, the development of assistive technologies such as articulated shower chairs is essential to face the challenges of the aging population in Brazil. Hence, there is a need for a multidisciplinary and integrated population.

References

1. IBGE (ed.). Censo 2022: número de pessoas com 65 anos ou mais de idade cresceu 57,4% em 12 anos. [S.l.]: IBGE, 27 out. 2023. Available at: https://agenciadenoticias.ibge.gov.br/agencia-noticias/2012-agencia-de-noticias/not icias/38186-censo-2022-numero-de-pessoas-com-65-anos-ou-mais-de-idade-cresceu-57-4-em-12-anos.
2. Galvão J.. Dados do IBGE revelam que o Brasil está envelhecendo. Jornal da USP, [S.l.], 11 jul. 2023. Available at: https://jornal.usp.br/radio-usp/dados-do-ibge-revelam-que-o-brasil-esta-envelhecendo/. Acesso em: 11 jul. 2024.
3. Moraes EN, Moraes FL, Lima SPP. Características biológicas e psicológicas do envelhecimento. Rev Med Minas Gerais, [S. l.] 2010;20(1):67-73. Available at: http://www.observatorionacionaldoidoso.fiocruz.br/biblioteca/_artigos/197.pdf.
4. Anastácio BS. PESQUISA-AÇÃO: um relato de experiência. EntreVer, Florianópolis 2014;4(6):208-2015.
5. Mello CHP, Turrioni JB, Xavier AF, Campos DF. Pesquisa-ação na engenharia de produção: proposta de estruturação para sua condução. Production, São Paulo, 2012;22(1):1-13. DOI https://doi.org/10.1590/S0103-65132011005000056. Available at: https://www.scielo.br/j/prod/a/BN5Yt8YSxPVk5RJZ3hNZmXK/?lang=p.
6. Engel GI. Pesquisa-ação. Educar, Curtiba, 2000;16:181-191. Available at: https://www.scielo.br/j/er/a/dDzfLYyDpPZ3kM9xNSqG3cw/?format=pdf&lang=pt. Acesso em: 6 ago. 2021.
7. Associação Brasileira de Normas Técnicas. NBR 9050: Acessibilidade a edificações, mobiliário, espaços e equipamentos urbanos. 2004. Rio de Janeiro, 2004.

Comparative Prospection of Bioethanol Production from *Musa* spp. Residues

Amanda Santos[1*], Emilly Anjos[1], Félix Santos[1], Luan Lucas Brito[1], Tatiana do Vale[1]
[1]SENAI CIMATEC University; Salvador, Bahia, Brazil

The present study explores the feasibility of bioethanol production using banana residues, focusing on its potential contribution to second-generation bioethanol. The research investigates the comparative prospecting of bioethanol production from different *Saccharomyces cerevisiae* strains, employing methods such as enzymatic hydrolysis and alcoholic fermentation. Results indicate the viability of utilizing banana residues for bioethanol production, highlighting its potential for sustainable fuel production. The findings underscore the importance of harnessing abundant agricultural byproducts for renewable energy generation, with implications for both theoretical and practical biofuel applications.
Keywords: Bioethanol. Banana Waste. *Saccharomyces cerevisiae*.

The growing demand for renewable and sustainable energy sources has driven notable advances in second-generation ethanol production. In this context, the production of 2G ethanol contributes to reducing dependence on fossil fuels and represents a significant step towards sustainability. This approach minimizes environmental impact by using waste and promotes an economically viable, socially beneficial, and efficient solution for disposing of this waste.

Banana farming residues have aroused significant interest in being used as raw material in manufacturing bioethanol. Due to its physical-chemical characteristics, it has significant potential for fuel generation [1]. According to the Food and Agriculture Organization of the United Nations (FAO) [2], in 2011, banana production in *Musa* spp. reached more than 106.54 million tons of fruit. As a result, the fruit can be considered one of the most consumed in the world; according to Souza and colleagues (2012) [3], for each ton of banana, approximately three tons of waste are generated, including peels, leaves, pseudostems, and banana tree remains.

As mentioned by Alvarenga (2011) [4], regarding sugars during banana ripening, the amylase enzyme acts by converting 17.5 to 25.9% of the starch present in the fruit into fermentable sugars, mainly glucose and fructose, which are found in more than 20%. As presented in Table 1, the residual starch will undergo a hydrolysis process. This procedure aims to convert the starch into simpler sugars, increasing the available sugars.

To produce bioethanol with raw materials that contain starch (polysaccharide), it is necessary to carry out the hydrolysis process so that fermentable sugars (monosaccharides) are created, as described in the following reaction [5]:

$$(C_6H_{10}O_5)n + (n+m)\,H_2O \rightarrow n\,glucose + m\,maltose$$

Hydrolysis aims to convert polysaccharide-rich biomass into smaller sugars. In enzymatic hydrolysis, specific enzymes convert cellulose and hemicellulose into fermentable sugars, essential for ethanol production. This method stands out for its efficiency and lower energy demand than chemical hydrolysis [6].

Ethanol (C_2H_6O) and carbon dioxide (CO_2) can be produced through enzyme-catalyzed fermentation. This process occurs mainly in yeast to produce energy in the form of ATP. Ethyl alcohol is a byproduct of fermentation and also acts as an inhibitor of other microorganisms [7]. According to Amorim (2005) [8], strains of *Saccharomyces cerevisiae* are the most used in converting sugar into ethanol. They have an optimum temperature

Received on 17 September 2024; revised 10 December 2024.
Address for correspondence: Amanda Santos. Av. Orlando Gomes, 1845, Piatã, Salvador, Bahia, Brazil. Zipcode: 41650-010 E-mail: amandaf412006@gmail.com.

J Bioeng. Tech. Health 2025;8(1):7-10

Table 1. Composition of banana sugars in the ripening phases.

Degree of Maturation	Starch (% m/m)	Total Sugars (% m/m)
Underripe	19.8	6.5
Mature	2.9	20.4
Very mature	0.63	22.7

Source: Alvarenga, 2011 [4].

of 26 to 35 °C. pH values develop in a range, with between 4 and 5 being suitable [9].

The present study aims to analyze the viability and efficiency of second-generation bioethanol production using three different *Saccharomyces cerevisiae* strains, collect data and banana residues, and evaluate residue/yeast combinations with higher alcoholic yields.

Materials and Methods

This article's methodological approach adopts a qualitative perspective, allowing a comprehensive analysis of bioethanol production from banana waste. The choice of three different commercial strains for industrial applications aims to provide comparative data for obtaining bioethanol.

Acquisition of Yeasts

The yeasts were purchased from Bahia Malt, a store selling supplies and equipment for brewing in Salvador - Bahia. The related strains of *Saccharomyces cerevisiae*, S-33, WB-06 It is K-97, were selected for the study due to their efficiency in producing beer and other alcoholic beverages.

Cultivation of Strains *Saccharomyces cerevisiae*

The cultivation of yeast strains was achieved through the use of medium Sabouraud Dextrose, in duplicate, with a composition of dextrose (20 g/L), a mixture of animal tissue peptic digestive (10 g/L) and casein pancreatic digestive (10 g/L), being autoclaved at 121°C, carrying out the inoculation of strains S-33, WB-06 It is K-97, and growth during 72h.

Preparation of Banana Waste Must and Enzymatic Hydrolysis

Hydrolysis began by treating the biomass and weighing and sanitizing the material. Approximately 782g of waste was collected and sanitized in a 10% sodium hypochlorite solution. The residue was cut, diluted in water, homogenized in a blender, and filtered. Thus, the must was prepared for enzymatic hydrolysis.

It was carried out in a 5000 mL container with a lid, in which a system was created to capture CO_2. 1,826 mL of the enzyme was inoculated into the system Attenuzyme for 4.565 kg of must was analyzed using the Dubois Sugar Determination method.

The test was monitored for 60 hours, with the analysis points removed at 0, 24, and 48 hours. The final volume of the test used for fermentation yielded 5L, and after filtration, 2.8L of the residue hydrolyzate was obtained *Musa* spp.

Alcoholic Fermentation

The alcoholic fermentation of the musts was carried out in 500 ml airtight containers, using an airlock system to monitor the fermentation process and exhaust the produced carbon dioxide. 380 ml of filtered banana hydrolysate and 20 mL of *Saccharomyces cerevisiae* inoculum was used at 23°C. The fermentation process lasted 48 hours and was halted by cooling. The alcohol content of the fermented product was measured with an alcoholmeter.

Results and Discussion

The following item provides data obtained through quantitative and qualitative analyses, such as determining Sugars by Dubois, Chemical, Enzymatic Hydrolysis, Alcoholic Fermentation, and Distillation, carried out through laboratory experiments to support the project hypotheses.

Growth of Strains *Saccharomyces cerevisiae*

The growth of the three *Saccharomyces cerevisiae* strains, which was analyzed using the Wet Weight method, showed a consonance between the growth of yeast strains in the first 24 hours, determining the minimum fermentation time.

Determination of Total Sugars in the Hydrolyzate

The analysis of total sugars using the Dubois method to attest to Attenuzyme's breakdown of complex sugars (starch) did not present significant results.

Since Table 1 indicates only 0.63% starch in the total composition of ripe bananas, it was assumed that hydrolysis did not guarantee results given the small amount of sugars to be converted into the must.

Therefore, it is suggested that the process is viable without the additional step, given that ripe bananas have a satisfactory sugar content, as described in Table 1.

Characterization of Hydrolyzed Wort

After hydrolysis and filtration, the volume obtained from the must was equivalent to 2.88 liters and presented 5°Brix, which was corrected by adding 217 g of commercial sugar, ending this process with 14.9°Brix.

Characterization of the Fermented Must of Each Strain

Based on Table 2, we assume that WB-06 is the yeast most likely to meet the parameters for the production of Hydrated Fuel Ethanol established by the National Agency of Petroleum, Natural Gas and Biofuels (ANP), as it has a higher alcohol content than the others.

Characterization of each Bioethanol Obtained

The fractional distillation process obtained ethanols. Each yeast strain provided a different volume of distillate from the same volume of wort, as shown in Table 3.

Among the three, the strain of *Saccharomyces cerevisiae* with the most significant identified productive potential is the WB-06, followed by S-33; both have notable sugar consumption and conversion capacity and ethanol production with a considerable and relevant volume of distillate. However, having observed the divergence of data obtained regarding the volume indicated by the alcohol content of the must and the distillate, an equation was developed to estimate the degree of purity of the ethanol produced:

$$P = M \times T \div D$$

Where:

P = Degree of Purity (%); M = Volume of Fermented Must (mL); T = Alcoholic Content of the Must (%); D = Distillate Volume (mL).

Table 2. Comparative analysis of fermented musts of each strain.

Yeast Strain	°Brix Post - Fermentation n	pH	Alcohol content (% v/v)
S-33	3.8	4	3
WB-06	4.5	4	4
K-97	7	4	0.5

Table 3. Volume of distillates from each strain *S. cerevisiae*.

S. cerevisiae strain	Must Volume (mL)	Distillate Volume (mL)
S-33	400	38
WB-06	400	33
K-97	400	23

Determining the degree of purity of the ethanol produced, described in Table 4, helps to compare one of the essential parameters to comply with ANP regulations. According to the requirements of this regulatory body, set out in ANP Resolution No. 907, the minimum alcohol content for Hydrated Fuel Ethanol (EHC) is 92.5%, and the minimum hydrogen potential (pH) is 6.0.

Table 4. Estimated purity content of ethanols obtained.

S. cerevisiae strain	Purity Content
S-33	31.58
WB-06	48.48
K-97	8.69

In this way, it was found that the bioethanol produced by strain WB-06 has the highest alcohol content and is close to that suitable for the Agency, followed by the ethanol from strain S-33. This information is crucial to understanding the productive potential of the analyzed strains, guiding future optimizations in the bioethanol production process from banana waste, and adapting the ethanol produced to the standards defined for Hydrated Fuel Ethanol by the ANP.

Conclusion

The present study analyzed the viability of bioethanol production from banana waste using three different strains of *Saccharomyces cerevisiae*: S-33, WB-06 It is K-97. The results demonstrated the feasibility of using banana residues for bioethanol production, confirming their potential as a sustainable source for renewable fuel generation and showing that converting them into bioethanol contributes to environmental development and provides a promising alternative to conventional biofuels. This integration involves developing advanced technologies, optimizing processing conditions, and significantly contributing to environmental sustainability with large-scale use.

Acknowledgments

We would like to express our deep gratitude to all individuals and institutions who contributed to completing this work. This research represents the collective effort of everyone involved and would not have been possible without each one's support and contributions.

References

1. Fernandes ERK. Valorization of waste generated in banana farming by thermochemical conversion by pyrolysis. 2012.
2. FAOSTAT. World Banana Production. Available at: <http://www.fao.org>.
3. Souza O et al. Alternative biomass energy: bioethanol from banana peel and pulp. Brazilian Journal of Agricultural and Environmental Engineering 2012;16:915-921.
4. Alvarenga RM. Evaluation of fermentation and distillation parameters to adjust the levels of secondary compounds in banana spirits. UFMG, 2011.
5. Yoosin S, Sorapipatana C. A study of ethanol production cost for gasoline. 2015.
6. Ferreira CG. Evaluation of the synergistic effect between xylanases and cellulases in the deconstruction of the lignocellulosic complex and the fermentability of the hydrolyzate generated in the production of lactic acid. 2019.
7. Motta V. Biochemistry. 2nd edition, 2011.
8. Amorim HV. Alcoholic Fermentation: Science and Technology. Piracicaba. São Paulo, 2005. Fermentec, 448p.
9. Alterthum F, Schmidell W, Moraes I. Industrial biotechnology: fermentative and enzymatic processes. 2nd edition ed. Blucher, 2019.

Determination of Chromosome Number and Ploidy Level in Five Species of *Agave* from Mexico

José Manuel Rodríguez Domínguez[1*], Vanessa Nataly Magaña Avalos[1], Sofia Anahí Real Covarrubias[1]
[1]Center for Research and Assistance in Technology and Design of the State of Jalisco, A.C., Mexico, Plant Biotechnology Unit; Guadalajara, Jalisco, Mexico

Cytogenetic analysis was carried out on five species of *Agave* genus collected in Mexico. Meristematic root cells were analyzed cytogenetically using a modified steam-drop method for chromosome counting. The analysis showed that in *A. guiengola*, *A. geminiflora*, *A. attenuata*, and *A. victoriae-reginae* species, the chromosome number was 2n=60 with bimodal karyotypes composed of five pairs of large chromosomes and 25 pairs of small chromosomes. On the other hand, *A. salmiana* also showed a bimodal karyotype consisting of 30 large + 150 small chromosomes. Considering the basic number x=30, *A. salmiana* is a hexaploid species (2n=6x=180), whereas the other four species analyzed are diploid (2n=2x=60). This is the first report on the chromosome number of *A. guiengola*.
Keywords: Cytogenetic Analysis. Bimodal Karyotype. Diploid. Hexaploid.

The genus *Agave* is distributed in the tropical and subtropical parts of the world and represents a large group of succulent plants cultivated because of its commercial importance. Its distribution extends from the southern United States to Colombia, Venezuela, and the Caribbean Islands [1]. The genus has a basic chromosome number x=30 showing different degrees of ploidy, from diploid (2n=2x=60) to octoploid (2n=8x=240) species presenting asymmetric and highly conserved bimodal karyotypes, which consist of x=5 large chromosomes and x=25 small chromosomes [2-3].

Chromosomes spread without cytoplasm, and overlapping chromosomes are essential for cytogenetic studies, including chromosome counting, karyotype, and ideogram construction. In plants, creating good-quality spreads is difficult due to the rigid cell wall, which complicates chromosome separation. Several methods for obtaining good chromosome spreads have been developed, including the modified steam-drop method, one of the most effective for plant chromosome counting [4].

Received on 10 September 2024; revised 22 December 2024.
Address for correspondence: José Manuel Rodríguez Domínguez. Avenida Normalistas, nº 800, Colinas de la Normal, Guadalajara, Jalisco, México. PO Box: 44270. E-mail: mrodriguez@ciatej.mx.

J Bioeng. Tech. Health 2025;8(1):11-14

This work aimed to determine chromosome number and ploidy level in five species of *Agave* from Mexico.

Materials and Methods

In the present investigation, ten plants (10 cm tall) of five different species of the *Agave* genus were collected from several states of Mexico on field trips over ten years: *A. guiengola* was collected from Oaxaca, *A. victoriae-reginae* from Nuevo León, *A. salmiana* from Hidalgo, *A. geminiflora*, and *A. attenuata* from Jalisco; the plants of each of the species mentioned were transported at the Centro de Investigación y Asistencia en Tecnología y Diseño del Estado de Jalisco, A.C. (CIATEJ) and maintained in an *in vivo* collection in a greenhouse.

One month before cytogenetic analysis, 10 plants of each of the five species were placed in a container with a moist substrate made of peat moss vermiculite (7:3) for root production. Metaphasic chromosome preparations were performed according to the method reported by Rodríguez-Domínguez and colleagues (2017) [4]. Each slide was stained with 1% acetoorcein and coverslipped for chromosome counting.

The best ten metaphases obtained of *Agave* plants of each of the five species analyzed were photographed using a Leica DMRA2 microscope (Leica Microsystems, Wetzlar, Germany) coupled to an Evolution QEI phase-contrast camera (Media-Cybernetics, Rockville, Maryland, USA). In order

to reduce noise in the images, the images were sharpened with a 9 x 9 Gaussian spatial filter.

Results and Discussion

Mitotic metaphases with a good chromosome spread were obtained through the modified steam-drop method in all species analyzed. *A. guiengola*, *A. geminiflora*, *A. attenuata*, and *A. victoriae-reginae* species showed a bimodal karyotype consisting of 10 large + 50 small chromosomes (2n=60) (Figure 1a-d), on the other hand, *A. salmiana* also showed a bimodal karyotype consisting of 30 large + 150 small chromosomes (2n=180) (Figure 1e).

This is the first report on chromosome number for *A. guiengola*. Concerning *A. victoriae-reginae* and *A. geminiflora* species, the chromosome number shown in this work is consistent with that published in other studies [5-6]. On the other hand, Lingling and colleagues (2009) [7] reported that the chromosome number of *A. attenuata* ranges from 45 to 62, while our results for this species was 2n=60. Regarding *A. salmiana*, chromosome numbers 2n=120 and 2n=180 have been reported previously [8-10]. Our findings showed that the chromosome number of the analyzed plants was 2n=180. Because the genus *Agave* has a basic chromosome number x=30, the species analyzed have different ploidy levels (Table 1).

Certain chemicals can induce polyploidy; these compounds are so-called spindle poisons, which interfere with the formation of the metaphase spindle; some examples are colchicine, oryzalin, and α-bromonaphthalene among others; sometimes, these mitotic inhibitors also produce endopolyploidy in several plant species [11]. According to Ullah and colleagues (2009) [12], endopolyploidy could be achieved by at least four different mechanisms: endoreduplication, endomitosis, acytokinetic mitosis, or cell fusion; endoreduplication is the most common mode of polyploidization in plants and is estimated to occur in over 90% of angiosperms [13].

Figure 1. Chromosome number observed in mitotic metaphase of five different species of *Agave*.

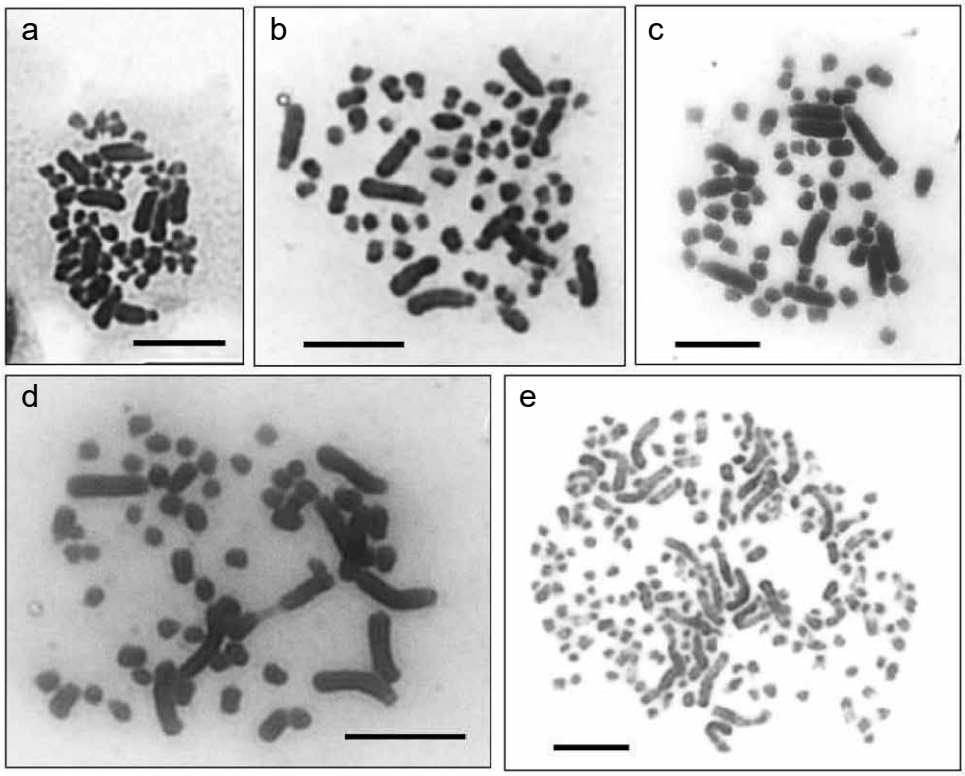

a. *Agave attenuata*; b. *Agave geminiflora*; c. *Agave guiengola*; d. *Agave victoriae-reginae*; e. *Agave salmiana*. Barr=10µm.

Table 1. Somatic chromosome number and ploidy level in five species of *Agave*.

Species	Somatic Chromosome Number	Ploidy Level
Agave guiengola	2n=60	Diploid (2n=2x=60)
Agave geminiflora	2n=60	Diploid (2n=2x=60)
Agave attenuata	2n=60	Diploid (2n=2x=60)
Agave victoriae-reginae	2n=60	Diploid (2n=2x=60)
Agave salmiana	2n=180	Hexaploid (2n=6x=180)

In this study, only one species of *Agave* showed endopolyploidy. The type of endopolyploidy detected was endoreduplication.

For *A. geminiflora* (2n=60) (Figure 2a), endopolyploid cells showed 2n=120 chromosomes (Figure 2b), with a low frequency (5%); this is in agreement with Rodríguez-Domínguez and colleagues, (2020) [11] who also reported a similar frequency of endoreduplication on *Polianthes howardii* (2n=2x=60), a diploid plant belonging to the same taxonomic family: Asparagaceae.

Conclusion

Based on the chromosome number obtained and considering the basic number x=30 for the *Agave* genus, *Agave salmiana* is identified as a hexaploid species (2n=2x=180), whereas *A. guiengola*, *A. geminiflora*, *A. attenuata*, and *A. victoriae-reginae* are diploid species (2n=2x=60). Notably, this study presents the first report on the chromosome number of *A. guiengola*.

One of the main challenges in counting chromosomes in polyploid species is obtaining preparations with well-spread metaphase chromosomes. However, this issue can be effectively addressed using the methodology described by one of our team members [4], which enabled the successful preparation of high-quality metaphase spreads in the hexaploid species *A. salmiana*. At CIATEJ, we continue our research to determine chromosome numbers in additional *Agave* species. The findings of this study provide valuable insights that will support future breeding programs within the *Agave* genus.

Acknowledgments

The authors express their gratitude to Project PlanTECC for funding this research.

Figure 2. Normal and endopolyploid cells in *Agave geminiflora*.

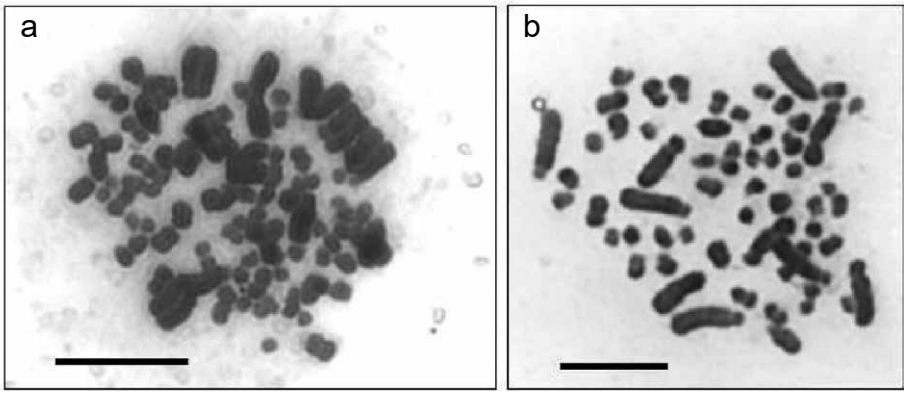

a. Endoreduplication with 4n appearance where the chromosomes are close to their homologous pair (2n=120); b. Normal cell (2n=60). Barr=10µm.

References

1. García-Mendoza A. Distribution of *Agave* (Agavaceae) in Mexico. Cactus and Succulent Journal 2002;74(4):177-187.
2. Thiede J. *Agave agavaceae*. In: Eggli U, Nyffeler R. (eds) Monocotyledons. Illustrated Handbook of Succulent Plants, Springer, Berlin, Heidelberg, p. 21-311, 2020.
3. Robert ML et al. Wild and agronomically important *Agave* species (Asparagaceae) show proportional increases in chromosome number, genome size, and genetic markers with increasing ploidy. Botanical Journal of the Linnean Society 2008;158(2):215-222.
4. Rodríguez-Domínguez JM et al. An improved technique for obtaining well- spread metaphases from plants with numerous large chromosomes. Biotechnic & Histochemistry 2017;92(3):159-166.
5. Bhattacharyya GN. Chromosomes in different species of *Agave*. Journal of Cytology and Genetics 1968;3:1-6.
6. González-Gutiérrez AG et al. Aspectos relevantes del desarrollo sexual en el género *Agave* y otras asparagáceas. Los *Agave*s y sus Derivados: Tendencias Científicas, Uso Sostenible y Patrimonio 2023:21-49, 2023.
7. Lingling LV et al. Determination of chromosomal ploidy in *Agave* ssp. African Journal of Biotechnology 2009;8(20):5248-5252.
8. Vignoli L. Cariologia del genere *Agave*. Lavori del Reale Istituto Botanico di Palermo 1936;7:176-217.
9. Granick EB. A karyosystematic study of the genus *Agave*. American Journal of Botany 1944;31(5):283-298.
10. García-Mensoza A. Los *Agave*s de México. Ciencias 2007;87:14-23.
11. Rodríguez-Domínguez JM et al. Detection of endopolyploid cells in root tips from two geophytic species pretreated with α-bromonaphthalene. Acta Horticulturae 2020;1288:117-122.
12. Ullah Z et al. Cip/Kip cyclin-dependent protein kinase inhibitors and the road to polyploidy. Cell Division 2009;4(10).
13. D'Amato F. Role of polyploidy in reproductive organs and tissues. Embryology of Angiosperms, B.M. Johri, ed. (New York: Springer-Verlag), p. 519-566, 1984.

Comparative Assessment for Forage Palm and *Agave sisalana* Biomass for Sustainable Biofuel Production

Valdeci Machado[1*], Evily Ribeiro Moura[1], Gabrielly de Moura Bezerra[1], Luciano Sergio Hocevar[1], Carine Tondo Alves[1], Marcos Machado da Rocha[1]

[1]Federal University of Recôncavo of Bahia; Feira de Santana, Bahia, Brazil

In recent years, interest in semiarid biomass has surged. This study examines the physical-chemical properties of *Opuntia ficus indica* Mill (*Palma forrageira*) and *Agave sisalana* Perrine (*Agave sisalana*). This study aimed to characterize these biomasses by analyzing key structural components: moisture content, ash content, cellulose, hemicellulose, and lignin. The results reveal that *Opuntia ficus indica* Mill contains 78.65% moisture, 3.65% ash, 54.11% cellulose, 18.60% hemicellulose, and 21.08% lignin. In contrast, *Agave sisalana* Perrine exhibits 82.36% moisture, 11.65% ash, 63.39% cellulose, 5.80% hemicellulose, and 18.67% lignin. Forage Palm, with its higher cellulose and hemicellulose content, may be better suited for biofuel production. Meanwhile, *Agave*'s elevated ash content warrants consideration when evaluating its combustion quality and energy yield. Balancing lignin levels in both biomasses is crucial for efficient utilization.

Keywords: Biomass. Biofuels. *Opuntia ficus indica* Mill. *Agave sisalana* Perrine.

The semiarid region of Brazil is home to a wide variety of plant species that have adapted to the harsh climate and soil conditions. Two noteworthy plants in this region are the forage palm (*Opuntia ficus indica* Mill) and *Agave sisalana* (*Agave Sisalana* Perrine), which have evolved to thrive in water-scarce environments with high temperatures, playing essential roles in the local economy and ecology [1]. There is increasing interest in sustainable energy sources, with bioethanol emerging as a promising option. Bioethanol is produced through the fermentation of materials rich in fermentable sugars or carbohydrates, leading to efforts focused on non-food biomass generation. This includes lignocellulosic biomass derived from forest residues, woody and herbaceous plants, non-food crops, municipal solid waste, and animal fat [2]. It is important to study the flora of the semiarid region to uncover its biomass potential.

Analyzing the physical-chemical composition of these resilient plants is crucial for developing technologies that support sustainable energy production and address the social and economic development needs specific to the semiarid region. This study is critical to diversifying Brazil's energy sources.

The forage palm, commonly used as livestock feed in the semiarid region, shows drought resistance and has high biomass productivity [1]. Apart from its role in local agriculture, this succulent plant holds significant promise for bioenergy production, contributing to the expansion of renewable energy sources in Brazil. Meanwhile, *Agave sisalana* Perrine, the predominant species cultivated in the Brazilian semiarid region, belongs to the Agavaceae family. Renowned for its robust fiber rich in cellulose and lignin, *Agave* has various industrial applications. Adapting to semiarid conditions further underscores its potential as a valuable biomass resource.

This study aimed to characterize some physical-chemical properties of Forage palm and *Agave sisalana* biomass, informing sustainable practices and contributing to diversifying Brazil's energy matrix.

Materials and Methods

This study evaluated the moisture, ash, lignin, cellulose, and hemicellulose of *Agave sisalana*

Received on 15 September 2024; revised 30 November 2024.
Address for correspondence: Valdeci Machado.Av. Centenário, 697 - Sim. Zipcode: 44042-280. Feira de Santana, Bahia, Brazil. E-mail: valmachado@aluno.ufrb.edu.br.

J Bioeng. Tech. Health 2021;8(1):15-19

and forage palm. All experiments were conducted in triplicate at the Laboratory of Energies (LEN) at the Federal University of Recôncavo of Bahia (UFRB). Samples of *Agave* were collected in the city of Araci-BA at CETEP SISAL II, located at 11°20'20.6" S 38°57'45.4" W on April 5, 2024.Samples of *Opuntia* spp. were collected at CETENS-UFRB in Feira de Santana-BA at 12°15'14.0 "S 38°55'34.0 "W on May 10, 2024. The flour production involved 829.98 g of forage cactus and 956.88 g of *Agave*, dried at 60°C for 72 hours, ground, and sieved.

The moisture content was determined using a digital moisture balance (Belithermo G163L) on samples of forage palm and *Agave sisalana*, dried at 105 °C in the oven for 50 minutes in triplicate. In the second stage, ash content was determined by drying the biomasses at 105 °C in an oven for 24 hours, weighing them, and then placing them in a muffle furnace at 575 °C for 24 hours. After cooling, the ash content was obtained following the method proposed by Sluiter and colleagues (2005)[4].

The method used in this study for cellulose determination was proposed by Wright and Walles [5]. It involved preparing a 1 L solution containing 90 mL of nitric acid, 732 mL of glacial acetic acid, and distilled water. Three samples weighing 1 g of dried biomass each were prepared (Fraction A), and the material was transferred to a 50 mL flat-bottom flask. A 25 mL aliquot of the nitric acid-glacial acetic acid solution was added, and the mixture was refluxed for 25 minutes at 120 °C. After cooling, the cellulose residue was vacuum-filtered through filter paper and washed with 500 mL of hot water and 25 mL of ethanol, followed by drying in an oven at 100 ± 5 °C until constant weight (Fraction B). After cooling in a desiccator, the filter paper with the residue was weighed. The cellulose content was determined using Equation 1.

$$Celullose\ (\%) = \frac{Mass\ of\ Cellulose\ (B)\ (g)}{Mass\ of\ dry\ Biomass\ (A)\ (g)}\ x\ 100 \qquad (1)$$

The lignin content was determined by adapting methodologies from Sluiter and colleagues [4] and Silwadi and colleagues [6] by the soluble lignin (ASL) method and by the insoluble lignin (AIL) method. Initially, 0.3 g of biomass was added to 3 mL of H_2SO_4 at 72% concentration, and the mixture was periodically agitated for 60 minutes at 30 °C in an ultrasonic water bath. The acid was then diluted with 84 mL of distilled water, and the sample was incubated at 120 °C for 60 minutes. After cooling, the sample was vacuum-filtered. Acid-soluble lignin was analyzed using a UV-visible spectrophotometer (Weblaborsp, WUV-M51) at 205 nm, and the values were converted to concentration using an absorptivity coefficient of 105 $L.g^{-1}.cm^{-1}$. The total of the ASL was determined using Equation 2.

$$ASL\ (\%) = \frac{Absorbance \times filtered\ volume \times dilution}{\varepsilon\ Absorbance \times mass\ of\ dry\ biomass \times path\ length\ of\ UV\ (cm)}\ x\ 100 \qquad (2)$$

The insoluble fraction, Acid-Insoluble Lignin (AIL), was thoroughly washed with distilled water until excess acid was removed. It was then dried overnight in an oven at 105°C until reaching a constant mass (Fraction A). Equation 3 determined the total AIL content of the sample.

$$AIL\ (\%) = \frac{The\ mass\ of\ lignin\ insoluble\ (A)(g)}{The\ mass\ of\ dry\ biomass\ (g)}\ x\ 100 \qquad (3)$$

The total lignin was determined by summing the AIL and ASL by Equation 4.

$$Total\ of\ Lignin\ (\%) = ASL\ (\%) + AIL\ (\%) \qquad (4)$$

The hemicellulose content was estimated according to Kapoor and colleagues [7] by adding 10 mL of 1 M NaOH to 1.0 g of dried biomass. The sample was incubated in an autoclave at 120 °C for 60 minutes, then cooled, filtered, and reserved. The soluble fraction was neutralized with HCl, and the resulting precipitate (Fraction A) was separated by filtration and reserved. 95% ethanol (1:1) was added to the remaining solution to precipitate the remaining soluble hemicellulose (Fraction B). The precipitates obtained were filtered, washed with distilled water, and dried in an oven at 105 °C overnight until a constant mass was achieved. The estimated hemicellulose content was calculated using Equation 5.

$$Hemicellulose\ (\%) = \frac{Mass\ of\ the\ hemicellulose\ (A+B)}{Mass\ of\ the\ dry\ biomass\ (g)}\ x\ 100 \qquad (5)$$

Results and Discussion

Chemical analysis of components such as moisture, ash, hemicellulose, and lignin is crucial for understanding prickly pear's structural and nutritional composition (*Opuntia ficus indica*) and *Agave* (*Agave* spp.). These parameters are essential for determining these plants' quality and potential use and understanding their biochemical and industrial properties. Following the completion of the laboratory study, the results obtained are presented in Table 1.

We observed that succulents like *Agave* and forage cacti have a high moisture content, indicating their ability to retain large amounts of liquid. This is due to their adaptation to long periods of drought, allowing them to survive in arid environments. This characteristic is particularly beneficial for processes such as alcoholic fermentation, as the high water retention in succulents means that less external water needs to be added during the fermentation process, making it more efficient and sustainable.

Additionally, the natural moisture of these plants can create a more favorable environment for the growth of yeast, which is essential for converting sugars into alcohol. Figures 1 and 2 visually present the values obtained through the methodologies described in the text in the context of analyzing the key constituents that enable alcoholic fermentation for bioethanol production.

Lignocellulosic biomass comprises cellulose (40-60%), hemicellulose (20-40%), and lignin (10-25%), which are intricately intertwined to form complex carbohydrates. These components play pivotal roles in bioethanol production through separate hydrolysis and fermentation. Lignin, a complex polymer with an amorphous structure composed of aromatic and aliphatic components, binds to lignocellulosic fibers, contributing to cell wall formation [8,9]. Characterized by a hydrophobic nature and a highly branched three-dimensional structure, lignin constitutes approximately 10-25% of plant composition [10]. It acts as an adhesive between cellulose and hemicellulose, essential structural elements of the cell wall. Removing lignin is essential to facilitate the conversion of cellulose and hemicellulose into sugars [11].

Figures 1 and 2 illustrate lignin contents of 18.67% in *Agave* spp. and 21.08% in *Opuntia* spp., indicating that *Opuntia* spp. has a higher percentage, making it less favorable than *Agave* spp. for bioethanol production. Pretreatment processes are necessary to degrade lignin for efficient sugar release, potentially increasing production costs or resulting in underutilizing biomass portions. Hemicellulose is a complex polysaccharide with a relatively low molecular weight, consisting of polymeric carbohydrates containing sugar units typically composed of five to six carbon atoms [10].

It can include sugars such as D-glucose, D-galactose, D-mannose, D-xylose, L-arabinose, D-glucuronic acid, and 4-O-methyl-D-glucuronic acid [12]. Structurally, hemicellulose bears more remarkable similarity to cellulose than to lignin. Rich in sugar composition, hemicellulose plays a crucial role in bioethanol production. *Agave* spp. Exhibits a lower hemicellulose content, which contrasts favorably with *Opuntia* spp., where hemicellulose content is more than three times higher. Pretreatment methods for hemicellulose breakdown are generally more efficient than those required for lignin [8].

Cellulose consists of dimeric units of anhydroglucose [$(C_6H_{10}O_5)$ n, where n is the number

Table 1. Chemical characterization results of *Agave* spp. and *Opuntia* spp.

	Moisture (%)	Ash (%)	Lignin (%)	Hemicellulose (%)	Cellulose (%)
Agave spp.	82.36 ± 0.82	11.65 ± 1.77	18.67 ± 1.71	5.80 ± 1.46	63.39 ± 12.82
Opuntia spp.	78.65 ± 3.10	3.65 ± 0.65	21.08 ± 3.17	18.60 ± 13.65	54.11 ± 7.95

Values represent mean ± standard deviation.

Figure 1. Chemical composition of the *Agave* spp.

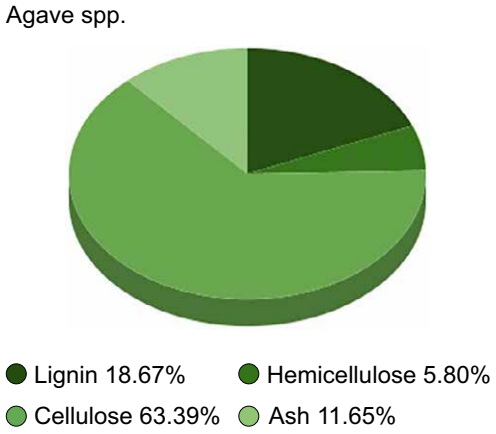

Figure 2. Chemical composition of the *Opuntia* spp.

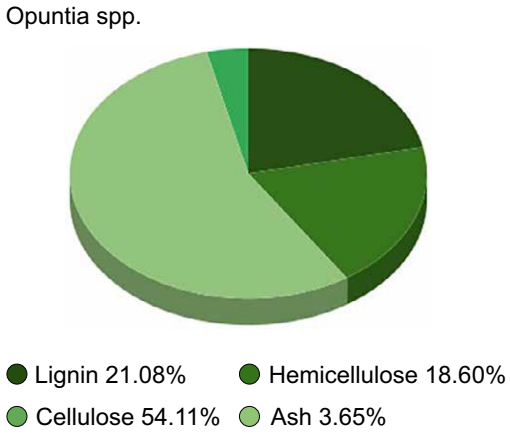

of repeat units per chain], arranged in a linear chain. These dimers are linked by glycosidic bonds between carbon 1 (C1) of one dimer and carbon 4 (C4) of the adjacent dimer, forming a β 1-4 linkage [9,10,13]. In the absence of lignin, the length and packing of cellulose chains, which predominantly constitute the crystalline regions of cellulose, significantly influence material accessibility. The crystallinity of cellulose can affect processes like saccharification, where cellulose is converted into glucose. Tighter packing and longer cellulose chains reduce substrate accessibility, posing challenges for catalysts and solvents involved in the process [10,13]. Despite both plants containing high cellulose content, effective pretreatment initially targets lignin breakdown to facilitate access to cellulose and hemicellulose. Therefore, process feasibility hinges on pretreatments that effectively separate lignin from hemicellulose and cellulose. Ash content refers to the residue left after the decomposition and elimination of organic matter, achieved through calcination, which releases associated elements. This process enables comprehensive plant identification, with the ash content as a fundamental metric for subsequent experiments. It provides insights into the presence of inorganic materials within the plant, forming a basis for analyzing extractives and other compounds that may potentially hinder processes. Thus, ash content establishes a foundational understanding of the inorganic composition of the plant material.

Conclusion

Based on the results of the chemical characterization of *Agave* spp. and *Opuntia* spp., several important characteristics for their use as biomass sources can be highlighted. *Agave* spp. A significantly lower lignin content was observed compared to *Opuntia* spp., which may facilitate processes such as bioethanol production, where lignin removal is essential to improve the accessibility of cellulose and hemicellulose. On the other hand, *Opuntia* spp. showed a higher hemicellulose content, making it a potential source of sugars for fermentation.

The high moisture content found in both plants indicates a natural ability to retain water, which can be advantageous in processes like alcoholic fermentation, minimizing the need for external water addition.

Furthermore, ash content analysis provides important insights into the mineral composition of the plants, which is essential for understanding their nutritional potential and for processes involving impurity removal. Cellulose, despite being abundant in both plants, is closely associated with lignin and hemicellulose, the removal of which is crucial for optimizing biofuel production. Therefore, pretreatment strategies to effectively remove

lignin and break down hemicellulose should be developed and optimized for efficient bioethanol production from these succulents. This maximizes biomass conversion into fermentable sugars and increases overall process efficiency, making it more economical and sustainable for future industrial applications.

Acknowledgments

The authors thank CNPq (nº 405778/2022-8), FAPESB (INCITERE nº PIE 0R008/2022), and UFRB (PIBITI and PIBIC).

References

1. Moura ER, Cabral PS, Rofrigues RJ et al. Explorando o potencial da palma forrageira (*Opuntia*): uma análise abrangente para impulsionar os biocombustíveis no semiárido brasileiro. Observatório de la Economía Latinoamericana 2024; 22(6):e5256. DOI: 10.55905/oelv22n6-137.
2. Halder P. Azad K, Shah S, Sarker E. Prospects and technological advancement of cellulosic bioethanol eco fuel production. In: Azad, Kalam (Ed.). Advances in Eco-Fuels for a Sustainable Environment. Woodhead Publishing Series in Energy. Woodhead Publishing, 2019:211-236. ISBN 9780081027288. https://doi.org/10.1016/B978-0-08-102728-8.00008-5.
3. Sousa EJS. Ocupação e uso do solo pela cultura do *Agave sisalana* no Território de Identidade do Sisal – Semiárido da Bahia. Dissertação (Mestrado em Solos e Qualidade de Ecossistemas) - Universidade Federal do Recôncavo da Bahia, Cruz das Almas, Bahia, 2015.
4. Sluiter A, Hames B, Ruiz R, Scarlata C, Sluiter J, Templeton D. Determination of ash in biomass. Laboratory Analytical Procedure (LAP) - National Renewable Energy Laboratory (NREL), 2005.
5. Wright PJ, Wallis AF. A Rapid determination of cellulose in plantation eucalypt woods to predict kraft pulps yields. Tappi Journal 1998;81(2):126-130.
6. Silwadi M, Mousa H, Azkawi AA et al. Pretreatment and acid hydrolysis of *Omani prosopis juliflora* wood. Journal of King Saud University - Engineering Sciences 2023;35:359-365. DOI: 10.1016/j.jksues.2021.07.003.
7. Kapoor K, Garg N, Diwan RK, Varshney L, Tyagi AK. Study the effect of gamma radiation pretreatment of sugarcane bagasse on its physcio-chemical morphological and structural properties. Radiation Physics and Chemistry. (Online). 2017. DOI: 10.1016/j.radphyschem.2017.07.010.
8. Pendse DS, Deshmukh M, Pande A. Different pretreatments and kinetic models for bioethanol production from lignocellulosic biomass: A review. Heliyon 2023;9(6). DOI: https://doi.org/10.1016/j.heliyon.2023.e16604.
9. Su T., Zhao D, Khodadadi M, Len C. Lignocellulosic biomass for bioethanol: Recent advances, technology trends, and barriers to industrial development. Current Opinion in Green and Sustainable Chemistry 2020;24:56-60. DOI: https://doi.org/10.1016/j.cogsc.2020.04.005.
10. Tian S, Zhao R, Chen Z. Review of the pretreatment and bioconversion of lignocellulosic biomass from wheat straw materials. Renewable and Sustainable Energy Reviews 2018;91:483-489. DOI: 10.1016/j.rser.2018.03.113.
11. Jardine JG, Peres MR. Considerações sobre o bioetanol lignocelulósico para subsidiar a elaboração de conteúdo da Árvore de Conhecimento Agroenergia. Campinas, SP: Embrapa Informática Agropecuária, 2009, 28p.
12. Santos FA, Queiróz JH, Colodette JL, Fernandes SA, Guimarães VM, Rezende ST. Potencial da palha de cana-de-açúcar para produção de etanol. Química Nova 2012;35(5):1004-1010. DOI: https://doi.org/10.1590/S0100-40422012000500025.
13. Wang S, Lu A, Zhang L. Recent advances in regenerated cellulose materials. Progress in Polymer Science 2016;53:169–206. DOI: https://doi.org/10.1016/j.progpolymsci.2015.07.003.

Analysis of the Main Production Routes of Biomethane and Dimethyl Ether (DME) from Biomass

Rozenilton de Jesus Rodrigues[1*], Carine Tondo Alves[2], Felipe Andrade Torres[2], Ednildo Andrade Torres[1]
[1]Federal University of Bahia (UFBA); Salvador, Bahia; [2]Federal University of Recôncavo of Bahia (UFRB); Feira de Santana, Bahia, Brazil

The present work comprehensively analyzes the technologies and processes involved in producing dimethyl ether (DME), from biomass gamification to biomethane synthesis. For this purpose, the technical aspects of the operational parameters must be addressed. This study aims to analyze the efficiency and technical feasibility of the main production routes of DME using biomass. The method used in this work is based on a comparative analysis of the significant DME production roads, comparing them through a systematic bibliographic review. The results suggest using more efficient routes, focusing on greater efficiency, biomethane quality, selectivity, and CO_2 reduction.
Keywords: Production of Dimethyl Ether. Biomethane. Biomass.

The growing interest in renewable fuels such as biomass is linked to environmental sustainability and the need to reduce reliance on conventional fuels. Exploiting alternative sources such as biomass, biomethane, and dimethyl ether (DME) from biomass presents a promising path to sustainable biofuel production. Sources of biomass for biomethane production include organic materials such as lignocellulosic biomass, agricultural, urban, and forestry, and energy-intensive crops such as corn, beet, sugarcane, and sweet sorgo, among others [1].

Dimethyl ether (DME) is a chemical compound widely used in industries as a propellant, serving as a substitute for diesel and oil gas (GLP). It can be synthesized from coal, oil, and biomass, including greenhouse gases. Known for its exceptional cleanliness and compressibility, the DME offers a promising alternative to diesel and GLP as a source of energy, both for combustion and as an energy source fuel, due to its self-ignition capacity and impressive octane index [2,3].

Biomass is a renewable source with great energy potential, used for power generation as a fuel, with excellent energy properties, low CO_2 emissions, and long-term economic advantages. The biomethane production process includes pretreatment, gasification, synthesis gas cleaning, hydrocarbon reforming, adjustment of the H_2/CO ratio, and biomethane synthesis [2].

Received on 10 September 2024; revised 21 November 2024.
Address for correspondence: Rozenilton de Jesus Rodrigues. Av. Milton Santos, s/nº - Ondina. Salvador, Bahia, Brazil. Zipcode: 40170-110. E-mail: leojrodrigues1111@gmail.com.

J Bioeng. Tech. Health 2025;8(1):20-25

Biomethane and DME Conversion Routes

Description of the main Biogas and Biomethane Production Routes

Biogas production mainly involves anaerobic digestion and thermal gasification [4]. Anaerobic digestion is a complex process that requires strict anaerobic conditions and microbiological activity to convert organic material into biogas, primarily composed of methane and carbon dioxide [5]. Thermal gasification, or thermochemical conversion, is influenced by temperature, pressure, and gasifying agents. The resulting biogas can be used for heating, electricity generation, and as a fuel for vehicles [4].

Biomethane to DME Conversion Processes

Biomass gasification involves gas cycling, refrigeration, and purification units directed to a synthesis gas reactor. After condensing and separating the gases, the gas is synthesized from its elementary components, suitable for use in transportation, power generation, industrial applications, and additional chemicals [7].

Figure 1: Biogas conversion and production by anaerobic digestion and thermochemical processes.

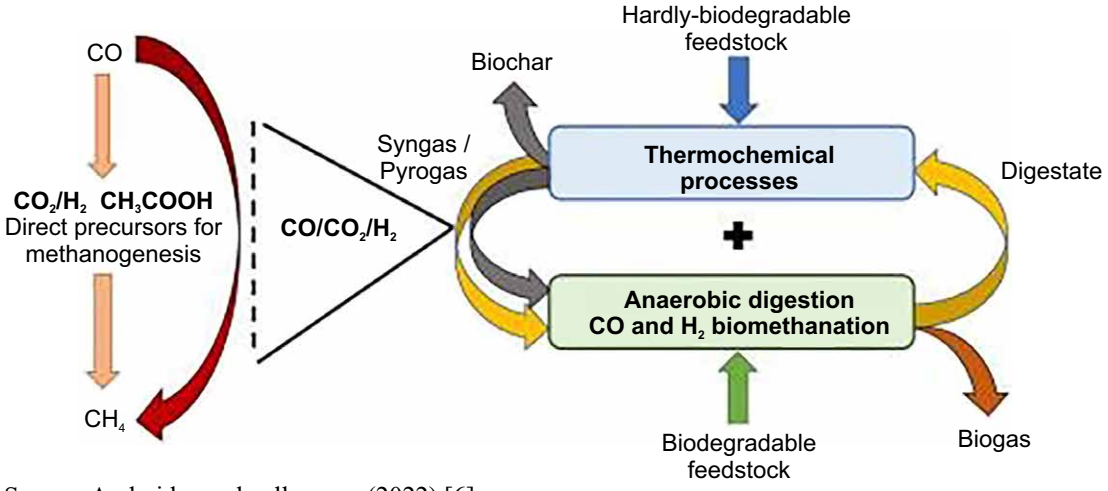

Source: Andreides and colleagues (2022) [6].

Dimethyl Ether (DME) Production Routes and Their Steps

The main processes for producing dimethyl ether from biogas include direct catalytic hydrogenation of CO_2 and the synthesis of DME from biomass-derived syngas [2,8]. The synthesized gas is converted to methanol using synthesis reactions, with CO reacting with water steam (H_2O) to generate CO_2 and H_2, followed by catalytic dehydration and fusion of methanol to form DME, according to the sequence of the following equations [9]:

Methanol formation: $CO + 2H_2 \leftrightarrow CH_3OH$ DHO = -90.4 kJ/mol (1)
Water-gas change: $CO + H_2O \leftrightarrow CO_2 + H_2$ DHO = -41.0 kJ/mol (2)
Methanol dehydration: $2CH_3OH \leftrightarrow CH_3OCH_3 + H_2O$ DHO = −23.0 kJ/mol (3)
General reaction: $3CO + 3H_2 \leftrightarrow CH_3OCH_3 + CO_2$ DHO = −258.3 kJ/mol (4)

Direct Biomass Synthesis Route

The direct pathway of DME synthesis involves partially hydrogenating carbon monoxide (CO) and the DME synthetic reaction. In the direct catalytic hydrogenation process, CO_2 is converted to methanol using bifunctional/hybrid catalyst systems, which combine metal and acid functions. Methanol is then dehydrated to DME using an acid catalyst (Figure 2) [10,11].

Route Indirect Synthesis Via Synthetic Gas

The methanol dehydration process is a necessary step in producing dimethyl ether. The DME-water-methanol mixture is not an ideal thermodynamic system, requiring the dehydration of methanol to form DME at a temperature of 534 K and a pressure of 0.5 MPa [13].

Methanol Dehydration on Solid Acid Catalytic

The indirect production synthesis involves two stages: the DME from biomass-derived synthetic gas undergoes a process using a $Cu/ZnO/Al_2O_3$ catalyst intended for methanol syntheses, and an acid catalyst (usually γ-Al_2O_3) is used for the dehydration of methanol to DME. The author highlights that the synthesis of DME by dehydration requires the conversion of methanol to DME in a fixed bed reactor with copper-based catalysts (Cu/Zn, Cu/3n/Al, Cu/Zn/CO) or solid-acid catalysts [14].

Materials and Methods

This study used as method the research of DME synthesis processes through a systematic bibliographic review of the production routes: direct

Figure 2. One-step process: Direct method via DME synthesis gas from anaerobic digestion of biomass.

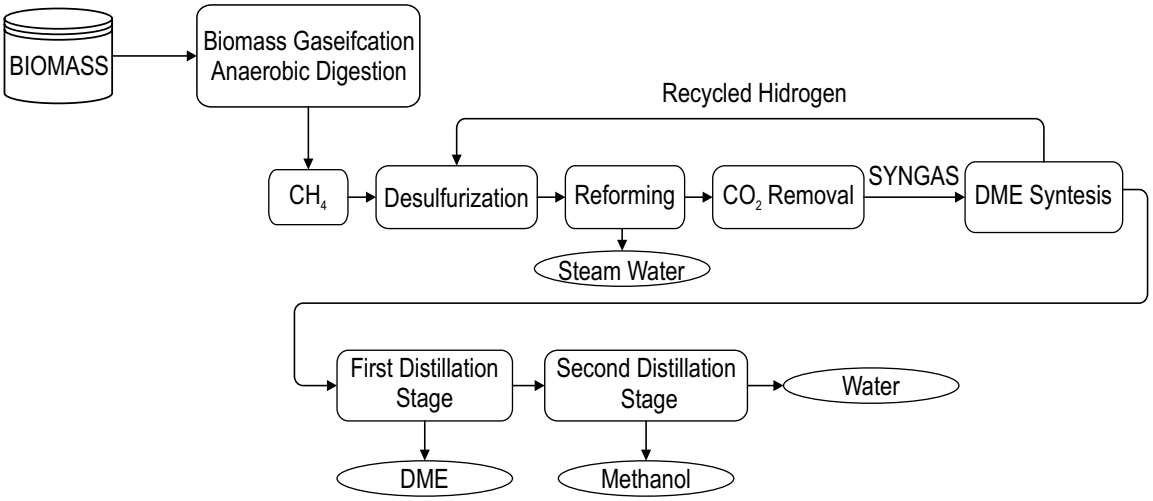

Source: Adapted from Falco (2020) and Wodołażski (2020) [12,13].

Figure 3. Two-stage process: Indirect method via DME synthesis gas from the anaerobic digestion of biomass.

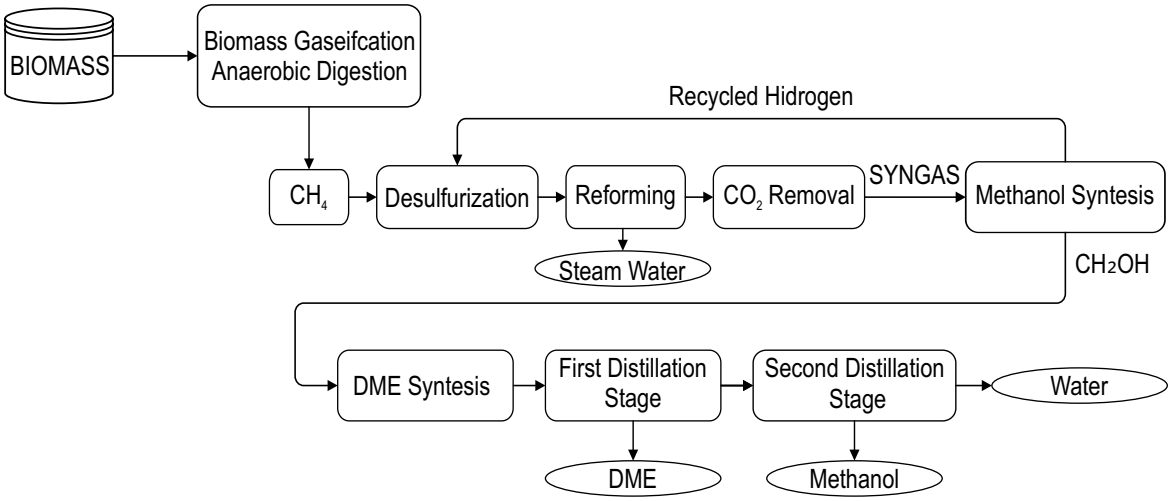

and indirect synthesis, biomethane dehydration, and methanol dehydration in solid acid catalysts resulting from the anaerobic digestion of biomass. The analyses resulted in an analysis of the experimental parameters of the studies presented, focusing on performance, selectivity, and relationship between reagents.

Results and Discussion

Yaripour and colleagues' research on solid-state catalysts for the catalytic dehydration of methane to DME highlights the benefits of a simple metal dehydration method that achieves high conversion rates to DME [15]. His process offers improved selectivity, minimized coke formation, and the option for selective coking using specialized catalysts like DME-AlS. However, it also underscores the importance of biogas pretreatment in two separate stages. Table 1 provides data on reactant generation percentages and catalytic performance, clearly indicating that the silica-modified c- Al_2O_3 catalyst modified with silica has the best performance [15].

Table 1. Methanol dehydration over reference and modified γ-alumina catalysts.

Catalysts Parameters	DME-AlS1	DME-AlS2	DME-AlS3	DME-AlS4	Catalysts	DME-AlS5	DME-SCAT2 (γ- Al_2O_3)
DME (wt%)	75.6	73.4	71.3	64.7	58.6	63.23	73.4
MeOH (wt%)	24.4	26.6	28.7	35.3	41.6	38.77	26.6
CH_4 (wt%)	0.0326	0.0128	–	–	–	–	–
Conversion (X%)	86.4	84.5	85.0	83.5	73.6	77.15	84.5

Source: Adapted from Yaripour and colleagues (2005) [15].

Eichler's study [1] highlights the importance and characteristics of biomass in influencing biomethane levels, which have an average range of 40–70% v/v—lower quality biomass results in a lower biomethane percentage, resulting in lower DME production. Insufficient methanol levels can also lead to reduced efficiency and incomplete inversions. However, biomass pretreatment is necessary to remove impurities and increase the biomethane percentage, which increases operating costs. Direct synthesis of DME from biomass waste using catalysts was analyzed in Liuzzi and Peinaldo study [10], identifying that a high CO_2/CO ratio affects the catalyst performance. The authors suggested that the addition of an aqueous solvent (zeolite 3A) to the reaction process can mitigate the detrimental effect of H_2O in the direct synthesis of DME from CO_2-rich waste, increasing the production of DME through catalysts such as zirconium and gallium.

In another study by Abreu [16], several models of chemical catalysts, several chemical catalyst models were evaluated for experimental settings, finding that the good performance of chemical modeling for biomethane dissolution depends on the experimental points, the conversion rate achieved, and the catalyst acidity. The dissolution of biomethane is crucial for species adsorption models, and constant values for methanol dissolution and water balance are temperature-sensitive.

The data presented in Figure 4 simulates this process using catalysts ZSM-5 and γ-Al2O3 m function of temperature in distinct reactions.

According to the study by Yasar [17], direct synthesis using hybrid catalysts is more advantageous than indirect synthesis, which uses bimetallic or multimetallic catalysts commonly used for biomethane synthesis (Table 2). The biomethane dehydration process utilizes solid catalysts such as Al_2O_3, HZSM-5, SapOS, and SiO_2.

Conclusion

The present work provided a comprehensive review of energy-to-liquid conversion technologies, including the use of DME, highlighting the potential of biomass in the production of aggregate and high-value chemicals and exploring the manufacture of biological-based chemical products from renewable biomass, emphasizing the need for efficient and sustainable conversion processes.

Production of DME can significantly reduce transportation and local labor costs, as well as the use of agro-industrial waste as precursors. DME is a clean alternative to diesel and is suitable for transportation and heating applications. It is a promising fuel and renewable solvent with numerous applications, including clean alternatives to diesel and GLP, offering high ketone numbers and reduced emissions, especially in heavy vehicles. The studies suggest that adding promoters like zirconium oxides and gallium can boost CO in synthesis gas, thereby enhancing DME production rates. Furthermore, adding a water sorbent to the

Figure 4. Conversion in function of temperature using catalyst simulation.

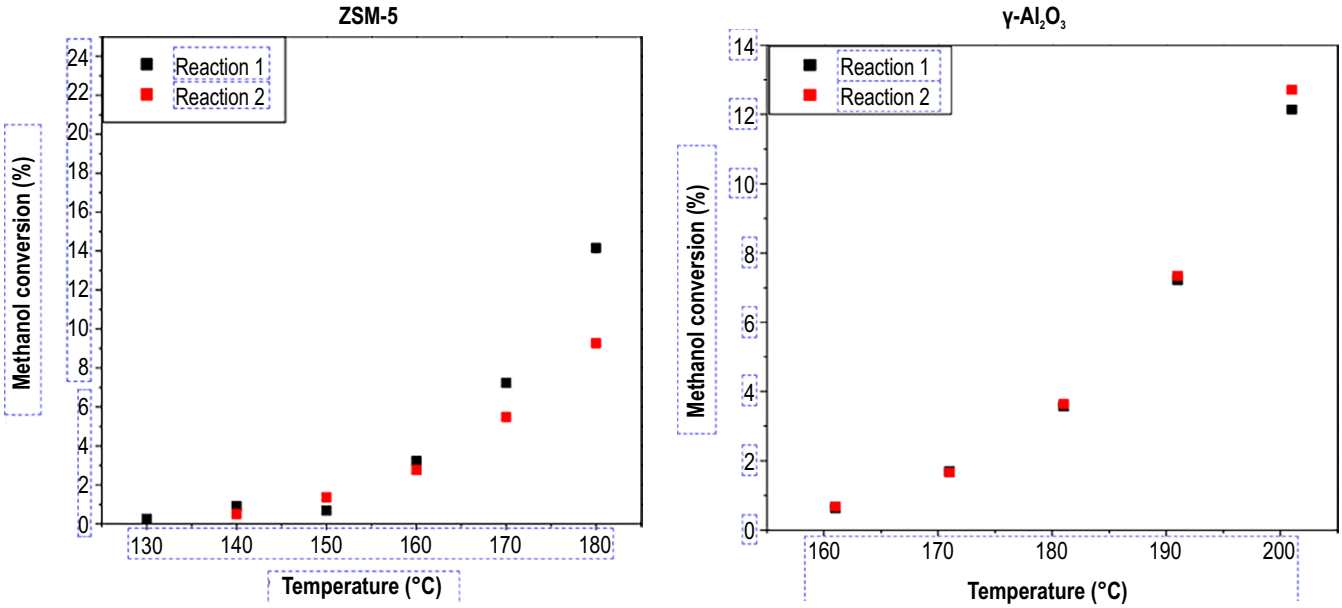

Source: Abreu, (2015) [16].

Table 2. Analysis operating parameters: Production of DME from direct synthesis to derivative of synthesized gas obtained from biomass.

Synthesis	Reactor Type	T (°C)	P(MPa)	Feed Composition/ Space Velocity	Catalysts	(X), (Y), (S)	Authors
Direct	Fixed Bed Reactor	840	2	0.6 kg biomass / h, ER 0.28, CO_2/biomass ratio 0.327	Cu-Zn-Al/ HZSM-5	XCO=2.5 Nm= 78.5% YDME = 379g DME kg^{-1}	Chang (2012)[18]
Direct	Fixed-bed isothermal reactor system	800	2	Raw CO_2 and biomass charcoal. CO_2 / CO =6.33	Ni/Al_2O_3	XCO_2=71.1% XCO=89% YDME=≈65.5 % YCO≈84.8%	Yong (2011) [19]
Direct	Fixed-bed isothermal reactor system	400	3	Similar to biomass-derived synthesis gas CO/CO_2 / H_2 / N_2 = 1/1.9/7.7/1.18	Cu/ZnO/ Al_2O_3 (CZA) Cu/ZnO/ Al_2O_3 (CZA) γ-Al2O3	YDME ≈70% XCO and XCO_2 ≈ 7.6 and 9.9%	Dalia and colleagues (2020) [20]
Direct	Fixed bed membrane reactor (PBMR)	240	3	H2/CO = 1 and biomass	Low pressured CZA	BioDME= 49,4% XCO= 96.24% SDME = 70%	FEDELI, (2022) [21]

T, temperature; P, pressure; X, conversion; Y, yeld; S, selectivity.

reaction medium can further boost DME production from CO_2-rich synthesis gas. It can be concluded, according to the analyzed work, that there are critical gaps in the production of DME, noting that industrial processes affect the costs with investment-related expenses (capex), as well as the general operating costs (opex) and that DME synthesis plants can support the current CO_2 capture and seizure plants.

Acknowledgments

The authors thank CNPq (nº 405778/2022-8), FAPESB (INCITERE nº PIE 0008/2022), UFBA, and UFRB.

References

1. Eichler P and colleagues. Bioethanol production via gasification of lignocellulosic biomass. Química Nova 2015;38:10.5935/0100-4042.20150088.
2. Mondal U, Ganapati DY. Perspective of dimethyl ether as fuel: Part I. Catalysis. Journal of CO_2 Utilization 2019;32:299-320.
3. Huang C, Zhu C, Zhang M et al. Design of efficient ZnO/ZrO_2 modified CuCoAl catalysts for boosting higher alcohol synthesis in syngas conversion. Appl Catal B Environ 2022:300.
4. Turco M, Ausiello A, Micoli L. Processes of Biogas Production: Anaerobic Digestion and Thermal Gasification. In: Treatment of Biogas for Feeding High Temperature Fuel Cells. Green Energy and Technology. Springer, Cham. 2016.
5. Stamatelatou KG, Antonopoulou G. 12-production of biogas via anaerobic digestion. Editor(s): Rafael Luque, Juan Campelo, James Clark. In: Woodhead Publishing. Series in Energy. Handbook of Biofuels Production. Woodhead Publishing, 2011:266-304.
6. Andreides D et al. Biological conversion of carbon monoxide and hydrogen by anaerobic culture: Prospect of anaerobic digestion and thermochemical processes combination. Biotechnology Advances 2022;58:107886.
7. Deka TJ, Osman AI, Baruah DC et al. Methanol fuel production, utilization, and techno-economy: a review. Environ Chem Lett 2022;20:3525–3554.
8. Mota N et al. Direct synthesis of dimethyl ether from CO_2: Recent advances in bifunctional/hybrid catalytic systems. Catalysts 2021;11:411. doi: 10.3390/CATAL11040411.
9. Peral EMM. Optimal production of dimethyl ether from switchgrass-based syngas via direct synthesis. Industrial & Engineering Chemistry Research. American Chemical Society 2015;54:7465-7475. doi: 10.1021/acs.iecr.5b00823.
10. Liuzzi D, Peinado MA, Peña J et al. Increasing dimethyl ether production from biomass-derived syngas via sorption enhanced dimethyl ether synthesis. Sustainable Energy and Fuels 2020;4:5674-5681. Doi: 10.1039/D0SE01172J.
11. Aristide G, Catizzone E, Freda C. Process Simulation and environmental aspects of dimethyl ether production from digestate-derived syngas. International Journal of Environmental Research and Public Health 2021;18:807. doi: 10.3390/IJERPH18020807.
12. de Falco M. Dimethyl Ether (DME) Production. In: Oil e Gas Portal, 23 December 2015, Available at: https://www.oil-gasportal.com/ dimethyl-ether-dme-production-2/?print=pdf. 2015.
13. Wodolazski A, Smoliński A. Modeling and process integration study of dimethyl ether synthesis from syngas derived from biomass gasification: Flowsheet simulation. Alexandria Engineering Journal 2020.59:4441-4448.
14. Rafiee A. Staging of diethyl ether (DME) synthesis reactor from synthesis gas (syngas): Direct *versus* indirect route. Chemical Engineering Research and Design 2020;163:157-168. https://doi.org/10.1016/j.cherd.2020.08.033.
15. Yaripour F, Baghaei F, Schmidt I, Perregaard Jens. Catalytic dehydration of methanol to dimethyl ether (DME) over solid-acid catalysts. Catalysis Communications. 2005;6:147-152. 10.1016/j.catcom.2004.11.012.
16. Abreu BMNB. Kinetic modeling of the dehydration of methanol to dimethyl ether. 2015. 107 p.: il. Dissertation.

Biomethane Production from Cassava Juice: The Usage of Manipueira as Biomass

Anderson Freitas Sales[1*], Rubens Pereira Martins[1], Calisto José da Silva Neto[1], Adley Diego Ferreira de Almeida[1], Carine Tondo Alves[1], Leandro Freitas Sales[2]

[1]Federal University of Recôncavo of Bahia, CETENS; Feira de Santana, Bahia; [2]SENAI CIMATEC University; Salvador, Bahia, Brazil

With the growing demand for alternative energy sources and environmental sustainability, waste biomass has gained prominence in the energy sector due to its wide availability. This study analyzes the production of biomethane from manipueira, a toxic and highly polluting byproduct of cassava processing, and evaluates its potential as an energy source. A biodigester was used to monitor manipueira temperature and gas production over 11 days to assess biomethane generation. The process yielded 91 mL/L of biomethane, demonstrating its viability as a biomass energy source. Additionally, the low production cost reinforces the feasibility of utilizing manipueira for sustainable energy generation.

Keywords: Manipueira. Biomass. Alternative Energy. Biogas. Biodigester.

Since 1970, the world has experienced a series of significant environmental impacts, mainly resulting from population growth, industrialization, and changes in consumption patterns. These environmental impacts have driven growing global awareness and action in sustainability activities. Initiatives such as the creation of protected areas, policies to reduce greenhouse gas emissions, the promotion of renewable energies, and sustainable agricultural practices are some of the responses developed to mitigate the adverse effects and promote an environmentally balanced future. Brazil generates tons of waste in the agricultural sector daily, most of which is disposed of inappropriately, contaminating the soil and emitting gases into the atmosphere. These gases are generated by animal confinement waste, grain cleaning waste, and produce that rots in warehouses, so adding the generation of bioenergy to agricultural production, whether through family farming or even through large rural producers, guarantees not only a reduction in the impacts caused to the environment but also an economic possibility, since, among the renewable energies available in rural areas, energy from residual biomass is more available for low-cost access and more cost-effective for the Brazilian reality [1].

Manipueira is the liquid waste from cassava pressing to produce flour and starch. Manipueira can be used as an alternative energy source for biogas production, as it is rich in carbon molecules, nitrogen, and mineral salts, which are essential for anaerobic digestion and do not require hydrolysis [2]. Through this process, the production of biogas, which is made up of a mixture of gases, with commonly 60%-70% biomethane (CH_4) and 25-35 % carbon dioxide (CO_2) as the leading gases [2], can be used as a fuel for generating thermal and electrical energy. This practice reduces negative environmental impacts and provides an alternative and sustainable energy source, promoting the circular economy and benefiting rural communities.

Firewood is often needed in rural areas for the roasting process of cassava flour. Soares (2022) [3] showed that a flour industry in Cianorte—PR replaced firewood with biogas obtained through anaerobic digestion of manipueira. The average firewood consumption between 2021 and 2022 was reduced by 50.04 %. We also observed that biogas proved more energetically advantageous as it has a higher calorific value than firewood, generating less CO_2 when burning the fuel and, therefore, better environmental performance.

Guimarães and colleagues (2019) [4] evaluated that produced electricity generation feasible in a

Received on 10 September 2024; revised 1 December 2024.
Address for correspondence: Anderson Freitas Sales. Universidade Federal do Recôncavo Baiano. v. Centenário, 697 - Sim. Zipcode: 44042-280. Feira de Santana, Bahia, Brazil. E-mail: andersonengfreitas@gmail.com.

J Bioeng. Tech. Health 2025;8(1):26-31

quilombola community, demonstrating great social, environmental, and energy performance when using manipueira biogas to generate electricity. According to the authors, the preparation of must and the use of inoculum indicated that the biogas potential is 1.389.312 cm^3 per year in a single-stage biodigester with a capacity of 60 liters, producing 115.776 cm^3 per round. The project is also estimated to generate 214 kWh/year of electricity. In this case, animal-origin inoculum was used, which provides more excellent conditioning for CH4 production. Finally, this is another example of the excellent energy potential that can be exploited for any site that produces manipueira in residual form.

According to Kunz and colleagues (2022) [5], anaerobic digestion involves four key stages: hydrolysis, acidogenesis, acetogenesis, and methanogenesis; each plays a crucial role in converting organic matter into biogas. In Alves and colleagues (2024), it is shown that the phases of anaerobic digestion occur as follows: hydrolysis: Complex organic matter → Simple compounds, acidogenesis: Simple compounds → volatile fatty acids (VFAs), alcohols and other intermediates, acetogenesis: VFAs, alcohols and intermediates → acetic acid, H_2 and CO_2 and finally methanogenesis: acetic acid, H_2, and CO_2 → CH_4 and CO_2 [6]. In the case of manipueira, which is liquid waste, producing flammable gases requires two phases in the biodigestion process: acetogenic and methanogenic. In the acetogenic phase, bacteria in an acidic environment with a pH between 5 and 5.5 will form the main products for the methanogenic phase, including acetate, which can account for up to 70 % of CH_4 production [7]. In the methanogenic phase, microorganisms use acetate, hydrogen, and CO_2 to form biogas in a neutral pH environment. In both phases, the ideal temperature should be 15-45 ºC, where anaerobic digestion occurs [2]. Biodigestion has the advantage of taking place in low-cost and simplified biodigesters, making biomass energy sources more accessible [7].

In this context, this work aims to verify the production of CH_4, analyzing in a mixed way the feasibility of a low-cost project, which can be used, for example, in rural areas that generate biomass as waste from the main product, as occurred in Soares (2022) [3] and discussed by Bley (2009) [1]. This was done in a digestion process inside an automated biodigester, capable of cataloging the generation of CH_4, a gas of interest for energy purposes and generated in the digestion process [7]. Automation was done using Arduino and sensors, which took daily measurements. The project's low cost influences its methodological simplicity, which could make any significant production of flammable compounds viable as an aid to conventional energy sources.

Materials and Methods

Manipueira was collected from local cassava processors in Irará (Bahia-Brazil) on May 11, 2024. The samples were then pre-treated using decantation and filtration to remove larger solids. The acetogenic phase took place in an open plastic biodigester for 4 days. Subsequently, with the pH measuring 4.7 in the acetogenic phase (conventional tape pH meter), 3 liters of manipueira were neutralized with 500 mL of NaOH at a concentration of 1 mol/L, reaching a pH of 7.1 to suit the methanogenic phase in biodigestion. The sample was then transferred to a simple closed biodigester with a capacity of 5 liters, operating at room temperature of approximately 27 ºC, and kept in a shaded location in Irará (Figure 1).

The bioreactor (Figure 1) was equipped with inlet ports for the pre-treated manipueira at neutral pH 7 and an outlet for the biogas generated by a valve. Properly sealed with epoxy glue putty to create an anaerobic environment suitable for bacterial activity and gas storage, an Arduino board was used to operate the data from the submerged temperature (DS18B20) and CH_4 (MQ-4) sensors.

The body of the biodigester comes from recycling, and the Arduino is connected to the sensors via a protoboard, which is used to connect a 4.7 kΩ resistor to stabilize the temperature sensor reading signals.

In the same line, Alves and colleagues (2024) presented an automated biodigester that controls

Figure 1. Biodigester.

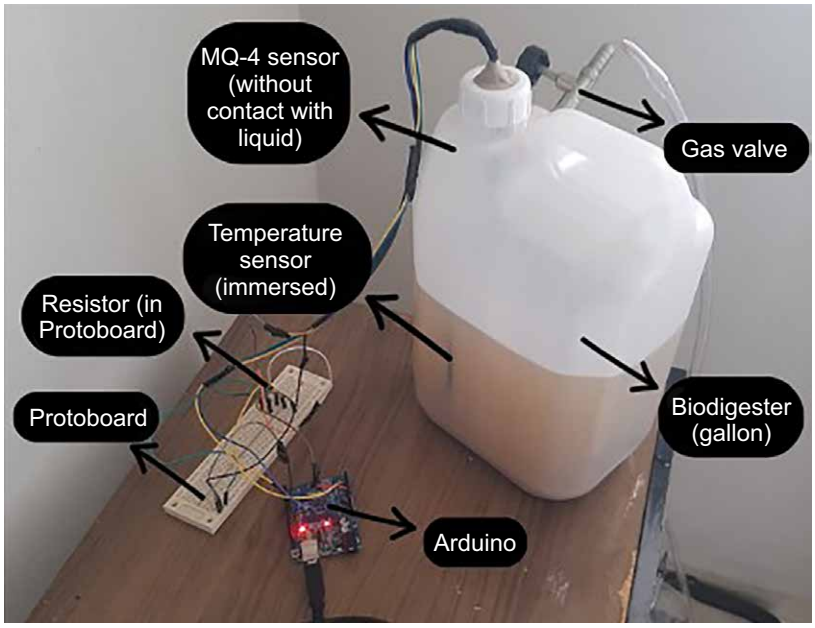

the temperature and monitors the formation of hydrogen and CH_4 in real time, as well as the pressure and temperature control variables [6].

Their results indicated higher biogas production at around 35 ºC [6]. This work demonstrated that manipueira can produce biogas even in conditions without temperature control and without the need to add inoculants, so this technology can be implemented in rural areas that do not have access to more sophisticated equipment.

System Configuration

Sensor connection: The Arduino's input ports must be connected to the sensors. The DS18B20 sensor needs three wires (signal, ground, and power), while the MQ-4 is connected to the Arduino's analog input ports. Arduino programming: The code was developed to read sensor data using Excel. Its structure is simple and available from the manufacturer on online sites.

Sensor Calibration and Data Collection

The sensors were calibrated before continuous use to ensure the accuracy of the readings. This includes sensitivity adjustments for the CH_4 sensor and checking the temperature sensor's accuracy. The collection is done with a GPU connection to the Arduino, which has been configured to export the temperature reading in degrees Celsius and the CH_4 volume in part per million directly to the Excel platform.

Results and Discussion

Upon initiating the bioreaction, a 12-hour interval was established for measuring CH_4 production and depressurizing the biodigester, owing to its basic sealing mechanism.

Measurements were systematically recorded at 8:00 PM and 8:00 AM daily, corresponding to nocturnal and diurnal readings. Table 1 presents the measurement days, the quantity of CH_4 generated at successive time intervals, and the temperature at the time of measurement. The data reveals that 12 hours after neutralizing the pH of the manipueira and confining it in the biodigester, a production pattern emerges, which remains consistent over the subsequent 3 days for the morning measurements. Production levels are observed from May 18, the fourth day, with a more significant rise in the afternoon. This aligns with the findings of Kunz

and colleagues [5], which indicate that the daytime production interval results in higher temperatures than nighttime. The increased incidence of light during the day also enhances bioremediation by activating methanogenic microorganisms more effectively.

Figure 2 shows the daily production of CH_4, adding up the values in Table 1, which is the biogas part of interest. The curve grows approximately linearly over the days up to the 5th day, with production increasing significantly on the 6th and 7th days. According to Neto and colleagues (2010), this is due to the reproduction of methanogenic microorganisms, in which the non-use of inoculum does not allow fermentation to be so expressive, especially at the beginning [2]. After the 7th day, there is a drop in daily production, which returns to the constant trend of the curve from the 9th - 11th, with a slight slope. This suggests that production is significant over the next few days, from day 11 onwards, although not cataloged in this study.

Figure 3 shows the accumulated volume production of CH_4. The production was evaluated in 11 days of fermentation. It is possible to see the viability of the process, given the proportion at the end of the 11th day of 91 mL of CH_4 per liter of manipueira cataloged. Although the production of this work is lower, proportionally, than in Neto and colleagues (2010) [2] or Guimarães and colleagues (2019) [4], for example, it is still possible to characterize the viability of the work since the costs are minimal and on a larger scale can generate great low-cost/benefit energy potential that is simple to obtain in terms of preparing the biomass and the biodigester [2,4]. This production tends to be even higher over a more extended period, as the curve in Figure 2 still shows excellent production on day 11. Including an inoculum with a more significant presence of CH_4-producing microorganisms and efficient temperature control can significantly increase biogas production.

Conclusion

This work shows that the production of CH4 from manipueira, a fluid derived from cassava, can reach up to 91 mL of CH_4 per liter of manipueira in the bioreaction process in the first 11 days. Daily production showed a notable increase after the 6th day due to the natural proliferation of microorganisms in digestion. Daytime production

Table 1. CH_4 production.

	Night production		Daytime production	
Date	**Temperature (ºC)**	**Volume (mL)**	**Temperature(ºC)**	**Volume (mL)**
05/15	27.75	9.34	29.19	14.08
05/16	27.56	8.67	27.94	13.01
05/17	26.31	9.44	27.87	14.16
05/18	25.81	10.27	25.87	15.40
05/19	25.25	11.03	26.56	16.54
05/20	25.69	14.18	27.87	21.27
05/21	26.00	13.94	26.36	20.91
05/22	25.19	10.96	26.50	16.43
05/23	25.81	13.39	27.56	20.08
05/24	25.81	13.56	27.56	20.33
05/25	26.06	12.76	26.00	19.14

Figure 2. Biomethane daily production.

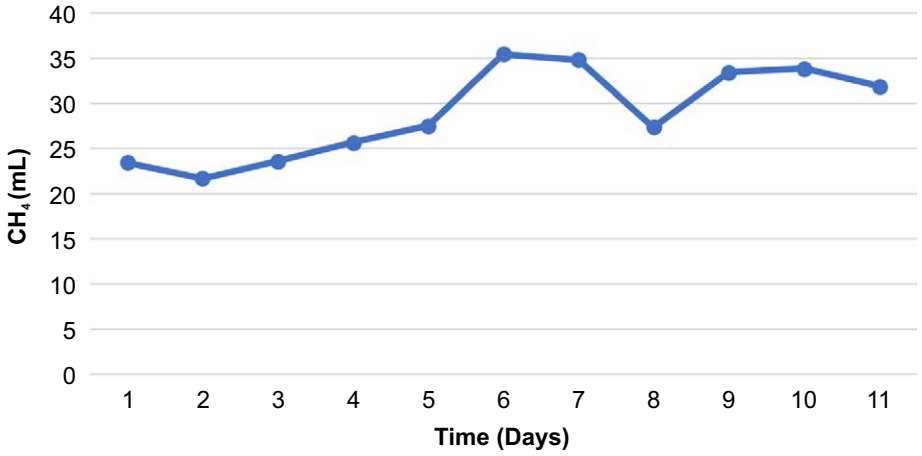

Figure 3. Biomethane accumulated production.

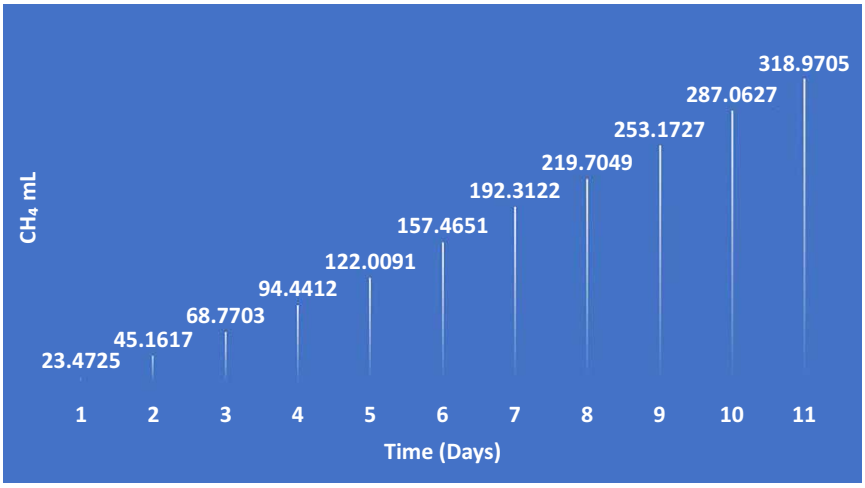

was higher than nighttime production, with production almost doubling after the 6th day due to the incidence of light and temperature, which increases the activity of anaerobic microorganisms. The cataloged production of 91 mL of CH_4 per liter is limited to the sampling period of the work, 11 days, the non-use of inoculums, and a more simplified biodigester methodology. Given the relative production cataloged, these decisions make the process very cheap for large-scale production and make using biomass as an energy resource viable. However, for more elaborate processes with a more extended sampling period, the amount of CH_4 cataloged could be much more significant and obtained more efficiently over days.

References

1. Bley JR, C. Geração elétrica a partir do biogás com saneamento ambiental: a experiência da Itaipu Binacional. Simpósio Internacional sobre Gerenciamento de Resíduos de Animais 2009;1:56-62.
2. Neto EDD. et al. Implementação e avaliação de um biodigestor de produção descontínua. E-xacta 2010;3(2).
3. Soares IAF. A Biodigestão Anaeróbica Com Uso da Manipueira: Alternativa Energética e Sustentável em uma Farinheira no Município de Cianorte-PR. Trabalho de conclusão de curso de graduação em Bacharel em Engenharia Ambiental, Universidade Tecnológica Federal do Paraná (UTFPR), Orientadora: Prof.ª Dr.ª Maria Cristina Rodrigues Halmeman. Campo Mourão, 2022.
4. Guimarães A et al. Electricity generation from biogas of cassava using cattle manure as inoculum: An assessment of potential in the quilombola community (Brazil).

International Journal of Advanced Engineering Research and Science 2019;6:200-205.
5. Kunz A, Steinmetz RLR, Amaral AC. Fundamentos da digestão anaeróbia, purificação do biogás, uso e tratamento do digestato: 2ª Edição. Sociedade Brasileira para o Progresso da Ciência (Sbera): Embrapa Suínos e Aves. Concórdia-SC, 2022.
6. Alves CT, Freitas L, Hocevar LS et al. Automatised bioreactor to produce biogas from biomass: development and evaluation. Journal of Bioengineering, Technologies and Health 2023;6(4):301-307. Available at: https://doi.org/10.34178/jbth.v6i4.325.
7. Nunes AN. Produção de hidrogênio a partir da manipueira em reator anaeróbio de leito fixo. Universidade Federal de Alagoas (UFA), Tese de mestrado em Recursos Hídricos, Orientador: Antônio Pedro de O. Netto. Maceió, 2015. Available at: https://www.repositorio.ufal.br/handle/riufal/5207.

Study of the Applicability of pH Mediators in Bioplastic Formulations for Use in Food Packaging

Camille Victória Carvalho[1*], Gabrielle Honorata Barbosa[1], Joaquim Dantas[1], Wendel Costa[1], Ingrid Lessa Leal[1], Paulo Romano[1], Tatiana Vale[1]

[1]SENAI CIMATEC University; Salvador, Bahia, Brazil

This work proposes the manufacture of bioplastics for food packaging using starch, carboxymethylcellulose, and green coconut waste (*Cocos nucifera*), with the addition of acid-base mediators to indicate the pH of the food. The method was based on experimental research, in which films were produced using the casting technique and incorporated mediators at a concentration of 1% (v/v). The results showed a high percentage of solubility, with an average of 95.09%, and low moisture content on a dry basis, with an average of 0.95%, and presented visually noticeable colorimetric changes in the pH ranges from 2 to 9. The research highlights the importance of using biodegradable materials and valorizing waste, which aligns with circular economy and sustainability practices.

Keywords: Bioplastics. Renewable Resources. Smart Packaging.

Economic development and urbanization are changing human behavior and the production of goods, leading the food industry to create packaging that guarantees the quality and safety of food on a large scale. However, the growing use of oil-based polymers has increased waste generation and damaged the environment, highlighting the need for better solid waste management strategies. In response, innovative packaging made of biodegradable polymers with pH indicators, such as corn starch, carboxymethylcellulose, and green coconut fiber, is emerging, improving food preservation by detecting spoilage and reducing the environmental impacts of conventional plastics.

Packaging production has been fundamental to the development of commerce and urban growth since human sedentarization, which led to the creation of artifacts to preserve and store food. With the First Industrial Revolution, there was an increase in industry and innovation in packaging to maintain product quality, using advanced materials and technologies [1]. According to ABRE (Brazilian Packaging Association), in partnership with FGV [2], in 2022, the gross value of packaging production in Brazil was R$123.2 billion, an increase of 3.9% compared to 2021. The food and packaging sector constantly evolves to reduce losses, reuse by-products, and increase food safety. Scarce resources and rising food costs drive demand for sustainable packaging that ensures product quality and safety.

Economic development, population growth, urbanization, and the technological revolution have changed consumption and production patterns, significantly increasing solid waste from various sources [3]. Excessive consumption and improper disposal of packaging saturate landfills and dumps, hinder waste degradation, cause environmental pollution, and favor the proliferation of diseases [4]. In Brazil, the National Solid Waste Policy (PNRS), established by Law No. 12.305/2010 [5], is crucial for managing this waste, promoting shared responsibility, and encouraging sustainable practices to meet ecological and social challenges.

Biodegradable Polymers

Polymers are macromolecules with a chemical structure and covalent intra- and intermolecular interactions. They can be derived from organic and inorganic matter, being highly malleable and moldable through heat and pressure to manufacture various products. Biodegradable

Received on 26 September 2024; revised 17 December 2024.
Address for correspondence: Camille Victória Carvalho. SENAI CIMATEC University. Avenida Orlando Gomes, 1845. Zipcode: 41650-010. Salvador, Bahia, Brazil. E-mail: camille.carvalho@ba.estudante.senai.br.

J Bioeng. Tech. Health 2025;8(1):32-41

polymers, as defined by ISO 1472:1998 [6], are films that undergo significant changes in their chemical structure under specific environmental conditions due to the action of microorganisms and are a sustainable and viable alternative to replace conventional plastics in production.

The size of the global bioplastics market is expected to grow from around 1.78 million tonnes in 2023 to 3.95 million tonnes by 2028, with a CAGR of 17.25% during the forecast period [7], presenting itself as a field in development, making it an area of great potential for studies to make its use viable. The application of polymer materials of natural origins, such as starch and cellulose derivatives, can generate continuous, naturally abundant, renewable, non-toxic, and biodegradable matrices, demonstrating thermoplastic behavior, presenting advantages over conventional plastics in terms of cost and functionality, reducing energy consumption, and making manufacturing cheaper [8], characteristics of industrial interest.

Starch is a plant polysaccharide characterized by semi-crystalline granules of different sizes and shapes. In recent years, corn starch has been the predominant raw material for producing biodegradable polymers as it is one of the primary sources of starch produced worldwide - approximately 64% [9]. Among the advantages of using biodegradable packaging made from starch are the following characteristics: transparency, barrier against oxygen and carbon dioxide, biodegradability, and compatibility with most materials during production.

Carboxymethyl cellulose (CMC) is an anionic biopolymer derived from cellulose, obtained by the alkaline reaction and etherification of cellulose with alkali and monochloroacetic acid successively. It is widely used in the food and pharmaceutical industries because it is biodegradable, soluble in cold or hot water, and transparent when in solution [10]. Its excellent properties, such as high water content, biocompatibility, and permeability, make it promising for the production of food packaging. Brazil is one of the largest global producers of green coconuts. Still, large-scale consumption generates up to 70% of the waste in coastal urban areas, mainly due to the fruit'sfruit's fibrous husks, which are bulky and heavy, making it challenging to manage municipal solid waste and negatively impacting the helpful life of landfills due to their slow decomposition. This waste is rich in lignin, hemicellulose, and cellulose and is used in various applications due to its strength and durability, similar to natural wood. Green coconut fiber has potential as a raw material for biodegradable bioplastics, offering a sustainable alternative for managing solid urban organic waste [11].

Smart Packaging

According to ABRE (Brazilian Packaging Association), the packaging is designed to store products in a way that prolongs their durability, protects them, and facilitates their distribution and consumption. In the case of food packaging, it preserves food against environmental factors such as light, humidity, gases, and microorganisms, keeping it unchanged during transportation and storage [12]. Oxidation by microorganisms reduces the shelf life of food, affecting taste and nutritional quality and generating toxic compounds [13].

The WHO [14] points out that millions of people fall ill and die every year from water- and food-borne diseases, underlining the importance of effective systems for handling and sanitizing packaging. Interest in intelligent packaging, such as biodegradable films with pH indicators, is growing to monitor food quality and safety [15]. Controlling the growth factors of microorganisms is essential in the production, transport, storage, and marketing of perishable foods to maintain the quality of these products [16].

Indicators are devices capable of transmitting information to consumers about food quality, considering the development of microorganisms [17].Real-time monitoring of specific characteristics, such as the absence or presence of biological or chemical compounds, can be carried out through, for example, visible colorimetric change using acid-base indicators

such as anthocyanin, bromothymol blue, or phenolphthalein. This simple technique quickly detects signs of food deterioration through pH change.

Materials and Methods

The study adopted an experimental qualitative-quantitative approach, starting with bibliographical research and preliminary topic analysis. Data collection was based on relevant scientific articles, including studies by Sugimoto (2000) [18], Leow and colleagues (2022) [19], Vedove (2019) [20], and Guglielmi and colleagues (2008) [21].

The following materials will be used in this work: corn starch, Carboxymethylcellulose - CMC, green coconut fibers (obtained from establishments in Salvador and São Sebastião do Passé - BA - used as a matrix for bioplastic formulations – separate as Sample A and B, respectively), distilled water, Glycerin P.A, citric acid, bicarbonate, Petri dishes, anthocyanin (extracted from red cabbage), phenolphthalein (from ACS Científica) and bromothymol blue (from Êxodo Científica) - used as pH indicators in an experiment in the Biotechnology Laboratory at SENAI CIMATEC. To obtain the bioplastic formulations, the solutions were obtained by the casting method (Tables 1 and 2), spread on glass plates, and left to dry at room temperature for 72 hours.

The CMC film solutions were prepared by heating and stirring the polymer containing water and glycerol as plasticizing agents. The films were obtained by casting, spread on glass plates, and left to dry at room temperature for 72 hours.

To obtain the bioplastic formulations from green coconut fiber, formulations from the Sugimoto patent (2000) [18] were adapted by processing the mesocarp of the green coconut (Table 3).

As materials used, the green coconut (Coccus Nucifera L) was obtained from establishments after use for manual separation of the Exocarp, Mesocarp, and Endocarp of the green coconut, separately stored and preserved in refrigerators at 4º C, avoiding the proliferation of microorganisms. The green coconut mesocarp was washed with distilled water and subjected to acid hydrolysis

Table 1. Bioplastic formulations from cornstarch by casting method.

Formulations	Components
F1	Starch; Water; Glycerol; Sodium hydroxide; Hydrochloric acid.
F2	Starch; Water.
F3	Starch; Water; Glycerol.
F4	Starch (4%); Water; Glycerol; Sodium Bicarbonate.
F5	Starch (5%); Water; Glycerol; Sodium Bicarbonate.
F6	Starch; Glycerol; Citric Acid.

Table 2. Bioplastic formulations from carboxymethyl cellulose by casting method.

Formulations	Components
F1	CMC; Water.
F2	CMC; Water; Glycerol.
F3	CMC; Water; Starch; Glycerol.
F4	CMC; Water; Glycerol; Sodium Bicarbonate.
F5	CMC; Starch; Water; Citric Acid.

Table 3. Bioplastic formulations from coconut fiber by casting method.

Formulations	Components
F1	Coconut fiber; Water; Carboxylic Acid; Starch.
F2	Coconut fiber; Water; Glycerol; Carboxylic Acid.
F3	Coconut fiber; Water; CMC.
F4	Coconut fiber; Water; Glycerol; Starch; CMC.

for 4 to 8 hours in a 6% (m/v) NaOH solution to delignify and remove impurities. After soaking, the suspended fibers were washed with distilled water until they reached a neutral pH and dried in an oven at 100ºC for 24 hours to lighten and reduce humidity. The fibers were then ground and sieved to obtain powdered fibers.

Hemicellulose quantification was performed on green coconut fiber mesocarp samples adapted from the patent from Leow and colleagues (2022) [19]. The process involved weighing 1g of dried green coconut fiber mesocarp and adding it to a 0.5 M NaOH solution in a Shaker Incubator for 4 hours at 500 rpm. After cooling to room temperature, the sample was vacuum-filtered and washed with distilled water until it reached a neutral pH. The remaining residue was dried in an oven at 100°C until the following day. The difference between the initial weight and the weight of the dried residue determined the hemicellulose content of the sample. Lignin quantification was performed on green coconut fiber mesocarp samples adapted from the patent from Leow and colleagues (2022) [19]. To do this, 1g of dried green coconut fiber mesocarp was added to a solution of 8 ml of 72% sulfuric acid and 7 ml of distilled water in a Shaker Incubator for 4 hours at 500 rpm. After cooling to room temperature, the sample was vacuum-filtered and washed with distilled water until it reached neutral pH. The remaining residue was dried at 100°C until the following day, and the weight of the dried residue was used to determine the lignin content of the sample.

The selected biofilms were prepared and dried for 72 hours at room temperature for the solubility test. After drying, the films were placed in Erlenmeyer flasks containing 50 mL of distilled water, then placed in a shaker with 80 rpm agitation at 25°C for 24 hours. After that, they were dried in an oven at 70°C for 24 hours to determine the final mass. The films were weighed before and after to obtain the initial and final mass. The solubility was calculated using Equation 1.

$$S = \frac{Wi - Wf}{Wi} \times 100 \quad (1)$$

Moisture content, on a dry basis, was determined according to AOAC method 930.04 [22] is determined by quantifying the mass before and after being dried in an oven at 105° C for 24 hours. The moisture content is obtained by calculation using Equation 2.

$$M = \frac{Wi - Wf}{Wi} \quad (2)$$

The mechanical tests were carried out using the EMIC Universal Shear and Tensile Testing Machine for adhesives (ASTM), provided by the Microscopy Laboratory at SENAI CIMATEC. Four specimens, F1 (CMC), F3 (CMC), F3 (coconut fiber), and F4 (coconut fiber), with an area of 5.5 mm2, were used.

For the pH colorimetric transition test, formulations were prepared in triplicate for each bioplastic sample using the indicators Anthocyanin, Phenolphthalein, and Bromothymol Blue at a concentration of 1% (v/v). These formulations were developed during the production of the bioplastics at room temperature. After formulation, the samples were placed in glass Petri dishes in a controlled environment for drying, without constant lighting and with air circulation. After

drying, the colorimetric transition test was carried out by adding 2 mL of buffer solutions (from ACS Científica) with pH 2, 7, and 9 at a concentration of 1 M. This procedure allowed visible color changes to be observed as the acidic, neutral and basic substances were added to the samples.

Results and Discussion

The study of bioplastic formulations with corn starch and CMC revealed that citric acid caused changes to the surface, making film formation incompatible. In contrast, sodium bicarbonate gave the formulations more elasticity and moisture, making them biocureatives. After drying, only two formulations containing starch showed positive results (F4 and F5) with smooth and adherent surfaces. The formulations with CMC (F1, F2, F3, and F4) exhibited the appearance of conventional plastics and desirable characteristics such as transparency, resistance, lightness, and malleability. The formulations with green coconut fiber (F3 and F4) were also successful, showing resistance and rigidity despite the lack of transparency (Figure 1).

The results of the extraction of samples revealed the removal of soluble lignin-cellulose components, resulting in a reduction in the total mass of the samples (Tables 4 and 5). Previous studies have indicated variations in the lignin and cellulose content of different green coconut cultivars, ranging from 37.2 ± 0.8%to 43.9±0.7% and from 31.5±0.1% to 37.4±0.5% for the lignin and cellulose content, respectively [23]. The concentration of hemicellulose and lignin in the residual samples was evaluated in comparison with non-residual green coconut fibers, showing that waste in the manufacture of composites remains within the natural values of the original raw material.

The results of the mechanical tests were analyzed based on the Stress at Maximum Breaking Strength, Specific Deformation at Breaking, and Modulus of Elasticity, shown in Figures 2, 3, and 4, respectively. Two used 2 samples each of the formulations that exhibited the appearance of conventional plastic, with the main characteristics desired for the experiment: resistance, lightness, and malleability, observed in the samples F1 (CMC), F3 (CMC), F3 (coconut fiber) and F4 (coconut fiber) – described the formulations in the Tables 2 and 3 – showed greater rigidity, indicated by the higher values of Modulus of Elasticity and lower elastic deformation under tension.

Figure 1. Developed formulations with desirable characteristics.

Table 4. Hemicellulose quantification.

	Starting weight (g)	Final Weight (g)	Hemicellulose Content (g)	Hemicellulose Percent (%)
Sample A	1,1855	0.8506	0.2979	29.79
Sample B	1,0678	0.6846	0.2999	29.99

Table 5. Lignin quantification.

	Starting weight (g)	Final Weight (g)	Lignin Percent (%)
Sample A	1,0683	0.3349	33.49
Sample B	1,0201	0.3842	38.42

Previous studies have highlighted the superior mechanical strength of formulations with CMC and water due to the specimens' smaller grain size and more excellent compaction [21]. However, due to the limited number of samples and the lack of structural uniformity, discrepancies were observed in the results, suggesting the need for more samples and more excellent uniformity for future studies.

The moisture and solubility results for the films with satisfactory visual results made with starch, CMC, and coconut fiber powder are indicated in percent as 0,95% and 95,09%, respectively Table 6). The presence of plasticizers, such as glycerol, contributes to an increase in the amorphous regions of bioplastics, making them easier to permeate with water. Due to the high solubility of CMC in water, it was possible to observe that the

Figure 2. Maximum strength tests.

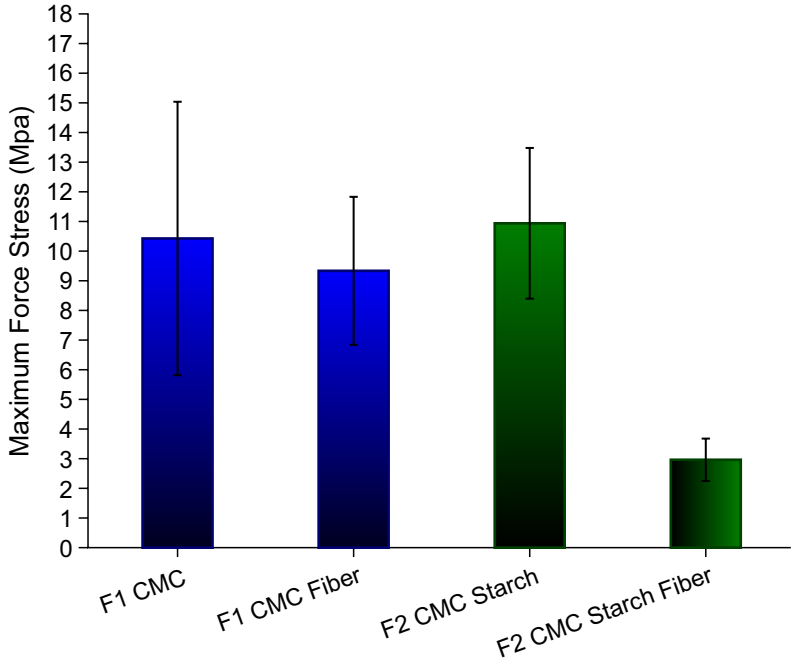

Figure 3. Modulus of elasticity testing.

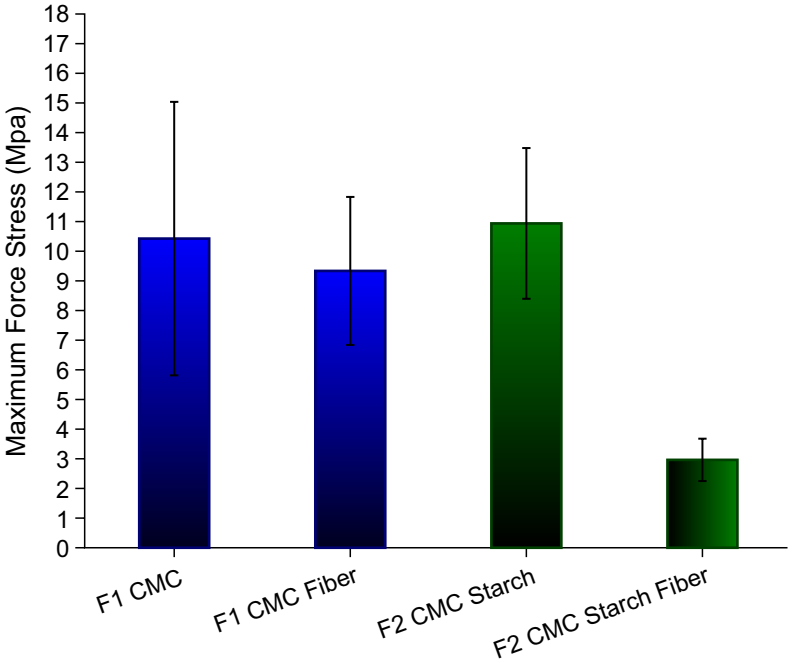

Figure 4. Tests for specific deformation at the break.

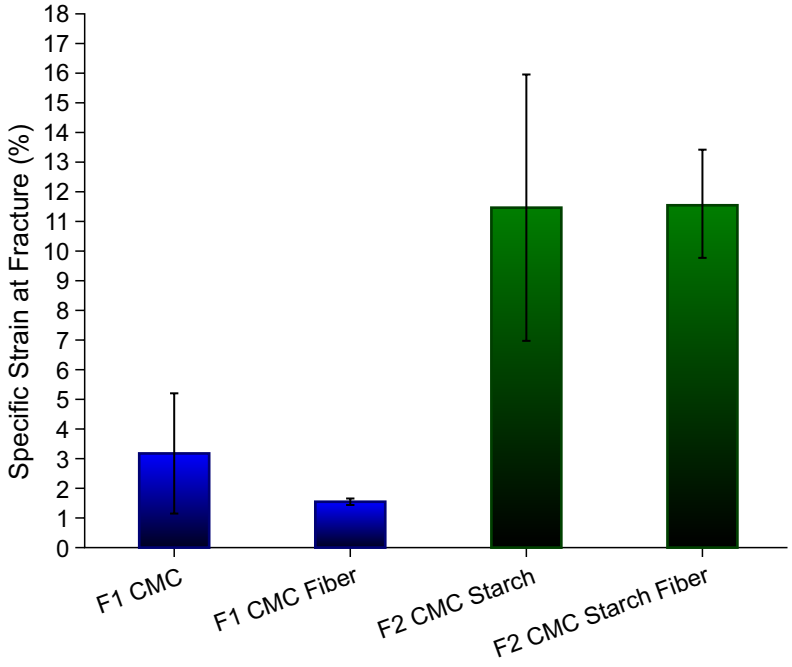

Table 6. Moisture Content on a dry basis.

Samples	Moisture Content (%)
Sample 1 (F4 Starch)	0.9748
Sample 2 (F5 Starch)	0.9756
Sample 3 (F1 CMC)	0.9714
Sample 4 (F2 CMC)	0.8902
Sample 5 (F3 CMC)	0.9022
Sample 6 (F4 CMC)	0.9470
Sample 7 (F3 Coconut fiber)	0.9784
Sample 8 (F4 Coconut fiber)	0.9492

formulations containing the natural polymer had high solubility content values and low moisture content on a dry basis (Table 7).

The study analyzed the ability of formulations that met the research criteria to change color, using triplicates and incorporating pH indicators (bromothymol blue, anthocyanin, and phenolphthalein). Most of the samples showed consistent test results, especially the formulations with bromothymol blue and phenolphthalein, which responded satisfactorily to acid, neutral, and basic pH variations (2, 7, and 9) (Figure 5). Although cellulolytic fungi contaminated some plates (Figure 6), the acid-base indicators effectively detected pH changes in contaminated areas, demonstrating their potential as microbiological markers.

Conclusion

The study used principal component analysis to evaluate films composed of starch and CMC, highlighting higher solubility and lower moisture on a dry basis. Adding green coconut fiber waste increased the strength, reduced the films' flexibility, and decreased the solubility compared to other samples. This waste was combined with natural bioactive compounds to produce biodegradable composites with low toxicity, contributing to the management of organic urban waste. Glycerol improved film formation as a plasticizer, making it an economically viable by-product for producing new products. Colorimetric analysis revealed that the films with phenolphthalein and bromothymol blue effectively detected pH variations, indicating potential for intelligent packaging and as

Table 7. Determination of solubility content.

Samples	Solubility Content (%)
Sample 1 (F4 Starch)	98.4250
Sample 2 (F5 Starch)	94.8920
Sample 3 (F1 CMC)	94.9713
Sample 4 (F2 CMC)	95.4002
Sample 5 (F3 CMC)	95.0424
Sample 6 (F4 CMC)	95.6640
Sample 7 (F3 Coconut fiber)	93.8670
Sample 8 (F4 Coconut fiber)	92.4661

Figure 5. Developed formulations with pH indicators.

Figure 6. Formulations 1 and 3 (CMC) were contaminated with unknown microorganisms with phenolphthalein and bromothymol blue indicators, respectively.

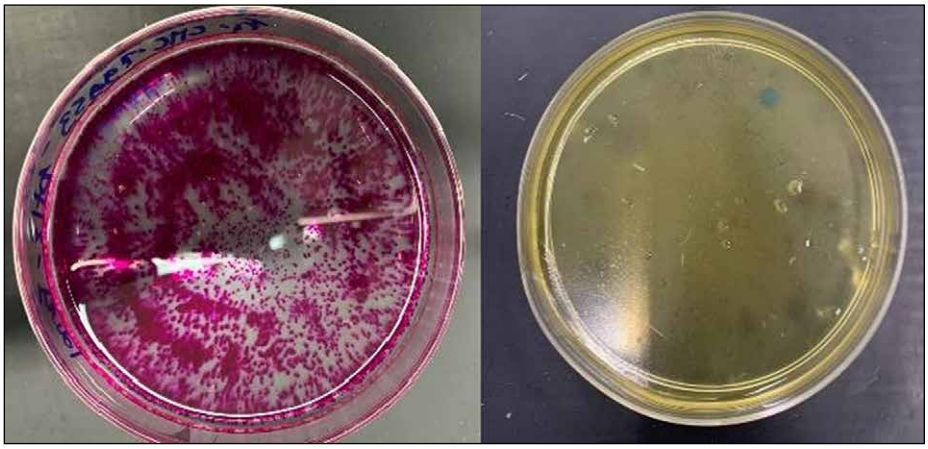

microbiological markers to monitor contamination during product storage and distribution. These results contribute to the development of new materials using advanced production techniques.

Acknowledgments

We want to thank everyone who has supported us throughout these years of effort, especially our family and friends. We also thank SENAI CIMATEC and its staff, mainly our advisor, Tatiana Vale, who enabled us to complete this work through her teachings, dedication, and patience.

References

1. Vedove TMARD. Thermoplastic starch with potential indicator of pH change for food packaging. [s.l: s.n.]. Available at: https://teses.usp.br/teses/disponiveis/33137/tde-21102019145359/publico/ThaisMariaAimolaRoncaDaleVedoveCorr19.pdf>.
2. FGV. Development of new regulatory dynamics for brazilian food packaging legislation based on the european international model: legal viability in the domestic regulatory system, characterisation and application in concrete situations filling gaps in anvisa'sanvisa's collegiate board resolution (rdc) 326/2019 based on commission regulation. [s.l.: s.n.]. Available at:<https://direitosp.fgv.br/sites/default/files/arquivos/127.pdf>.

3. Gouveia N. Urban solid waste: socio-environmental impacts and perspective of sustainable management with social inclusion. Science & Public Health, 2012;179(6):1503-1510.
4. Loureiro SPA, Noletto R. The concept of intelligent packaging. Available at: < https://www.ital.agricultura.sp.gov.br/arquivos/cetea/informativo/v28n1/artigos/v2 81_article1.pdf.
5. Law No. 12.305. Augusto 2010. Available at:<https://www.planalto.gov.br/ccivil_03/_ato2007-2010/2010/lei/l12305.htm>.
6. For O. ISO 14972:1998. Available at: <https://www.iso.org/standard/26128.html>.
7 Mordor intelligence. Available at: <https://www.mordorintelligence.com/industry-reports/plastic-packaging-market>.
8. Piatti T, Augusto R, Rodrigues F. Series: Talking about Sciences in Alagoas Plastics: characteristics, uses, production and environmental impacts.Available at:<https://usinaciencia.ufal.br/multimidia/livros-digitais-cadernos- tematicos/Plasticos_caracteristicas_usos_producao_e_impactos_ambientais.pdf>.
9. Luchese CL. Development of biodegradable packaging from starch containing by-products from food processing.Availableat:http://hdl.handle.net/10183/178251.
10. Zhong L et al. Construction of strong and tough carboxymethylcellulose- based oriented hydrogels by phase separation. International Journal of Biological Macromolecules. 2023;225:79–89.
11. Silva ECD et al.Use and energy potential of green coconut biomass. Magazine of Cases and Consulting 2018;9(3):e933–e933.
12. Landim APM et al. Sustainability regarding food packaging in Brazil. Polymers 2016;26:82–92.
13. Vermeiren L et al. Developments in the active packaging of foods. Trends in Food Science & Technology 1999;10(3):77–86.
14. Food safety is everyone'severyone's responsibility - PAHO/WHO | Pan American Health Organization. Available at: <https://www.paho.org/pt/noticias/6-6-2019-seguranca-dos-alimentos-e-consciente-todos>.
15. Soares NFF, Strigheta PC, Teixeira SC. Development of intelligent packaging with colorimetric change incorporated with anthocyanins: a critical review. Brazilian Journal of Food Technology 2021;24.
16. Nuin M et al. Modelling spoilage of fresh turbot and evaluation of a time– temperature integrator (TTI) label under fluctuating temperature. International Journal of Food Microbiology 127:193-199.
17. Assis OBG, Britto D. Review: protective edible coatings in fruits: fundamentals and applications. Brazilian Journal of Food Technology 2014;17(2): 87-97.Available at: https://www.scielo.br/j/bjft/a/PSw3gjR3H8Q3Z7DDV5vNPcL/?format=pdf&lang=pt.
18. Sugimoto I. Biodegradable Plastic Product Made From Coconut Husk Fiber powder Mixture. Patent Number: 6.083.621. United States Patent. Jul.4, 2000.
19. Leow Y et al. A tough, biodegradable and water-resistant plastic alternative from coconut husk. Composites Part B: Engineering 2022;241:110031.
20. Vedove TMARD. Thermoplastics starch with potential pH change indicator for food packing. Dissertation (Master's Degree) – Escola Politécnica, University of São Paulo, São Paulo, Brazil, 2019, 147 p. Available at: https://teses.usp.br/teses/disponiveis/3/3137/tde-21102019145359/publico/ThaisMariaAimolaRoncaDaleVedoveCorr19.pdf.
21. Guglielmi D, Neves WF, Das BA.Characterization of Commercial Carboxymethylcellulose. Cerâmica Industrial 2008;13(5).
22. AOAC. Official Methods of Analysis of the AOAC. In: Helrich, K.C., Ed., Official Methods of Analysis of the AOAC, Association of Official Analytical Chemists Inc., Arlington, 1298., 1990.
23. Corradini E, Medeiros ES, Carvalho AJF et al. Mechanical and morphological characterization of starch/zein blends plasticized with glycerol. Journal of Applied Polymer Science, New York, 2006;101(6): 4133-4139.

Carbon Credit Market: A Comparative Analysis of Consolidation in Brazil and the World

Natália Fernanda Santos Silva[1]*, Victor Menezes Vieira[1]
[1]SENAI CIMATEC University; Salvador, Bahia, Brazil

The carbon credit market has established itself as an essential mechanism for mitigating climate change. Its relevance is evidenced by the persistent growth in annual project submissions, reflecting global engagement in sustainable initiatives. This article aims to analyze the number of submissions of carbon credit projects in Brazil over the years and the performance of other countries, seeking to identify submissions and stratify them according to the type of market, the most active certification companies, the type of project, and the Brazilian regions most active in these initiatives. The methodology used was document analysis and bibliographical research through certification databases and studies that dealt with the topic.
Keywords: Carbon Credits. Kyoto Protocol. Regulated Market. Voluntary Market. Environmental Sustainability.

The carbon credit market, which emerged as a direct response to the global challenge of climate change, represents one of the most innovative and promising tools in the fight against greenhouse gas (GHG) emissions. This market was conceived through the Kyoto Protocol, signed in 1997, which established flexible mechanisms such as the Clean Development Mechanism (CDM) to encourage global emissions reduction through sustainable development initiatives. Companies and governments from different nations are increasingly involved in the creation and trading of carbon credits, either through regulated markets, such as the European Union Emissions Trading System (EU ETS), or through voluntary markets (Figure 1) [1].

The carbon credit market has gained significant relevance over the last two decades. Its main objective is to create an economic incentive to reduce GHG emissions, allowing companies and countries that reduce their emissions beyond established targets to sell excess credits on the voluntary market to those unable to achieve their reduction objectives. This system encourages initiatives to reduce greenhouse gas emissions and stimulates technological innovation, energy efficiency, and sustainability associated with economic activities. Since its creation, the carbon credits market has maintained constant growth, which can also be confirmed through the evolution of global revenues from taxes arising from the commercialization of carbon credits. Initially dominated by projects in developing countries, mainly in Asia and Latin America, it has expanded to include a variety of sectors such as renewable energy, reforestation, sustainable agriculture, and industrial efficiency (Figure 2) [2].

Globally, the carbon credit market is maturing. The implementation of the Paris Agreement in 2015 gave a new boost to this market, with more ambitious emissions reduction targets and greater private sector participation. Countries like China and the European Union are ahead of others in implementing robust emissions trading systems and establishing strict policies to reduce GHGs. The regulated carbon credits market in Brazil is currently in the process of being implemented following the enactment of bill (PL 182/2024) in the national Congress. This legislation involves the creation of the Brazilian Greenhouse Gas Emissions Trading System (SBCE), which holds great potential due to the country's vast forest coverage and rich biological diversity [1].

Despite advances, the carbon credit market has faced adversities such as the volatility of credit prices, the complexity of verification and certification mechanisms, and the need for transparency and environmental integrity. Furthermore, the

Received on 8 September 2024; revised 20 November 2024.
Address for correspondence: Natália Fernanda Santos Silva. SENAI CIMATEC University. Avenida Orlando Gomes, 1845. Zipcode: 41650-010. Salvador, Bahia, Brazil. E-mail: natalia.fernanda@fbter.org.br.

J Bioeng. Tech. Health 2025;8(1):42-49

Figure 1. Types of carbon credit mechanisms and market segments [2].

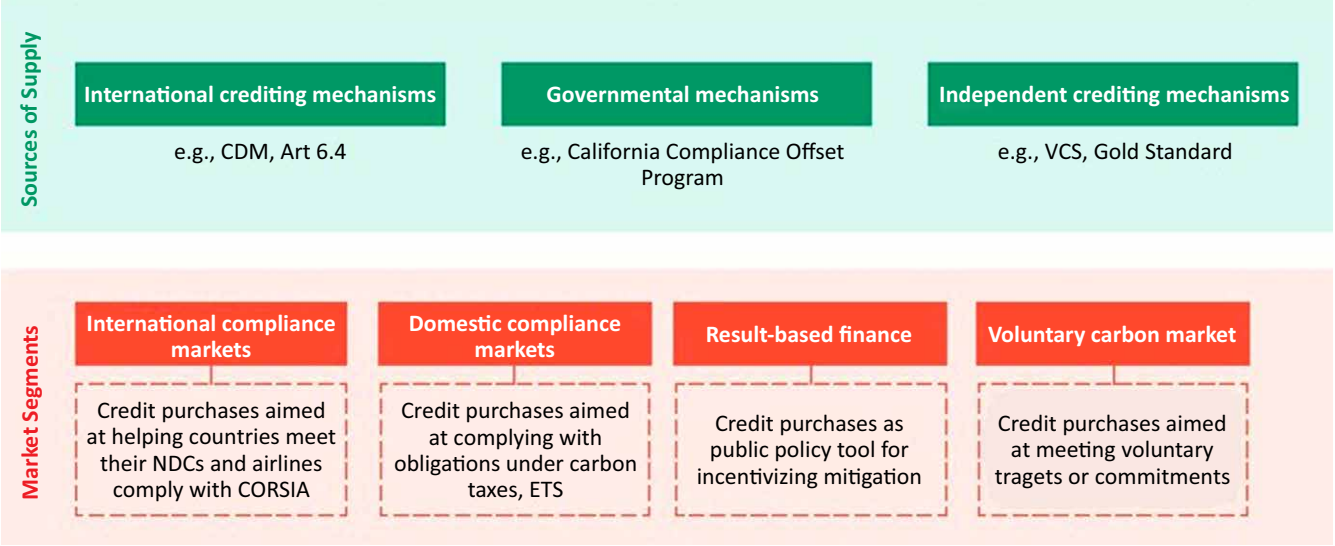

Figure 2. Evolution of global revenues obtained from the carbon credits market [2].

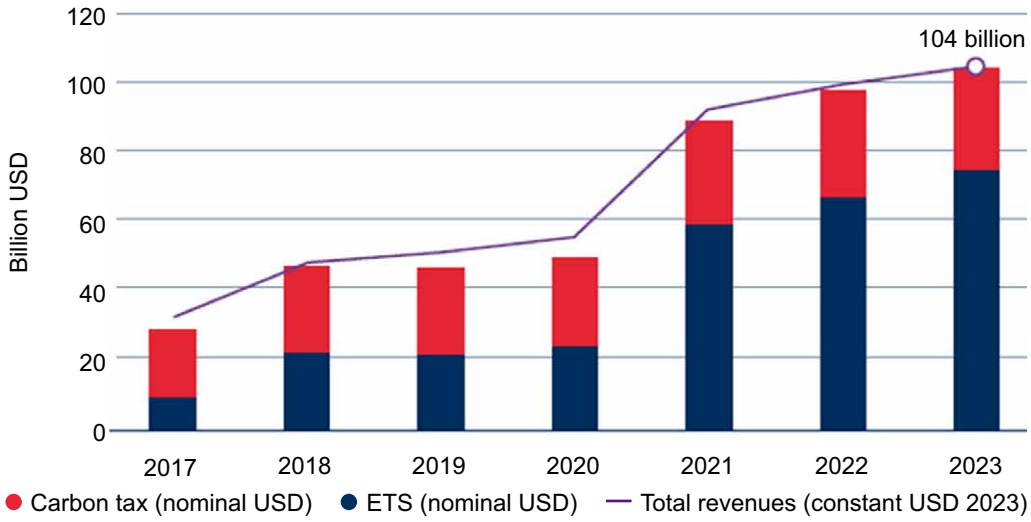

heterogeneity of regulations between countries and the lack of a unified global market complicates the negotiation and commercialization of credits. Forest restoration initiatives, biodiversity conservation, and clean energy projects are key areas that can boost the generation of credits and attract international investments in Brazil. In this way, the country can become a leader in the carbon credit market [3, 4].

The future of the carbon credit market looks promising, with a forecast of continued growth driven by stricter climate policies and increased environmental awareness. Therefore, this article aims to analyze the evolution of the global and Brazilian carbon credits markets based on data points illustrating market evolution, project categories, regional distributions, and sectors covered.

Materials and Methods

The method adopted followed a process of prospecting, selection, analysis, and documentary synthesis, which involved scientific publications, reports from organizations, and databases from carbon credit certifiers (Table 1).

Table 1. Scope of the literature review.

Scope of Bibliographic Review	
Analysis Period	The search covers recently released publications and reports, ensuring up-to-date and relevant data is included.
Data Sources	Reports from organizations such as the World Bank Group, Ecosystem Marketplace, and FGV, as well as information from carbon credit certifiers such as Verra, Gold Standard, and UNFCCC, were selected.
Inclusion Criteria	Reports that presented quantitative and qualitative data, trend analyses, and recommendations for public policies were included. Furthermore, the projects considered, extracted from the certification bodies' databases, were only those registered; they were not considered projects rejected or in the analysis process.
Data Extraction	Data was extracted from publicly available databases on these certifiers' platforms, including information on certified projects, the number of credits issued, methodologies used, and project locations.

Results and Discussion

The global carbon credit market has evolved in recent years, expanding to include initiatives such as the Paris Agreement, which sets more ambitious and comprehensive targets for reducing GHG emissions. Despite the variations over the years due to possible political and/or economic interference, it is still possible to observe a persistence in the evolution of the markets. It is possible to use Brazil as a reference since it is one of the countries that has grown in this area, is consistently positioned among the Top 10 countries with the most significant presence in the carbon credit markets, and is also affected by external influences that directly impact the annual volume of credits generated (Figure 3).

Comparing the volume of credits generated in the clean development mechanism (CDM) and the voluntary carbon market in Brazil is essential to understanding the contribution of each mechanism to the country's carbon economy. Figure 3 shows consistent growth in the voluntary market, with significant spikes in specific years that may be related to stricter environmental policies, demand for carbon credits, or the price of credits.

Considering the evident growth of the voluntary market, it is important to provide an example of where these carbon credits are being generated, as project records are categorized according to area of activity (Figure 4). The diverse categories, ranging from reforestation to carbon capture and storage technologies, indicate a broad and varied market. It is important to highlight the growth of the "domestic/community devices" category over the years, gaining greater prominence than the other categories in 2023. Another important point to be observed is the decline in the volume of projects in the renewable energy sector.

Globally, it is possible to see a big difference in the volume and value of carbon credits generated in different regions. Variations in the volume and prices of transactions within these classifications show that some regions are more active and valued in the carbon market, as shown by the information obtained in the report on the situation of the voluntary carbon market published in 2024, which in 2022 had Asia with a volume of 102.7 MtCO2 and sold per ton at 7.45 dollars and Europe with a volume of 0.61 MtCO2 and sold at 13.82 dollars. Regions with more excellent activity may receive more investment and technical support, while others may fall behind. This raises questions about public policies, access to opportunities in the carbon market, and trust in regional projects [3]. Different mechanisms can operate in the same

Figure 3. Volume of credits generated in Brazil's clean development mechanism (CDM) and voluntary carbon market from 2006 to 2021 [4].

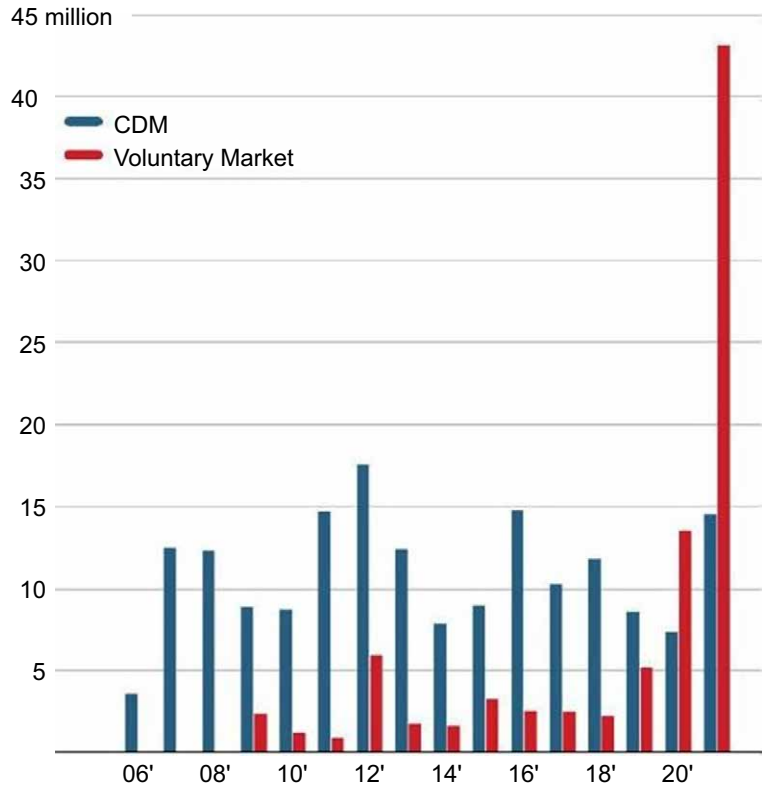

Figure 4. Register of carbon credit projects by category from 2019 to 2023 [3].

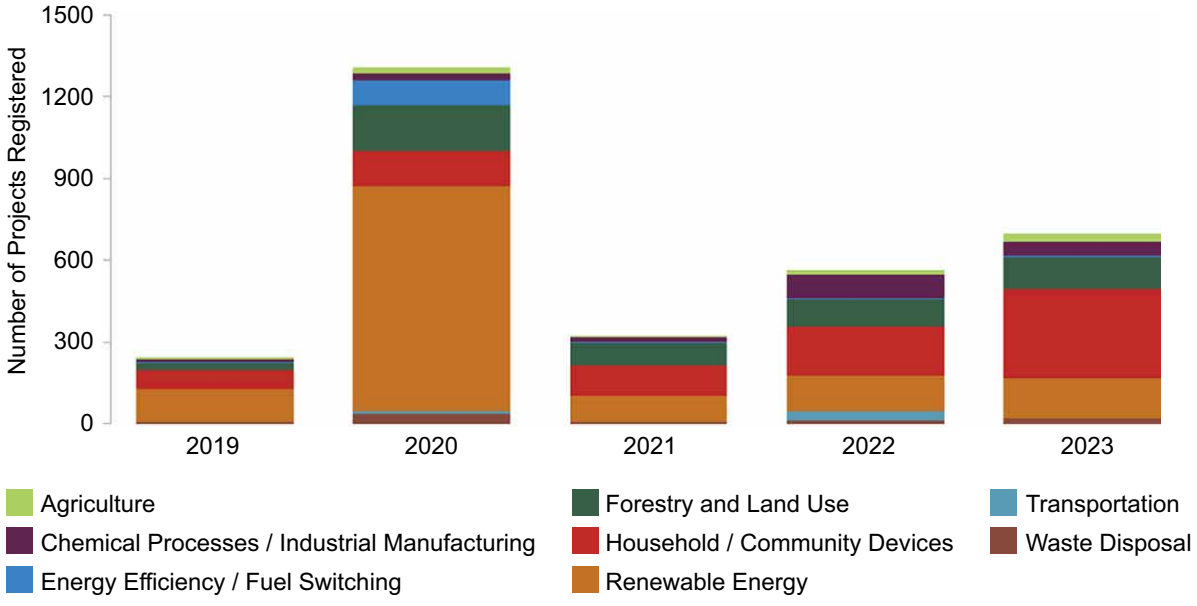

Note: Includes data on project registrations from ACR, CAR, CDM, City Forest Credits, Global Carbon Council, Gold Standard, Plan Vivo, and VCS registries.

region, but some are sometimes restricted to some regions because they are governmental mechanisms (Figure 5).

Figure 5 presents annual project registrations by type of credit mechanism, highlighting which mechanisms are most used and how preference for these mechanisms has evolved over the years. However, there may be mechanisms that, despite being less popular, are more effective or suitable for specific regions or sectors, such as the government mechanisms created to meet the needs of Thailand and Australia. These mechanisms have stood out, but in addition to other government mechanisms, they represent a significant portion. Due to their time of operation, reliability, and broad global presence, Gold Standard and Verra are mechanisms that play an important role in the voluntary carbon credits market and the United Nations Carbon Offset Platform (UNFCCC) in the global market through CDM projects. Based on this, seeking to understand the performance of these mechanisms in registered projects from Brazil and around the world, graphs were generated with the variation in the annual number of these projects submitted on the platforms (Figure 6).

Over the years, the variation in the number of projects registered on the UNFCCC, Gold Standard, and Verra platforms reveals a pattern of growth and decline possibly influenced by global events, initiatives, and government policies such as those listed in Table 2.

Conclusion

The carbon credits market, both globally and in Brazil, represents a strategic tool for tackling the global climate emergency. Despite the adversities, its prospects are positive, with the potential to promote environmental and economic sustainability on a global scale, as can be seen throughout the article given the data presented. It was found that the number of projects registered over the years can be closely linked to global events, government policies, and international initiatives. The initial growth of this market was driven by policies such as the Kyoto Protocol, the Clean Development Mechanism, and financial incentives. The decline after 2012 can be attributed to political uncertainty and the global economic crisis, while the stimulus for recovery can be

Figure 5. Comparison of annual project registrations by type of credit mechanism [2].

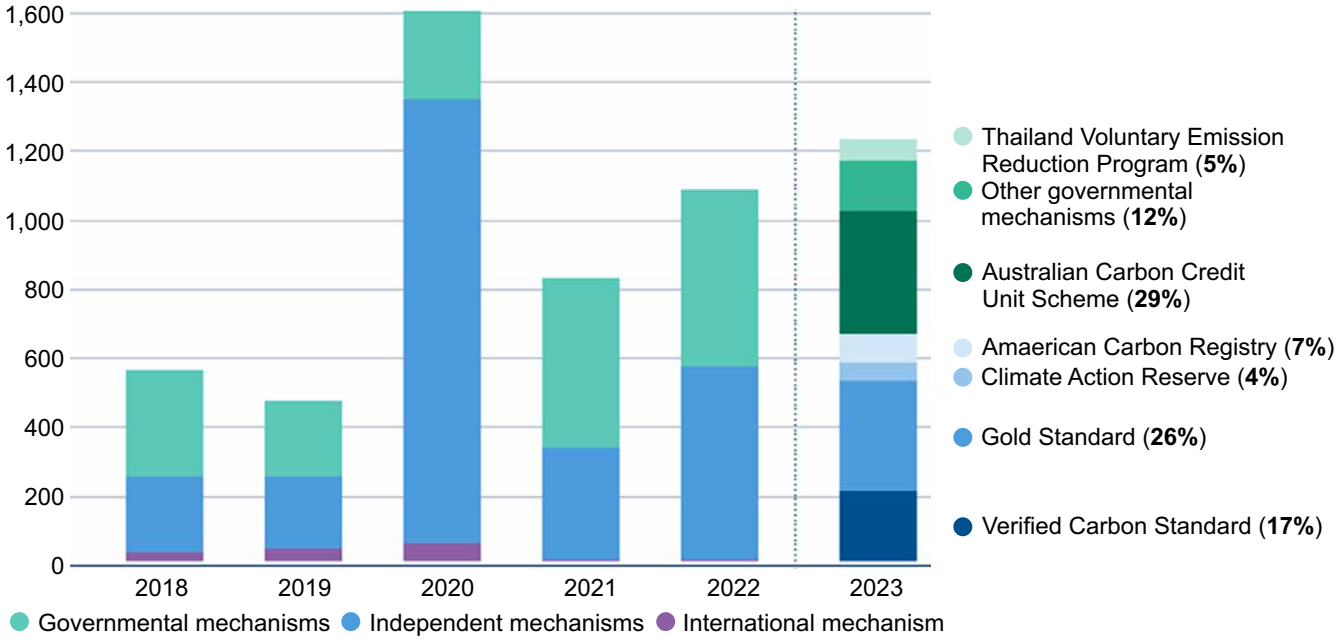

Figure 6. Comparison of the number of projects registered in Brazil and around the world in UNFCCC, b) Gold Standard, and c) Verra [5-7].

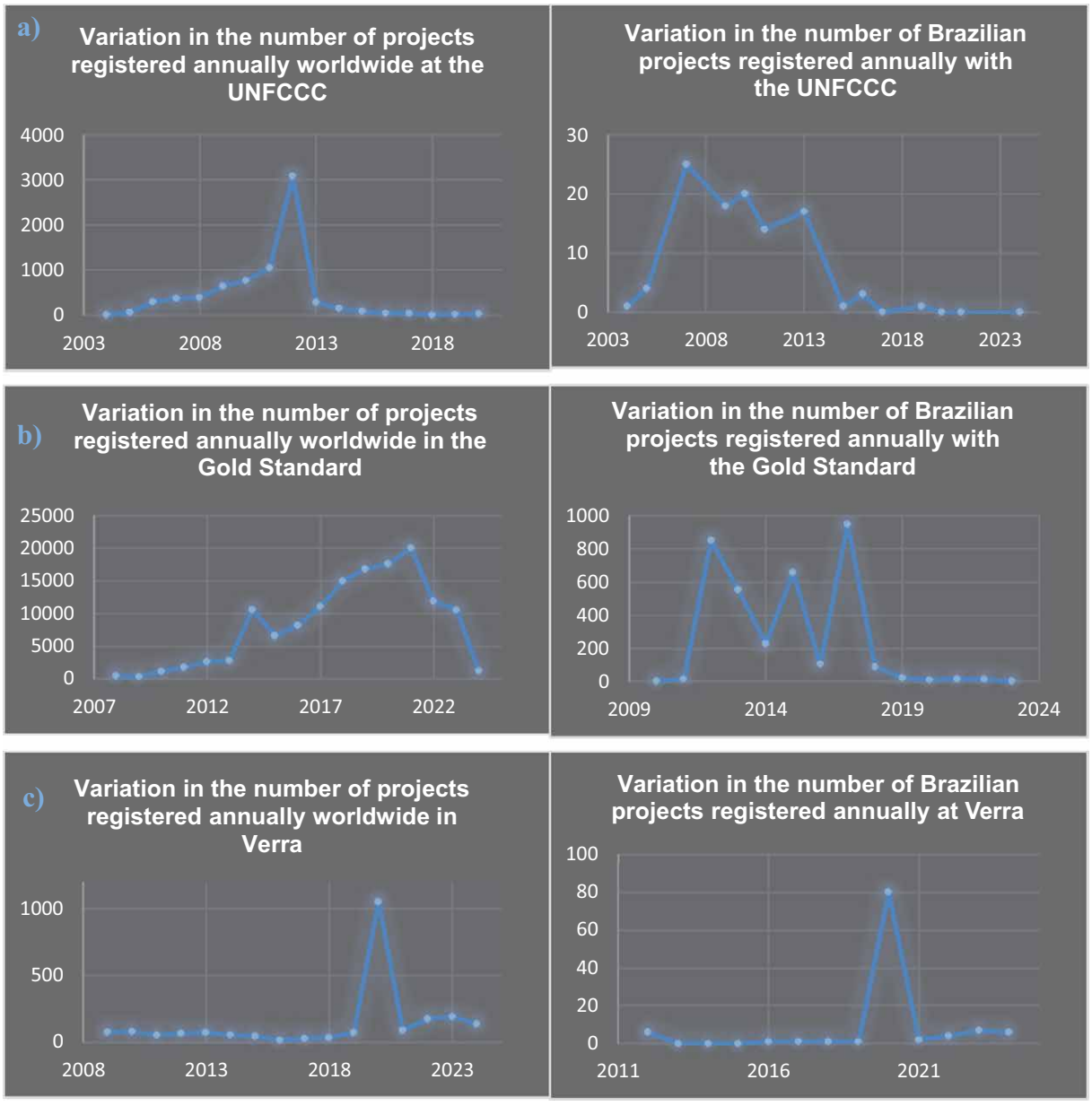

Table 2. List global events, initiatives, and government policies that may have affected the carbon credits market [1-7].

Global Events, Initiatives, and Government Policies	
Initial Growth (2005-2012)	**Global Policies and Initiatives**: The creation of the Kyoto Protocol (1997) and its implementation in 2005 encouraged many countries to register emission reduction projects. Several environmental policies and initiatives were implemented globally, stimulating significant growth in registrations until 2012. **Financial Incentives**: The CDM and other financial incentives, such as the carbon credit market, encouraged companies and countries to register projects that were particularly attractive in developing countries such as China, India, and Brazil.
Decline (2013-2014)	**End of the First Kyoto Protocol Period:** The first commitment period ended in 2012, leading to uncertainty about the future of climate policies and financing mechanisms. This uncertainty decreased project submissions as many countries waited for precise directions on new policies. **Global Economic Crisis:** The 2008 global economic crisis also delayed project registrations. The slow economic recovery in many countries limited investment in new environmental projects, contributing to declining submissions after 2012.
Recovery and New Peaks (2015-2021)	**Paris Agreement**: The signing of the Paris Agreement in 2015 revitalized global efforts to combat climate change, increasing project submissions on platforms such as Gold Standard and Verra. The Paris Agreement established clear targets and commitments to reduce emissions through Nationally Determined Contributions (NDC), encouraging new registrations. **National Initiatives**: countries launched national initiatives to meet their Paris Agreement goals, and from this, new mechanisms emerged, mainly governmental, which gained prominence, such as those created in Australia and Thailand. In Brazil, policies such as the National Plan on Climate Change and incentives for renewable energy and reforestation projects contributed to the increase in submissions.
Recent Decline (2022-2024)	**Changes in Policies and Funding Availability**: Changes in international funding policies and the completion of some support programs also contributed to the decrease in submissions. The transition to new post-Paris Agreement financial mechanisms is ongoing, causing uncertainty and a temporary reduction in registrations. Furthermore, the reduction in project financing was one of the late consequences of the COVID-19 pandemic, which can only be identified after the pandemic period as the bureaucratic procedures for project registration require a certain amount of time.

related to the Paris Agreement and national initiatives. The recent drop is likely linked to the consequences of the pandemic period, policy transitions, and the availability of financing.

Acknowledgments

The authors would like to acknowledge Shell Brazil and ANP (Agência Nacional do Petróleo, Gás Natural e Biocombustíveis) for the strategic support provided through regulatory incentives for Research, Development, and innovation. We also acknowledge EMBRAPII and Senai CIMATEC for the encouragement and funding.

References

1. United Nations Environment Program (2023). Emissions Gap Report 2023: Broken Record – Temperatures hit new highs, yet world fails to cut emissions (again). Available at: <https://wedocs.unep.org/20.500.11822/43922>.
2. World Bank. State and Trends of Carbon Pricing 2023. Available at: <http://hdl.handle.net/10986/39796>.
3. Ecosystem Marketplace. State of the Voluntary Carbon Markets 2024. Available at: <https://www.ecosystemmarketplace.com/publications/2024-state-of-the-voluntary-carbon-markets-sovcm/>.
4. Vargas DB, Delazeri LMM, Ferreira VHP. Voluntary carbon market in Brazil. Bioeconomy Observatory, FGV AGRO, 2022. Available at: <https://eesp.fgv.br/sites/eesp.fgv.br/files/ocbio_mercado_de_carbono_1.pdf>.
5. United Nations Framework Convention on Climate Change (UNFCCC). ActivitySearch. Available at: <https://cdm.unfccc.int/Projects/projsearch.html>.
6. Gold Standard. Impact Registry 2024. Available at: <https://registry.goldstandard.org/projects?q=&page=1>.
7 Verra. Verified Carbon Standard (VCS) 2024. Available at: <https://registry.verra.org/app/search/VCS/All%20Projects>.

Image-Based Underwater Liquid Leak Detection and Transfer Learning

Eric Oliveira[1*], João Paulo Barros[1], Misael Alves[1], Taniel S. Franklin[1]
[1]Department of Software, SENAI CIMATEC University;Salvador, Bahia, Brazil

This paper addresses the critical challenge of liquid leaks in the oil and gas industry by leveraging advanced computer vision and deep learning methodologies. The objective is to develop practical models for detecting underwater objects with low image quality in adverse conditions. We train and test CNN detectors using Facebook's Detectron2 Faster R-CNN. The model was evaluated on a custom dataset of underwater oil spill videos, focusing on detection accuracy and processing speed. The results demonstrated that even using images of smoke in the sky as training made it possible to detect the underwater oil leak accurately.
Keywords: Leak Detection. Deep Learning. Artificial Intelligence. Computer Vision.

The offshore oil and gas industry is one of the most profitable industries in the world. However, due to the nature of its deep subsea operations, these industries could face some issues, such as safety concerns and environmental impact. Such issues can directly impact enterprise profit and generate life risk. Machinery fluid and crude oil leakages are examples of issues that can affect the external environment and normal operation conditions. Several studies have tried to address the task of underwater leakage detection.

Most of them use acoustic sensors, fluorimeters, and vibration sensors to obtain the data post-processed by a machine or deep learning algorithm to extract and analyze patterns indicating the presence of leakages; these methods can be inaccurate and relatively expensive [1]. Underwater object detection is generally achieved by sonar, laser, and cameras. Compared to sonar and laser, the cameras are low-cost and can capture more visual information with high temporal and spatial resolution.

Our proposal in this work is to offer an accurate and cost-efficient solution for underwater leak detection using imaging and deep learning techniques. By incorporating the Faster Region-based CNN (Faster R-CNN) [2] models, we aim to enhance the identification capability of liquid leaks in key infrastructure components. Harsh underwater environments negatively impact methods that rely on edge information by reducing object detection accuracy. Convolutional neural networks (CNNs) dominate current object detection research to improve detection speed and accuracy. CNN-based methods can be divided into two main categories: Region Proposal-Based Frameworks(two-stage) and Regression/Classification-Based Frameworks(one-stage).

Object detection is one of the tasks of computer vision, where the goal is to recognize objects and locate them in an image. Deep learning models can recognize and extract information from images in challenging environments while simultaneously working with vast data.

Underwater object detection is generally achieved by sonar, laser, and cameras. Compared to sonar and laser, the cameras are low-cost and can capture more visual information with high temporal and spatial resolution. Underwater leak detection using deep learning is an active and rapidly evolving field of research, with some published studies on this topic, such as Bansod [3] that describe the use of thermal images to enhance leak identification by deep neural and Rehman [4] that address the topic of using sensor signals as input along with images to create an attention-based model.

Various studies have tried to solve the leakage detection task using object detectors. Going in the opposite direction, the paper written by Padovese

Received on 25 September 2024; August 18 November 2024.
Address for correspondence: Eric Oliveira. Avenida Orlando Gomes, 1845. Zipcode: 41650-010. Salvador, Bahia, Brazil. Zipcode: 40170-115. E-mail: eric.santoss@fbter.org.br.

J Bioeng. Tech. Health 2025;8(1):50-55

[5] uses a Passive Acoustic Monitoring (PAM) system for leakage detection on offshore CO_2 geological storages. It takes advantage of the signal disturbance caused by the emission of bubbles to classify the acoustic signal and detect gas leakage.

The main benefit of PAM use is the investment cost of sensor equipment and the extended range of the sensor. However, this system could not detect fluid leakage on offshore equipment located in the seabed. PAM sensors can be affected by other sources of signal (noise), which introduces complexity to the detection task. Beyond that, passive acoustic is mainly used in wildlife studies.

Traditional sensors face significant challenges in high-pressure environments, such as deep ocean ones. These sensors are not low-cost, and the detection complexity increases due to adverse conditions. Other works carried out research in leak detection underwater using deep learning based on pressure measurements, integration of surveillance thermal cameras, and sound and vibration sensors.

As a positive point, these techniques improve the data available for training deep learning models. From another perspective, using sensors can increase investment costs, in addition to the fact that these tools can be inaccurate and fail in specific scenarios of high pressure, such as deep water. The present study proposes an innovative solution based on deep learning and object detection using only underwater images, without the need for vibration, sound, or pressure sensors. This approach offers cost reduction and several advantages compared to related works. Using cameras and deep learning eliminates the need for expensive and sophisticated sensors, such as acoustic and pressure sensors, resulting in a significantly more economical solution. Deep learning models can quickly process large volumes of image data, enabling real-time or near-real-time leak detection, which is crucial for rapid interventions.

Materials and Methods

Next, we present deep-learning models utilized in our study, explain the training and test pipelines, and introduce an augmentation technique to overcome the lack of accurate data representing the underwater scenario with wildfire smoke.

Alternatively, images of wildfire smoke and crude oil leaking that share similar features to underwater leakage have become data to train the AI models. It is done because deep learning models require an extensive data set to achieve good results and generalization capabilities. Due to this lack of data, obtaining evaluation metrics with expressive results is a great challenge, especially in real scenarios.

The algorithms for object detection are based on supervised learning, which requires image samples with objects to be detected and their corresponding bounding boxes represented as labels. Similarly, the leak detection model needs videos or images of comparable liquid leaks in different scenarios for training. The wildfire smoke dataset, consisting of 737 images and annotations, was used to train the models. This dataset was selected because it contains properties and characteristics like liquid leaks. It becomes a quick and cheap solution to overcome the lack of liquid leak data under the sea. Figure 1 shows a frame extracted from the dataset.

After preparing the source data by applying a set of transformations, the total number of images has been split into 3 groups: training, validation, and test. The first two are used during the learning stage of the deep neural network; the training set provides the data distribution from where the model will learn, while the validation one is used to check how well the model evolves its training. Once the training stage is finished, the model weights learned during this phase are used to make inferences on the test set to verify the model performance. Its performance is measured using a mean Average Precision mAP metric based on three metrics: Intersection-over-Union (IoU), Recall, and Precision. The IoU role is to define if a predicted bounding box is a true positive or a false positive by defining a threshold. Boxes with IoU values that fall below that range are considered false, and the ones above are considered valid. Generally, the higher the IoU

Figure 1. Sample of wildfire smoke frame.

threshold, the more challenging the detection task. IoU is computed by dividing the area of overlap by the total union area, subsequently, with the computation of false positives, true positives, and false negatives. Recall and Precision are measured. These metrics measure how well the model is to predict accurate positive samples and how precise the model detections are, respectively. So, the computed value of those two metrics is used to plot the precision-recall curve from where the map will be calculated. Two proofs of concept (POC) were created where one used training only from the wildfire smoke dataset (Only smokesmoke) and another used (Transfer Learning) with the addition of underwater oil spill frames. Both POCs were evaluated on another set of underwater oil spill images (Figure 2).

Results and Discussion

The computer vision community created the mean average precision (mAP) metric to evaluate the efficiency of an object detection model and compare its performance against other models. A high Average Precision (AP) means the model has a low false negative rate and a low false positive rate. A false negative occurs when the model infers the object as a region that is part of the image's background. A false positive occurs when a background region is mistakenly identified as an object. The higher the map, the more accurate and with more excellent recall the model will be. Accuracy measures the proportion of correct samples predicted as positive (correct inference), that is, how often the model predicts correctly. Recall measures the proportion of positive samples obtained from the total existing samples, both samples that were correctly detected and those that were not detected. In other words, how many positive samples could the model find in the total number of existing predictions? In other words, the model predicted every time it should have predicted. The mAP combines precision and recall into a single metric. It measures how accurately the model identifies objects by comparing the predicted bounding boxes' Intersection over Union (IoU) with the ground truth bounding boxes. IoU values are calculated for a range of threshold values, from 0.5 to 0.95, with a step of 0.05. The Average Precision (AP) is then calculated from these IoU values, and the mAP value is the average AP value of all detected classes. A higher IoU value closer to 1 indicates better detection quality (Table 1).

In Figure 3, we present underwater leak detection results for different implementations of the POCs carried out on the same custom test dataset. In machine learning, specifically statistical

Figure 2. Sample of oil spill frame used in transfer learning model train.

Table 1. mAP values for the developed POCs.

Model	mAP 50	mAP 50-95
Transfer Learning	91.41	31.28
Only Smoke	13.09	2.89

Figure 3. Confusion matrix to compare prediction results.

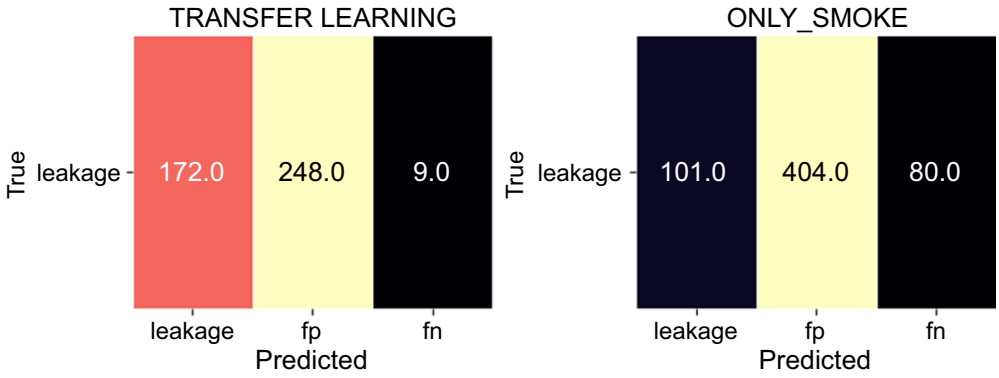

classification, a confusion matrix, also known as an error matrix, is a specific table layout that allows visualization of the performance of an algorithm, typically supervised learning. Each row of the matrix represents the instances in an actual class, while each column represents the instances in a predicted class, or vice versa. View the confusion matrices of the most promising POCs in Figure 3.

These results in Figure 4 suggest that the TRANSFER LEARNING model outperforms the ONLY SMOKE model in detecting oil leaks, mainly due to its high recall, indicating it captures most true leaks. TRANSFER LEARNING exhibits a higher precision (0.41) and a significantly higher recall (0.95) compared to ONLY SMOKE, resulting in a superior F1-Score (0.57 *vs.* 0.29). ONLY SMOKE

has a considerably low precision (0.20), indicating a high number of false positives and a moderate recall (0.56).

The precision-recall curve presented illustrates the performance comparison between two models, Transfer Learning and Only Smoke in detecting oil leaks. The Transfer Learning model demonstrates superior performance in terms of precision across various levels of recall compared to the Only Smoke model. Figure 5 compares the detections with the models in a specific frame. This shows the efficiency and precision in generating the bounding boxes, mainly for the model frame trained with transfer learning. View all inference results in the drive.

Conclusion

In this study, we introduced an approach to underwater liquid leak detection using image-based techniques and transfer learning. Our model significantly improved detection accuracy and

Figure 4. Precision *vs*. Recall curves.

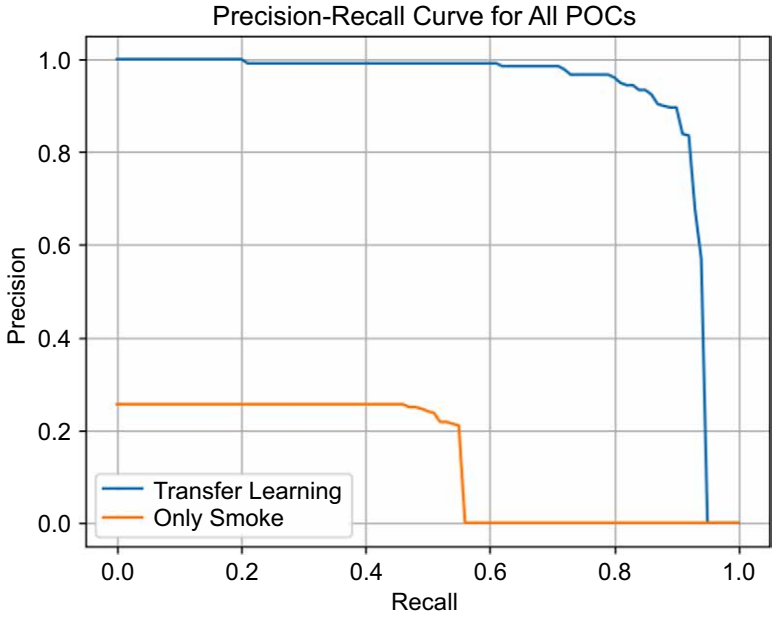

Figure 5. Detection for Transfer Learning model.

Figure 6. Detection for Only Smoke model.

processing speed by leveraging Faster R-CNN and training on a custom dataset of underwater oil spill videos and wildfire smoke images. The transfer learning model outperformed the single-source model, demonstrating superior precision and recall. This research highlights the potential of deep learning in providing cost-effective, efficient, and real-time leak detection solutions, offering a viable alternative to traditional, sensor-based methods. Future work should focus on refining models and expanding datasets for enhanced robustness.

Acknowledgments

This research was executed in partnership between SENAI CIMATEC and Shell Brasil. The authors would like to acknowledge Shell Brasil Petroleo LTDA, the Brazilian Company for Industrial Research and Innovation (EMBRAPII), and the Brazilian National Agency for Petroleum, Natural Gas and Biofuels (ANP) for the support and investments in RD&I.

References

1 Mysorewala M, Cheded L, Ali I. Leak detection using flow-induced vibrations in pressurized wall-mounted water. IEEE 2020;8.
2. Ren SJ. Faster R-CNN: Towards real-time object detection with region proposal networks. Advances in Neural Information Processing Systems 2018;28.
3. Kalpak Bansod YWYR. Liquid leak detection using thermal images 2023.
4. Ur Rehman. Attention-based underwater oil leakage detection. CAI 2023;1:214-217.
5. Padovese LR. A machine learning approach for underwater gas leakage detection. CS 2019;1.

Enhancing Neural Network Performance for Water Quality Forecasting with Principal Component Analysis in Intensive Aquaculture

Guilherme Freire de Almeida[1*], Lucas Cruz da Silva[2], Valéria Loureiro da Silva[3]
[1]Embedded Systems Department, [2]Robotics Department, [3]Optics and Photonics Laboratory; SENAI CIMATEC University; Salvador, Bahia, Brazil

This work investigates the application of Principal Component Analysis (PCA) to enhance the performance of a neural network regression model for water quality forecasting in intensive aquaculture. The dataset from an intensive cultivation study includes daily readings of controlled pond biochemical parameters. The standard and PCA-enhanced models had their performance evaluated based on the MSE, MAE, and R^2. The results demonstrate that the model incorporating PCA outperformed the standard model. The PCA model achieved lower training and testing MSEs, with a notable reduction in MAE. These findings highlight the effectiveness of PCA in improving the accuracy and efficiency of neural network models by reducing dimensionality and emphasizing the most informative features.
Keywords: Principal Component Analysis. Neural Network. Water Quality Forecasting.

In aquaculture, water quality forecasting has become an important area of research, especially for high-density cultivation methods such as semi-intensive and intensive systems. Predicting water quality parameters helps maintain optimal conditions for marine life, which is essential for sustainable aquaculture practices [1]. This approach often relies on artificial intelligence (AI) algorithms that use biochemical measurements to predict other critical parameters, such as dissolved oxygen and pH [2].

Principal Component Analysis (PCA) is a widely used statistical method for dimensionality reduction and feature extraction in neural network (NN) training datasets. This matrix-based technique transforms the data into a new feature space, retaining the essential characteristics while enabling a reduction in the number of features. This transformation can lead to more efficient models, particularly useful in scenarios with memory and processing constraints, as it enables a more compact and representative data representation [3].

Received on 21 September 2024; revised 12 December 2024.
Address for correspondence: Guilherme Freire de Almeida. Avenida Orlando Gomes, 1845. Zipcode: 41650-010. Salvador, Bahia, Brazil. Zipcode: 40170-115. E-mail: freireg1503@gmail.com.

J Bioeng. Tech. Health 2025;8(1):56-61

This work explores the application of PCA in improving the performance of a regression neural network model for water quality forecasting. Specifically, it investigates two models: a typical neural network regression model that takes ammonia, nitrate, and temperature as inputs to predict dissolved oxygen and pH levels [4] and a second model that applies PCA to the input data before training the neural network. The objective is to assess whether PCA can enhance the model's efficiency and accuracy in predicting critical water quality parameters in intensive aquaculture systems.

Theoretical Background

Principal Component Analysis

Principal Component Analysis (PCA) is a technique used in dimensionality reduction. It transforms a large set of variables into a new, smaller set known as principal components. These principal components are linear combinations of the original variables and capture the most significant patterns in the data. The main objectives of PCA are to:

- **Preserve variance**: The method ensures that the new components retain as much of the original dataset's variability.
- **Eliminate redundancy**: PCA can reduce redundancy and highlight the most important

features by identifying and combining correlated variables.

In addition to dimensionality reduction, PCA can be used for feature extraction. Feature extraction through PCA transforms data into a new set of features that more accurately represent the underlying structure by emphasizing components that capture the most variance. This process reduces noise and highlights the most important aspects, enhancing machine learning models' performance.

$$\boldsymbol{P = KX} \quad (1)$$

The method achieves this through a linear transformation (Eq. 1), where K is a transformation matrix obtained by diagonalizing the covariance matrix of the original data set X. The new representation, P, retains the same dimensionality as the original data but orders the components by their contribution to total variance [5]. Typically, only the first few principal components are retained as they explain most of the variance, allowing the less significant components to be discarded. This reduces the dimensionality compared with the original representation and decreases the complexity of subsequent classification systems [6].

Neural Networks

Artificial Neural Networks, or simply Neural Networks (NN), are machine learning models designed to recognize patterns and make predictions inspired by the human brain's structure and function. These networks consist of interconnected layers of nodes, known as neurons, that process input data and generate outputs based on learned relationships within the data [3].

A basic neural network comprises three main types of layers:

- **Input Layer**: The input layer receives the raw data that the network will process. Each node in this layer represents a different feature or variable from the dataset. In this layer, no data computation is done.
- **Hidden Layer**: The hidden layers are situated between the input and output layers and perform most of the network's computation. These layers consist of neurons that apply weighted transformations to the input data, followed by an activation function. NNs can have multiple hidden layers.
- **Output Layer**: As the name suggests, the output layers represent the last layer in the network, producing the prediction output.

During training, the neural network learns by adjusting the weights associated with each connection between neurons. This is achieved through a process known as backpropagation, where the model's prediction error is propagated backward through the network, updating the weights to minimize the error. This iterative process continues until the network's predictions are sufficiently accurate [7].

Materials and Methods

The data used for this demonstration were collected from an intensive tilapia cultivation study at the aquaculture research site of Fazenda Oruabo in Santo Amaro, Bahia. The cultivation occurred from July 30th, 2018, to December 11th of the same year in a controlled tank exposed to sunlight, with artificial oxygenation and a regular feeding schedule. The dataset includes daily readings of dissolved oxygen, pH, temperature, ammonia, and nitrite at 8:00 am each morning. The dataset had 134 samples with a 70%, 15%, and 15% split for training, validation, and testing, respectively.

Initially, a network was designed to take raw temperature, ammonia, and nitrite samples as input to forecast oxygen and pH values. Following this, a new model will achieve the same forecasting task and be trained using the same raw data but preprocessed with PCA. Figure 1 shows the component analysis referring to the object in evaluation, where the first component represents 65.98% of the total variance, the second one is 28.25%, and the last is only 5.77%. Removing the third component would not severely

Figure 1. Explained variance for each component.

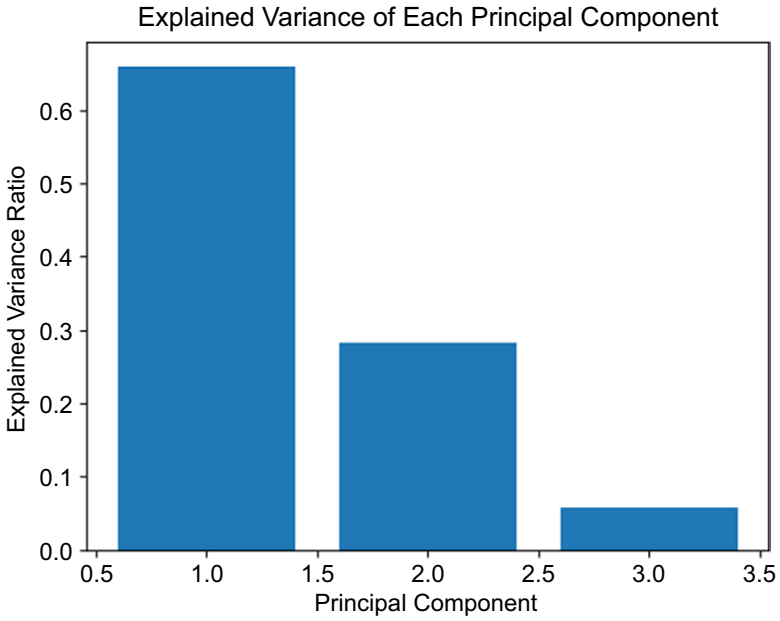

disturb the system's variance in that context. This is important during the NN training, where, after the preprocessing, this component could be removed to reduce the model's input dimensions.

The trained models were feedforward neural networks with four hidden layers, each consisting of 128 and two output nodes. The ReLU (Rectified Linear Unit) activation function was used, and the Adam optimizer was employed for backpropagation with a 0.001 learning rate.

The models' training performance was evaluated using mean squared error (MSE) as the loss function and mean absolute error (MAE) as a secondary metric. In contrast, their real-world performance was assessed using MSE and the coefficient of determination (R^2).

MSE measures the average squared difference between the predicted and actual values, indicating how close the model's predictions are to the valid values. R^2 represents the proportion of the variance in the dependent variable explained by the model's independent variables. A higher R^2 value indicates that the model explains a more significant portion of the variability in the data, demonstrating a better fit [8].

All the development was executed on Google's Colab platform, utilizing a cloud-based Linux environment with 12GB of RAM, and implemented using TensorFlow and the Keras API.

Results and Discussion

The standard neural network regression model and the model with PCA-applied inputs were trained for 400 epochs as performance improvements plateaued beyond this point. The training history illustrates the progression of training loss, validation loss, training mean absolute error, and validation MAE throughout the training process.

Analysis of Training and Validation Loss

Figure 2 shows that the training and validation loss decreased significantly during the initial epochs and stabilized as training progressed. The training loss converged to around 0.78, while the validation loss reached a similar level. The gap between training and validation loss suggests that the model generalizes well to unseen data with minimal overfitting. The training and validation MAE followed a similar trend to the loss values, with both metrics decreasing over time. The training MAE decreased steadily to approximately 0.40, while the validation

Figure 2. Model training Loss and MAE.

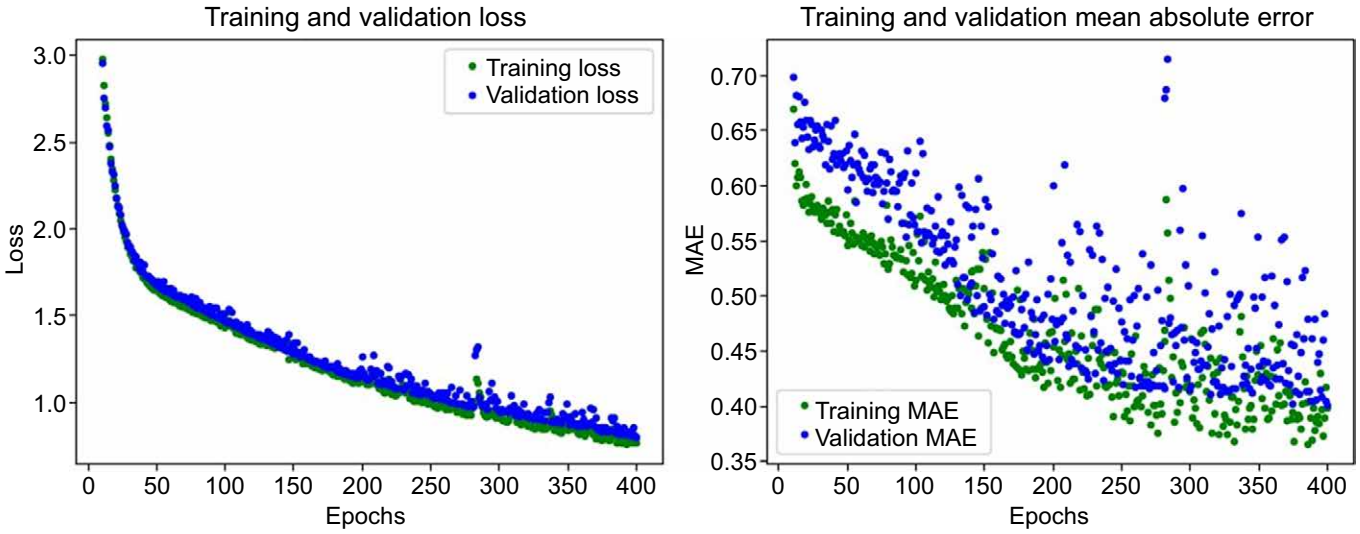

MAE also showed a steady decline, indicating good predictive performance.

In Figure 3, the training and validation loss started at higher values than the standard model, reflecting the initial higher error. However, both losses decreased rapidly and converged to lower values, around 0.38, suggesting better performance. The close superposition of the training and validation loss curves indicates minimal overfitting and good generalization. The training and validation MAE also started at higher values than the first model but presented a faster stabilization profile. Both metrics reached approximately 0.26, with the validation MAE closely following the training MAE curve, further indicating strong model performance and generalization.

Analysis of Testing Results

Table 1 summarizes the test performance metrics for both the standard neural network model (without PCA) and the model incorporating PCA.

Model Training Metrics

- **Without PCA**: The model achieved a training MSE of 0.7849 and a training MAE of 0.4042.
- **With PCA**: The PCA model demonstrated improved training performance, with a significantly lower training MSE of 0.3887 and MAE of 0.2605.

Testing Metrics for Oxygen Prediction

- **Without PCA**: The testing MSE for dissolved oxygen was 0.3998, with an R^2 value of 0.0248, indicating poor predictive accuracy and low variance explanation.
- **With PCA**: The PCA model achieved a notably lower testing MSE of 0.2148 for oxygen prediction, with an R^2 value of 0.4758. This substantial increase in R^2 indicates that the PCA model discriminates more of the variance in the oxygen data, leading to more accurate predictions.

Testing Metrics for pH Prediction

- **Without PCA**: The testing MSE for pH prediction was 0.1551, with an R^2 value of 0.0601.
- **With PCA**: The PCA model showed a significant improvement, with a testing MSE of 0.0562 and an R^2 value of 0.6591. This indicates a much better fit and higher accuracy in predicting pH levels.

Figure 4 and Figure 5 display the test outputs for both scenarios, showing that the enhanced

Figure 3. Model training Loss and MAE with PCA.

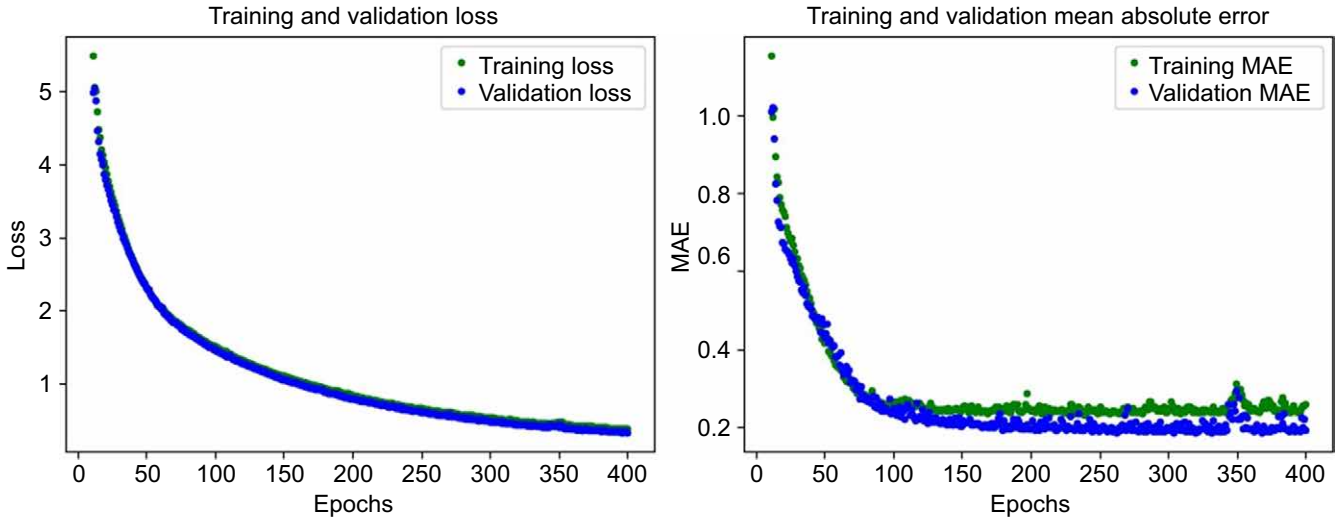

Table 1. Results comparison.

	Standard Model	PCA Model
Model Training MSE	0.7849	0.3887
Model Training MAE	0.4042	0.2605
Oxygen Testing MSE	0.3998	0.2148
Oxygen Testing R^2	0.0248	0.4758
pH Testing MSE	0.1551	0.0562
pH Testing R^2	0.0601	0.6591

Figure 4. Standard model test results.

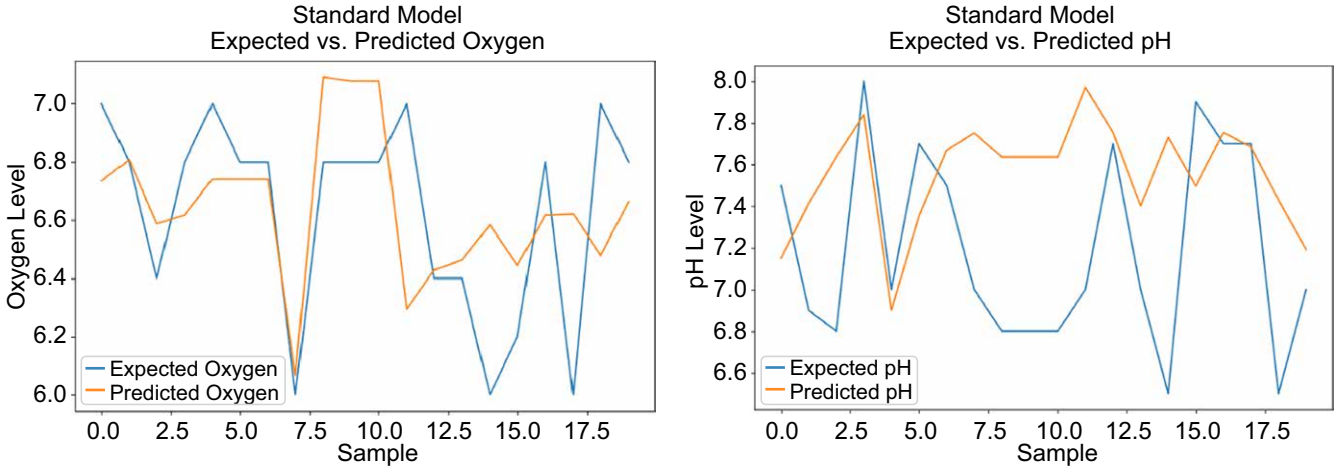

Figure 5. PCA model test results.

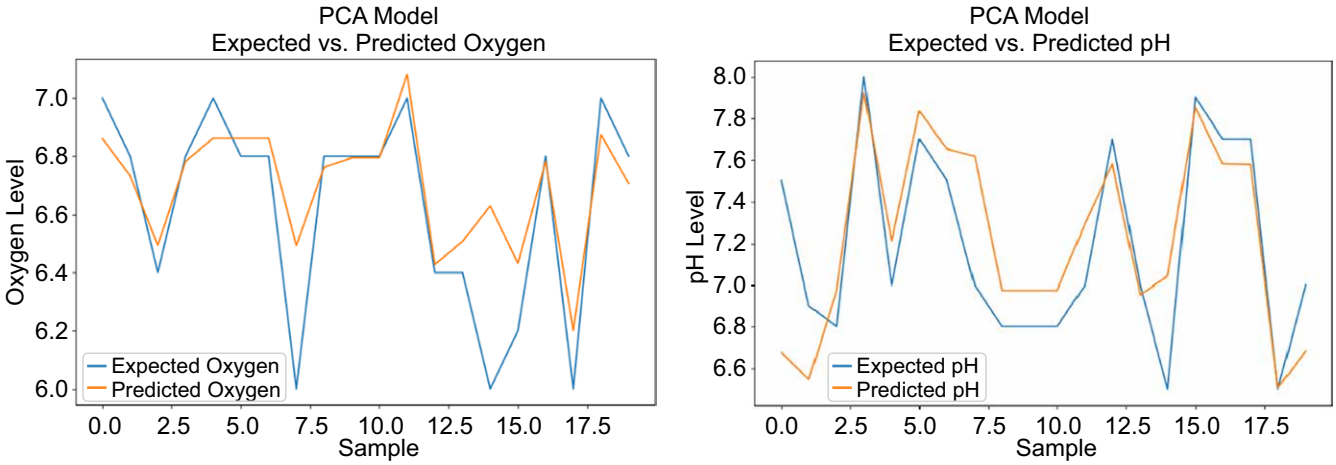

model provides a better fit. This is evidenced by the prediction graph shapes, which resemble the expected output more closely than the standard model.

Comparative Analysis and Discussion

The PCA-applied model significantly reduced training and validation losses more than the standard model. The minimal gap between training and validation losses suggests that the PCA model generalizes better, likely due to the reduced dimensionality and elimination of redundant information, which helps mitigate overfitting.

The test MSE and R^2 metrics confirmed the superior performance of the PCA model when compared to the standard model, with lower errors and a higher proportion of explained variance. This indicates that PCA effectively enhanced the model's ability to predict dissolved oxygen and pH levels from the input parameters.

Conclusion

The findings from this work underscore the importance of feature extraction techniques like PCA in enhancing the performance of neural network models, even in non-high-dimensional datasets like the one presented. By reducing noise and emphasizing the most informative aspects of the data, the method has proven to be a valuable tool in improving both the accuracy and efficiency of the built predictive model compared with its standard counterpart.

Moreover, investigating the impact of these techniques in different aquaculture environments and with various water quality parameters could provide more generalizable insights. It would also be beneficial to explore real-time implementation and the computational trade-offs associated with these advanced preprocessing methods, particularly in resource-constrained settings.

References

1. Yu C et al. Water Quality Management in Intensive Aquaculture in China. Springer, p. 1243–1252, 2008.
2. Zhao S et al. Application of machine learning in intelligent fish aquaculture: A review. Aquaculture 2021;540:736724.
3. Haykin SS. Neural Networks. Upper Saddle River, N.J.: Prentice Hall, 1999.
4. Han H-G, Chen Q, Qiao J-F. An efficient self-organizing RBF neural network for water quality prediction. Neural Networks 2011;24(7):717–725.
5. Silva LC et al. Embedded decision support system for ultrasound nondestructive evaluation based on extreme learning machines. Computers & Electrical Engineering 2021;90:106891.
6. Ferrani DG, Nunes L. Introdução a mineração de dados. [s.l.] Saraiva Educação S.A., 2017.
7. Aggarwal CC. Neural Networks and Deep Learning.
8. Li T et al. Predicting aquaculture water quality using machine learning approaches. Water 2022;14(18):2836.

Neural Networks for Classification and Regression Applied to Public Lighting Project

Matheus O.C. Cerqueira[1*], Wild F.S. Santos[1-3]
[1]Federal University of Bahia;[2]SENAI CIMATEC University; Salvador, Bahia; [3]State University of Feira de Santana;Feira de Santana, Bahia, Brazil

This paper explores using neural networks to evaluate public lighting projects according to Brazilian Standard 5101/2018. Employing Multilayer Perceptron (MLP) models, the study performs regression to predict illuminance, uniformity, and classification to assess compliance with the standard. The regression model achieved a mean squared error (MSE) of 0.002. The classification model attained an accuracy of 97.26%, with a precision of 97.0%, a recall of 96.5%, and an F1-score of 96.7%. These results underscore the effectiveness of MLP networks in improving compliance evaluation and optimizing public lighting projects.
Keywords: Public Lighting. Neural Networks. Multilayer Perceptron. Regression. Classification.

Recent estimates indicate that Brazil has over 18 million public lighting points, representing 4% of the nation's electricity consumption and 3% to 4% of municipal budgets [1]. These data highlight the urgent need to ensure the effective implementation and quality of public lighting across all municipalities. Enhancements in quality, focusing on efficacy, efficiency, and effectiveness, can be significantly enhanced through innovations such as advanced project planning [1].

Ensuring quality in public lighting in Brazil involves municipalities, energy concessionaires, the National Electric Energy Agency (ANEEL), the National Institute of Metrology Quality and Technology (INMETRO), and the Brazilian Association of Technical Standards (ABNT). ABNT's Brazilian Standard (NBR) 5101/2018 provides recommended guidelines for public lighting implementations throughout the country. Adequate public lighting reduces nighttime accidents, improves traffic conditions, and enhances public safety by deterring crime [2].

However, traditional methods for evaluating compliance with standards like NBR 5101/2018 are often prone to errors and time-consuming (e.g., specialized software needs to process both calculations for predictions and rendering graphics). This study is justified by applying neural networks to improve the accuracy and efficiency of compliance evaluations in public lighting projects.

Several studies have explored the application of neural networks in public lighting. One study developed an Extreme Learning Machine (ELM) model for simulating public lighting projects, focusing on reducing simulation time, enhancing energy efficiency, and maintaining a low error rate [3]. The ELM-based model achieved an error rate of less than 6% compared to DIALux (lighting design software) simulations and processed 1,000 different typologies in 10 seconds, showcasing the potential of neural networks to optimize public lighting design and evaluation [3].

This study develops and evaluates two distinct Multilayer Perceptron (MLP) neural network models [4, 5] for assessing compliance with NBR 5101/2018. The newer NBR 5101/2024 standard is not applied in this study due to the absence of approved LED luminaires in the Brazilian market by INMETRO that meet the new standard [6] and because simulation software has not yet been adapted. The first model is a regression-based MLP, which predicts illuminance and light uniformity in a pathway. The second model is a classification-based MLP that uses these predicted parameters and classifications of roads and sidewalks to assess compliance with the NBR

Received on 15 September 2024; revised 20 November 2024.
Address for correspondence: Matheus O.C. Cerqueira. Rua Amado Coutinho, 243, Edf. Azalea, ap.804, Brotas. Zipcode: 40285-500. Salvador, Bahia, Brazil. E-mail: escrevaparamatheus@gmail.com.

J Bioeng. Tech. Health 2025;8(1):62-67

5101/2018. A thorough review of the guidelines in Brazilian Standard 5101/2018 is essential to identify the relevant parameters for evaluation. The study involves analyzing and preprocessing data from real-world public lighting projects to ensure its suitability for training neural network models. This process includes evaluating the models' precision, recall, and F1-score for classification tasks and the mean squared error (MSE) for regression tasks. The goal is to demonstrate the feasibility and effectiveness of using neural networks to optimize public lighting systems, ultimately contributing to safer and more efficient urban environments.

Theoretical Background

Brazilian Public Lighting Standards

Brazilian Standard 5101/2018 establishes comprehensive guidelines for public lighting systems in Brazil. These guidelines ensure safety, visibility, and efficiency in public spaces, particularly in urban areas. The standard specifies requirements for several critical parameters, including illuminance and its uniformity, to ensure that lighting systems meet the necessary criteria for safety and functionality. [2].

Illuminance is the total luminous flux incident on a surface per unit area, measured in lux (lx). It is a fundamental metric for assessing the adequacy of lighting in each region. The standard sets minimum and recommended illuminance levels for different classes of public roads and areas (e.g., high-traffic urban roads and highways require higher illuminance levels than residential streets or pedestrian pathways. This differentiation is vital to provide appropriate visibility for drivers and pedestrians, reducing the likelihood of accidents and enhancing overall safety [7].

Illuminance uniformity, now referred to as uniformity, measures the evenness of light distribution across a surface. It is expressed as a minimum-to-average illuminance ratio and is crucial for preventing areas of excessive brightness or darkness, which can cause visual discomfort or hazards. NBR 5101/2018 outlines specific uniformity ratios that must be achieved to ensure a consistent and comfortable visual experience for road users and pedestrians [7].

According to NBR 5101/2018, roads are classified due to their pedestrian and vehicle traffic intensity. Different classes of roads require specific illuminance and uniformity levels to ensure safety and visibility and enhance efficiency [7]. Table 1 summarizes these requirements, indicating the minimum and average illuminance values and uniformity ratios for various road categories.

Neural Networks

Artificial Neural Networks (ANNs) are machine learning algorithms inspired by the human nervous system. They consist of interconnected neurons called perceptrons that propagate information. ANNs optimize functions to either maximize or minimize an objective function. In supervised learning, the goal is to minimize an error function that measures the difference between predicted outputs and actual values. This optimization enables the network to learn from data and improve its performance over time, making ANNs powerful tools for various applications, including public lighting project evaluation and improvement [4,5].

Multilayer Perceptrons (MLPs), a type of ANN, consist of several interconnected neurons: an input layer, one or more hidden layers, and an output layer. Information is fed forward from the input layer through the hidden (intermediate) layers to the output layer. Each neuron in a layer is connected to neurons in the previous and subsequent layers, with links having weights and biases that are adjusted during training to optimize network performance. The input layer receives raw data processed by hidden layers using activation functions. Common activation functions include the Rectified Linear Unit (ReLU), which introduces non-linearity to capture

Table 1. Minimum average illuminance and uniformity for Road / Sidewalk classes [7].

Road Lighting class	Illuminance (lux)	Uniformity (dimensionless)	Sidewalk Lighting class	Illuminance (lux)	Uniformity dimensionless)
V1	30	0.4	P1	20	0.3
V2	20	0.3	P2	10	0.25
V3	15	0.2	P3	5	0.2
V4	10	0.2	P4	3	0.2
V5	5	0.2			

complex data patterns, and the Sigmoid function, which maps input values between 0 and 1 and is valid for binary classification tasks [4, 5].

Training MLPs involves adjusting the weights to minimize the error between predicted and actual targets using a backpropagation algorithm. This algorithm calculates the error gradient for each weight and updates the weights in the opposite direction of the gradient. This process repeats over many iterations, known as epochs, until the network converges to a solution that minimizes error [4, 5].

Due to the backpropagation algorithm and interconnected perceptrons (which suit non-linear situations), MLPs can handle large datasets and complex relationships [4,5]. This implies they are well-suited for applications beyond public lighting, including image and speech recognition, financial forecasting, and medical diagnosis. Based on input parameters such as road width, mounting height, installation angle, and lamp power, MLPs can predict illuminance and uniformity in public lighting. They can also classify whether a lighting project complies with Brazilian Standard 5101/2018.

Materials and Methods

Data

The first step of this project was to collect comprehensive data from public lighting projects. This data was provided by a company specializing in public lighting, 42LUX, allowing us to gather a substantial dataset containing over 250,000 projects. Each project includes the following parameters: power, installation angle, mounting height, recoil, projection, road width, adjacent and opposite sidewalk width, and distance between poles. Additionally, the dataset contains road and sidewalk classes and output parameters such as illuminance and uniformity, which are critical for assessing compliance with Brazilian Standard 5101/2018 and validating the accuracy of both the classification and the regression models.

We performed several preprocessing steps to ensure the dataset was adequate for training our neural network models. Initially, we removed incomplete or erroneous records to guarantee the dataset's integrity and prevent potential bias. Next, we divided the dataset into training and test sets. As the literature suggests, the train-test ratio was 70%—30% to have enough data to train the network and tune hyperparameters, minimizing overfitting [4,5].

Normalization techniques were applied to address the different scales of the input parameters. Determining the most suitable data format for processing the dataset was essential. This understanding justified the construction of a specific feedforward classification network with backpropagation to examine the different loss graphs per epoch during training. The most suitable was standardization (removing the mean

and dividing by the standard deviation of the values set) [4].

Proposed Models

Two types of Multilayer Perceptron (MLP) models were developed for this study: one for regression and the other for classification. The regression model aims to predict the illuminance and uniformity values based on the project input parameters (reflecting the lighting devices and their spatial settings). In contrast, analyzing its illuminance and uniformity, the classification model determines whether a public lighting project complies with Brazilian Standard 5101/2018.

The regression model has an input layer with nine neurons, each corresponding to one of the parameters (power, installation angle, mounting height, recoil, projection, road width, adjacent and opposite sidewalk width, and distance between poles). The model includes one hidden layer with 100 neurons using the Rectified Linear Unit (ReLU) activation function and an output layer with six neurons, representing the illuminance and uniformity of the road and both sidewalks. The Adam optimizer minimizes the mean squared error (MSE) between predicted and actual values. The model was trained for 250 epochs.

The classification model uses the six output neurons from the regression model as inputs, sidewalks, and road classes. It has a hidden layer of the same dimension as the regression model but features a single neuron in the output layer with a sigmoid activation function. This neuron outputs a probability between 0 and 1, indicating whether the project complies with NBR 5101/2018. The Adam optimizer was used with the same learning rate and early stopping criteria as the regression model, and the model was trained for 250 epochs. Performance was evaluated using accuracy, precision, recall, and the F1-score.

Evaluation

After training, the models were evaluated using the test set. The mean squared error (MSE) and the coefficient of determination (R^2) were calculated for the regression model to assess prediction accuracy. For the classification model, accuracy, precision, recall, and the F1-score were used to evaluate performance [4,5].

The Receiver Operating Characteristic (ROC) curve was plotted, and the area under the curve (AUC) was calculated to assess discriminative ability. The ROC curve plots the valid positive rate against the false positive rate at various thresholds, and the AUC represents the probability that the model ranks a randomly chosen positive instance higher than a randomly chosen negative instance.

Results and Discussion

The regression model achieved an MSE of 0.002 and an R^2 of 0.047, contrasting the proposed model's evaluation. The very low MSE indicates that the predictions are very close to the actual values within the data context, implying high precision in individual predictions. However, the low R^2 value suggests that the model does not adequately capture the overall variability in the data, indicating limited explanatory power regarding the data's variance. This discrepancy is likely related to the data imbalance and the scale difference between the regression model outputs.

To improve the R^2, addressing data balancing issues and applying more effective normalization or standardization techniques are recommended.

Figure 1 illustrates the ROC curve for the classification model. The training process resulted in a loss of 0.08, suggesting a well-trained model with potential overfitting. However, as the confusion matrix analysis suggests, this was not observed in practice. The confusion matrix provides a detailed breakdown of the classification model, showing the number of true positives, true negatives, false positives, and false negatives. As shown in Table 2, the model accurately classified 31,125 compliant projects and 43,171 non-compliant projects. However, it misclassified 1,124 compliant projects as non-compliant and 967 non-compliant projects as compliant. This detailed

Figure 1. ROC curve and AUC of the classification MLP.

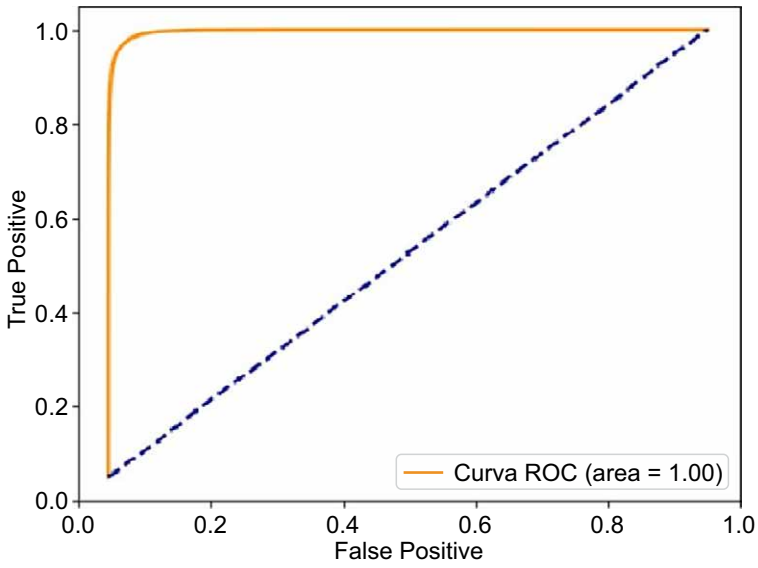

Table 2. Confusion matrix of classification model.

	Predicted Positive Class	Predicted Negative Class
Real Positive Class	31,125	1,124
Real Negative Class	967	43,171

analysis highlights the model's high accuracy and effectiveness in distinguishing between compliant and non-compliant public lighting projects.

As demonstrated in Table 2, the model achieved an accuracy of 97.26%, precision of 97% (indicating that most projects classified as compliant were correctly identified), recall of 96.5% (showing that most truly compliant projects were correctly detected), and F1-score of 96.7% (reflecting a strong balance between precision and recall), along with the ROC curve (showing an area under the curve (AUC) of approximately 1). The metrics confirm the effectiveness of the classification model in the public lighting context since it efficiently determines whether a set of illuminance and uniformity parameters meets the NBR 5101 standard.

In summary, the results show the potential of neural networks, particularly MLPs, to enhance the evaluation and implementation of public lighting projects. These models offer valuable tools for urban planners and engineers, helping them design and maintain lighting systems that comply with standards and improve public safety and efficiency.

Conclusion

This study demonstrated the feasibility of using MLP neural networks to evaluate the compliance of public lighting projects with Brazilian Standard 5101/2018. The obtained results are promising, indicating that this approach can help optimize the implementation of public lighting systems. We successfully implemented, trained, and evaluated the MLP neural network models. The regression model achieved an MSE of 0.002, demonstrating high precision in individual predictions. The classification model attained an accuracy of

97.26%, with a precision of approximately 97.0%, a recall of about 96.5%, and an F1-score of around 96.7%. These metrics indicate that the classification model is highly effective in identifying compliant projects and minimizing misclassification. Future research can explore the inclusion of additional variables or the application of other neural network architectures to enhance model performance and accuracy further.

Potential extensions of this work include experimenting with various hyperparameters, such as using variable or adaptive learning rates that adjust based on the loss function's convergence. Another possibility for future research could involve modifying the problem to identify the closest configuration for parameters that do not initially comply with NBR 5101/2018 but could be adjusted to meet the standards.

Additionally, a comparative analysis with commercial software designed for public lighting scenario simulations could be conducted, evaluating their accuracy and processing times against the neural network models used in this study. Finally, an update to the study could involve applying the proposed models by the new NBR 5101/2024 standards once approved LEDs and suitable simulation software become available, providing deeper insights and further advancements in applying neural networks to public lighting projects.

References

1. Meyer M et al. Lighting Brazilian Cities: Business Models for Energy Efficient Public Street Lighting. World Bank, Washington, DC, abr. 2017. Available at:<https://openknowledge.worldbank.org/entities/publication/244cea4e-dbde-5bdb-b733-ba150ac6834f>.
2. Associação Brasileira da Indústria de Iluminação. Guia para Iluminação Pública. 2021;1 Available at: <https://www.abilux.com.br/docs/Abilux_Guia_IluiminacaoPublica_2021_volume- 01.pdf>.
3. Costa V, Santos WFS. Street Lighting Simulation based on Extreme Learning Machine. Conference: ICISNA'23 (International Conference on Intelligent Systems and New Applications). London, 2023.
4. Faceli K et al. Inteligência artificial: uma abordagem de aprendizado de máquina. Rio de Janeiro: LTC, 2011.
5. Goodfelow I, Bengio Y, Courville A. Deep Learning. Cambridge, MA, USA: MIT Press, 2016.
6. Rosito L. ABNT NBR 5101: 2024 – Norma em vigor; e agora?. OSetorElétrico. 19jul.2024.Availableat<https://www.osetoreletrico.com.br/abnt-nbr-5101-2024-norma-em-vigor-e-agora/>.
7. Associação Brasileira de Normas Técnicas. Norma Brasileira 5101: Iluminação pública - Procedimento. 2018. Available at: <www.abnt.org.br>.

Panda Manipulator Control with Obstacle Avoidance Through Reinforcement Learning in a Simulated Environment

Marcelo Albergaria Paulino Fernandes Ferreira[1*], Taniel Silva Franklin[1],Oberdan Rocha Pinheiro[1]
[1]SENAI CIMATEC University; Salvador, Bahia, Brazil

Robotic systems with learning capabilities have many powerful applications in unstructured environments. Through reinforcement learning, robots can quickly adapt to new situations and learn from direct environmental interaction. This work proposes a simulation environment based on Robotics Toolbox for Python to solve a classic problem of the inverse kinematics of manipulators, ensuring that the robot reaches the desired position without colliding with the obstacles present in the scene. The potential of this reinforcement learning method is illustrated through simulation using the Franka-Emika Panda manipulator trained by the Deep Deterministic Policy Gradient algorithm.
Keywords: Reinforcement Learning. Machine Learning. Robotics.

Commercial and industrial robots nowadays have a wide range of applications. They often assist humans in dangerous, repetitive, and exhausting tasks. Many extreme environments are challenging to access or require expensive logistics to transport specialized personnel. One of intelligent robotics's main challenges is creating robots capable of interacting directly with the world around them to achieve their goals [1]. The wide variety of usage scenarios and environmental variations suggests that an effective manipulator must be able to cope with environments that neither it nor its designers have foreseen or encountered before. The growing availability of computational resources has boosted the development of machine learning, enabling the emergence of promising technologies such as recommendation systems, autonomous vehicles, video games, energy management, and robotics, among others [2].

Deep Reinforcement Learning (DRL) is the combination of Reinforcement Learning (RL) and Deep Learning (DL). Reinforcement Learning is a machine learning method where the Agent learns the ideal behavior in an environment through trial-and- error interactions to obtain the maximum reward. RL, the Agent has the function of taking actions to resolve complex problems, interacting with the environment that responds with observations or states, and rewards or costs [3].

These two components continuously interact so that the Agent tries to influence the environment; at each interaction step, the Agent receives an observation of the state of the world and then decides which action to take; for each action, he receives a reward signal from the environment (Figure 1). This reward needs to inform how successful the action was on the way to achieving the goal, so maximizing the total reward will lead the Agent to solve the problem by taking the best actions.

Training with a real robot is expensive because machine learning requires considerable data representing the robot's experience in the environment. Researchers have sought ways

Figure 1. Reinforcement learning scheme.

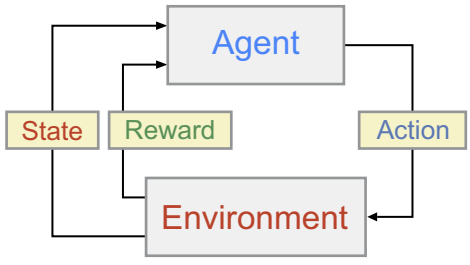

Received on 27 September 2024; revised 28 December 2024.
Address for correspondence: Marcelo Albergaria Paulino Fernandes Ferreira. Av. Orlando Gomes, 1845, Piatã. Zipcode: 41650-010. Salvador, Bahia, Brazil. E-mail: marcelo_albergaria@hotmail.com.

to reduce this dependency through training approaches by simulation due to the low risk to equipment parts and the availability of synthetic data acquired using many simulations. However, this approach needs to include strategies to minimize the reality gap.

Inverse kinematics is a classic problem in robotics. The aim is to determine the angles of a manipulator's joints to achieve a specific pose in space. This problem can be addressed in two main ways: analytical methods, which provide direct mathematical solutions, or numerical methods, which involve iterative algorithms such as optimization or solving systems of non-linear equations [4].

Reinforcement learning (RL) presents a model-free alternative to robot control. In this strategy, the robot learns a control policy by interacting with its environment and learning to make decisions that result in desired behaviors, such as reaching a pose or manipulating objects. This strategy is particularly effective when there is no perfect model of the system or when the environment is complex and non-deterministic, allowing the robot to adapt and improve its performance based on accumulated experience.

This project aims to solve the problem of inverse kinematics using a simplified environment built with Robotics Toolbox for Python [5]. This framework provides specific robotics functionalities to represent the kinematics and dynamics of rigid and mobile manipulators, making it possible to import a URDF file or use more than 30 models provided and create obstacles.

For the experiment, the Franka-Emika Panda collaborative robot was included to reach a final position, starting from a random initial position, without colliding with the obstacles in the scene.

In this context, it is useful to present a reinforcement learning environment for training robot manipulators in Python. The simulator is based on the Robotics Toolbox for Python. The environment provides training and visualization modules to compare standard DRL algorithms, such as the Deep Deterministic Policy Gradient (DDPG) algorithm.

Materials and Methods

The Robotics Toolbox for Python library was used to create the simulation environment and represent the kinematics of the manipulator. The floor, the table (obstacle), and the Panda manipulator were added in this step. A random initial position for the robot and target was used, as shown in Figures 2 and 3.

The Franka Emika company manufactures the Panda manipulator to achieve high performance and affordability, combining human-centered design. The responsive arm features 7 degrees of freedom with torque sensors at each joint, allowing for an adjustable fit and advanced torque control. It has a payload of 3kg and a reach of 855mm. The joints of the Panda robot have specific range limits to ensure safe and effective operation: Joint 0, joint 2, joint 4, and joint 6 have a range of -166° to 166°, joint 1 ranges from -101° to 101°, joint 3 ranges from -176° to 4° and joint 5 ranges from -1° to 215°.

Our main assumptions are that motion occurs in 3D, initial states are random (Figure 2), and actions are continuous with 7 active rotational joints, allowing for collisions with the table, floor, and joint boundaries (Figure 3).

The Deep Deterministic Policy Gradient (DDPG) algorithm was used for training. This algorithm is a variation of actor-critic suitable for environments with continuous action spaces. DDPG is based on using deep neural networks to estimate actor policies and critic values. This off-policy algorithm aims to learn a deterministic policy that maximizes expected returns in a continuous environment.

The method collects experiences, selects actions according to the actor's current policy, and stores rewards and states in the replay buffer. The Agent samples a batch of experiences, calculates discounted future rewards using the target crit network, and updates the critic weights. The actor's

Figure 2. Robot in starting position.

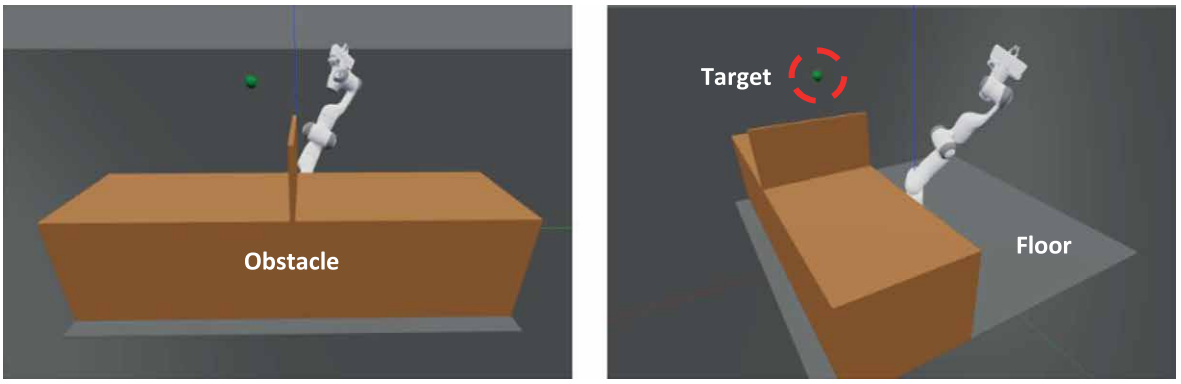

Figure 3. Robot in final position.

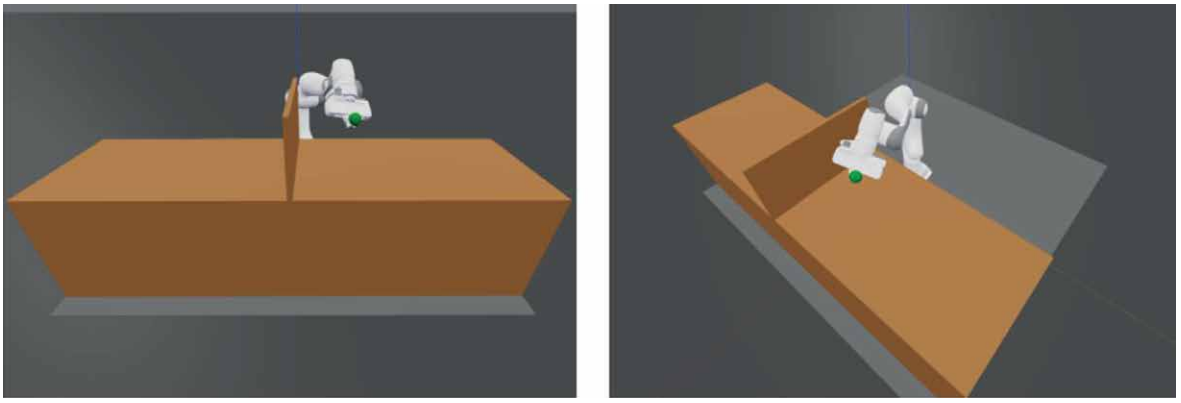

network is updated using an upward gradient to maximize the Q value estimated by the critic. Training continues iteratively, updating networks to improve policy and value estimation.

The neural networks are initialized during training, and the actor-network policy is applied to each episode. An exploration noise, known as Ornstein-Uhlenbeck, is added to the action taken by the Agent to ensure further exploration of the environment. The Agent acts as the environment and, in response, receives the next state, the reward obtained, and a flag indicating whether the episode has been completed. When the amount of stored experiences exceeds the batch size, the Agent updates its actor and critic networks using samples from the replay buffer. The actor-network is updated to improve the policy using the policy gradient method. Meanwhile, the critic network is updated to minimize the mean square error (MSE) between the estimated and desired Q-values.

The reward function used is a scalar reward function (1), which aims to balance two crucial aspects of the manipulator's behavior: the robot's proximity to the target and the magnitude of the action performed. The total reward is a weighted sum of two components and their coefficients.

(1)

$$R = \begin{cases} r_{col}, & \textbf{\textit{if collided}} \\ r_{suc}, & \textbf{\textit{if sucess}} \\ r(s,a) = \left(c_1 \times r_{tg}(s,a) + c_2 \times r_{action}(s,a)\right), & \textbf{\textit{otherwise}} \end{cases}$$

$C1$, weights the importance of proximity to the target, indicating a significant penalty for considerable distances to the target, and $C2$weights the magnitude of the action, encouraging more minor actions to promote efficient movements.

The object proximity reward $r$tg (2) encourages the manipulator to approach the goal precisely, where d is the manipulator's current distance from the goal and δ is a smoothing parameter. The action magnitude reward $r$action penalizes large action magnitudes, encouraging smooth and efficient movements, a is the applied action vector (3).

$$r_{tg}(d) = \begin{cases} \frac{1}{2} d^2, & if\ d < \delta \\ \delta(d - 0.5\delta), if\ d \geq \delta \end{cases} \quad (2)$$

$$r_{action}(a) = -\|a\| \quad (3)$$

Collision and step penalties ensure that the Agent minimizes excessive movements and avoids collisions. For example, the Agent receives a -0.5 penalty for each step taken during the episode, encouraging it to complete the task efficiently. Collisions with obstacles result in a significant penalty of -500 to avoid unsafe behavior. On the other hand, the Agent is rewarded with 500 when it reaches the goal. During agent training in the simulated Panda robot environment, fitness is calculated at each step to provide a metric for the Agent to adjust its actions and improve its performance. This metric continuously evaluates the position and orientation of the robot's end-effector relative to the desired target. Training involves applying the Agent's action, calculating the new state, evaluating the fitness, and deciding on the reward. The task is completed when the fitness value is smaller than the target of 0.004.

Results and Discussion

The training rounds were carried out using the Optuna optimizer [6] to automate adjusting the hyperparameters, saving time and computational resources. The result of this study provided the parameters for the best-performing model, aiming to achieve the manipulator's final position without any collision with obstacles (Table, Floor, Joint Boundaries) in the environment. Figure 2 represents the random initial position of the robot and the obstacles after resetting the manipulator, and Figure 3 represents the final state of the robot, with the objective achieved. The model's architecture includes neural networks for the actor and the critic. Both networks are configured with multiple densely connected layers, using Rectified Linear Unit (ReLU) activation functions in the hidden layers and a Tangent Hyperbolic (Tanh) activation function in the output layer of the actor network. This architecture allows the model to learn and generalize complex control patterns, optimizing the Agent's performance in the simulation environment.

The manipulator was trained with the parameters described in Table 1, and its average reward converged around 480. In the simulation phase, he obtained a total reward of 500 and completed the task in 1 step. After optimization on the hyperparameters, the Agent was trained with the reward function described by Eq. (1), converging on a successful positioning trajectory.

Figure 4 presents the best model's success rates, collision rates, and average reward values. The average reward stabilizes around 500, indicating policy convergence. The success and collision graphs demonstrate that the Agent quickly learns to avoid obstacles and reach the target efficiently.

Table 1. Training parameters.

Parameter	Value
Learning Rate	0.001
Total Number of Steps	200000
Batch Size	200
Fitness	0.004
Step Penalty	-0.5
Collision Penalty	-500
Sucess Reward	500
Gamma	0.99
Memory Size	50000
First Hidden Layer	1200
Second Hidden Layer	1800

Figure 4. Success rate, collision rate, and average reward.

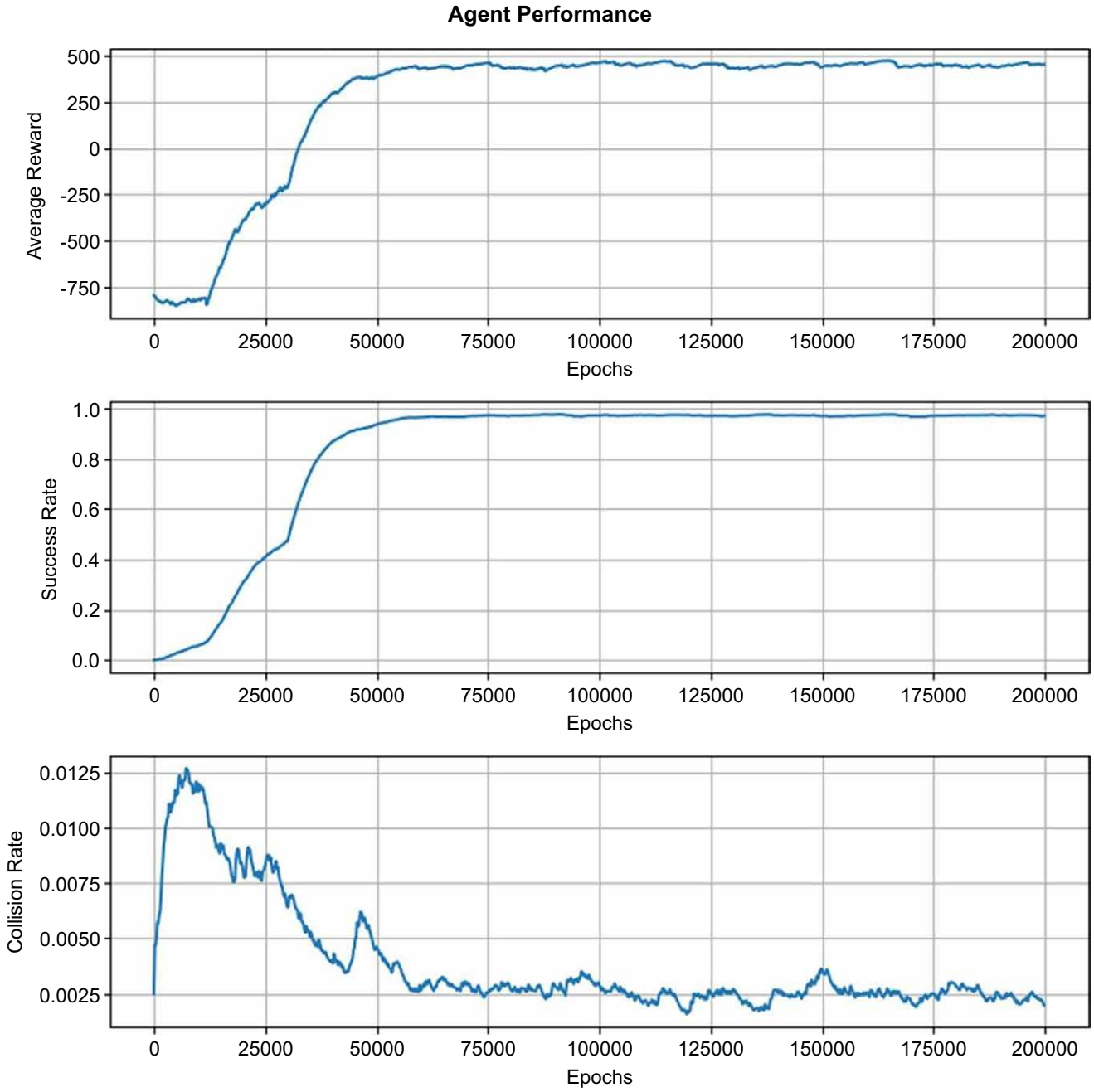

To illustrate the results, we have included a file (https://1drv.ms/f/c/f6931d804d905e8a/EhicS8adWDFIsr0h8sRQ0fgBCT1u13Vxfcqy29-j0Vwpnw?e=KI1WcZ) containing simulations that characterize successful tasks, failed tasks and random start positions of the manipulator based on the trained model.

Conclusion

This work demonstrated the applicability and use of the DDPG algorithm and the Robotics Toolbox for the Python environment for the classic inverse kinematics problem. The results indicate that the trained Agent could learn to interact with

the environment appropriately, reaching the goal in a minimum number of steps and avoiding collisions. The designed reward function, which balances the target's proximity and the actions' magnitude, proved effective in learning. The simulation environment allows the necessary skills to be developed in a safe, controlled, and easy-to-install interface without relying on a real robot, saving time and costs. These learnings can be transferred and tested on real manipulators after performing well in some situations. For future studies and improvements, implementing the task in a simulation environment with more realistic physics, such as Pybullet, would help to reduce the gap between simulation and reality. In addition, tests with reinforcement learning algorithms already used in other robotic tasks, such as Proximal Policy Optimization (PPO), could provide a solid comparative basis.

Acknowledgments

This research was carried out in partnership between SENAI CIMATEC and Shell Brasil. The authors would like to thank Shell Brasil Petróleo LTDA, Empresa Brasileira de Pesquisa e Inovação Industrial (EMBRAPII) and Agência Nacional do Petróleo, Gás Natural e Biocombustíveis (ANP) for their support and investments in RD&I. investments in RD&I.

References

1. Kroemer O, Niekum S, Konidaris G. A review of robot learning for manipulation: Challenges, representations, and algorithms. The Journal of Machine Learning Research 2021.
2. Elguea-Aguinaco I, Serrano-Muñoz A, Chrysostomou D, Inziarte-Hidalgo I, Bogh S, Arana-Arexolaleiba, N. A review on reinforcement learning for contact- rich robotic manipulation tasks. Robotics and Computer-Integrated Manufacturing 2023;81:102517,2023.
3. Liu R, Nageotte F, Zanne P, de Mathelin M, Dresp-Langley B. Deep reinforcement learning for the control of robotic manipulation: A focussed mini-review. Robotics 2021;10:22. doi:10.3390/robotics10010022.
4. CraigJJ.Introduction to Robotics: Mechanics and Control. Pearson/Prentice Hall, 2005.
5. Corke P, Haviland J. Not your grandmother's toolbox-The Robotic's Toolbox reinvented for Python. Proc. ICRA 2021.
6. Akiba T, Sano S, Yanase T, Ohta T, Masanori K. Optuna: A Next-generation Hyperparameter Optimization Framework. In KDD 2019.

Bibliometric Review on Planters and Transplanters

Vinícius Guimarães Rosa[1*], Alexandre Diogo Poltronieri[1], Danilo Jefferson Romero[1], Saulo Queiroz Figliuolo[1], Valter Estevão Beal[1]
[1]SENAI CIMATEC University; Salvador, Bahia, Brazil

This bibliometric review article aims to analyze scientific publications on various types of planting equipment, focusing on technological advances and emerging research areas. Data was collected from academic databases. The analysis covered articles from 1993 to 2023, identifying citation patterns, key authors, institutions, and countries involved. Results indicate a significant rise in publications, especially precision equipment and sustainable technologies. China and the USA lead in publications, with India and Brazil following. Interdisciplinary collaboration between agricultural engineers and data scientists is raising and promoting advancements. In conclusion, research on planting equipment is rapidly evolving, driven by the need for increased efficiency and sustainability in agriculture.
Keywords: Planter. Transplanter. Yield. Performance. Agriculture.

Agricultural transplanter and planter machines are vital in modern agriculture. They enhance planting efficiency, productivity, and resource utilization. These machines improve planting precision and speed, reducing labor costs and manual effort and making large-scale agriculture more sustainable.

Recent studies estimate that the agricultural sector must increase food production between 100% and 110% to meet global demands until 2050 [1] while addressing climate change, soil degradation, and resource depletion. Advanced machinery is crucial for sustainable practices, improving planting efficiency, reducing waste, and optimizing plant growth conditions, which minimizes the usage of fertilizers, herbicides, and pesticides.

New procedures and advanced technologies, such as automation, sensors, and renewable energy sources, enhance equipment performance. Automation and precision agriculture improve planting accuracy, maximizing crop yields and minimizing resource use. Sensors and IoT enable real-time monitoring, allowing data-driven decisions that enhance efficiency and sustainability.

Received on 18 September 2024; revised 17 November 2024.
Address for correspondence: Vinícius Guimarães Rosa. Avenida Orlando Gomes, 1845, Piatã. Salvador, Bahia, Brazil. Zipcode: 41650-010. E-mail: vinicius.rosa@fieb.org.br.

J Bioeng. Tech. Health 2025;8(1):74-80

The bibliometric review provides an overview of the research landscape and offers insights into the current state of research and development, highlighting influential studies, authors, and institutions. It reveals regional strengths and collaborations, guiding efforts to foster international cooperation and knowledge exchange and address global challenges in food security and sustainable agriculture.

In summary, this article provides a comprehensive understanding of the research landscape, highlighting key contributors to the evolution of agricultural machinery. It offers valuable insights for future research and development, promoting sustainable and efficient agricultural practices worldwide.

Materials and Methods

The study carried out in this work consists of a bibliometric review, which conducted a survey of articles published in the last 30 years (1993-2023) related to advances in agricultural planting machinery related to improvements in yield, performance, or efficiency. The search was conducted between May 29 and June 05, 2024, using the Scopus [2] and Web of Science [3] databases. The keywords used in the article were planter, transplanter, performance, efficiency, and yield.

After a preliminary analysis of the available publications, the search Booleans was defined for each interface, using the exact keywords and research fields. Still, in the interfaces themselves, filters were applied to remove articles unrelated to the area of interest from the results. The filter selection process removed 865 articles related to medicine, arts, pharmacology, and veterinary medicine (Table 1).

Next, the data were exported in "bibtex" file format, and pre-processing was carried out using the RStudio [4] software and its bibliometric review library Bibliometrix [5]. The two different datasets were merged into a single file, and duplicate information was removed, resulting in 1505 articles. After this initial process, the unified data were loaded into the Biblioshiny interface (a Bibliometrix development), and from there, graphs and maps were generated on quantitative and qualitative analyses to identify citation patterns, most frequent keywords, the timeline of the publication's evolution, relevant affiliations and authors, between other remarkable data.

Results and Discussion

The analysis of annual scientific production between 1993 and 2023 reveals a significant growth in the number of published articles, segmented into three distinct periods. From 1993 to 2004, stability was observed with moderate growth, with an average of approximately 11 annual articles, characterized by minimal variations and consolidation of research bases. From 2005 to 2014, there was accelerated growth (Figure 1), with the number of articles increasing from 14 in 2005 to 52 in 2014, possibly driven by technological advances, more significant investment in research and development, and expansion of scientific collaboration networks.

Between 2015 and 2023, scientific production has grown significantly, reaching 62 articles in 2015 and culminating in 160 articles in 2022, with a slight decrease to 150 in 2023. The analysis highlights the apparent growth trend in scientific production, reflecting advances in research and development and the importance of global scientific collaboration, which is essential for understanding the impact and direction of future scientific research.

Following the initial data evaluation, the publications in the period grouped by the country of production of the article were analyzed (Figure 2). In this analysis, it is possible to perceive that the USA was the dominant country in the number of publications until mid-2015, when it was then surpassed by the current country with the most articles published per year, China, which showed a progressive increase in the publication rate from 2008, reaching the current number of 1210 articles published in 2023. In second place, we have the USA with 467 publications, followed by India with 377, Brazil with 226, and Turkey in fifth place with

Table 1. Search inputs and results.

#	Source	Boolean	Search Results	Search Results After Filters
1	Web of Science	(TS=(planter) OR TS=(transplanter)) AND (TS=(performance) OR TS=(yield) OR TS=(efficiency))	1,053	761
2	Scopus	((TITLE-ABS-KEY (planter) OR TITLE-ABS-KEY (transplanter)) AND (TITLE-ABS-KEY (performance) OR TITLE-ABS-KEY (yield) OR TITLE-ABS-KEY (efficiency)))	1,829	1,256

Figure 1. Annual scientific production.

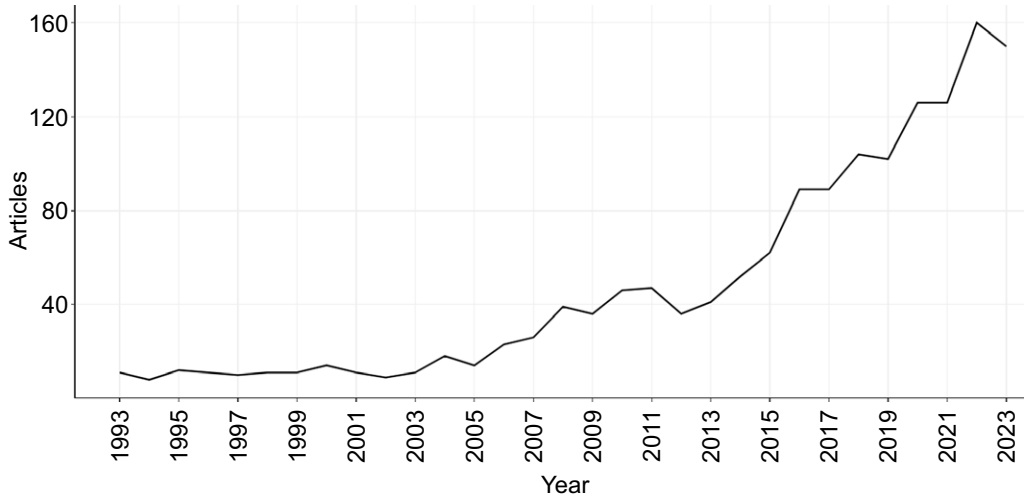

Figure 2. Ten countries with the most articles published per year (1993 - 2023).

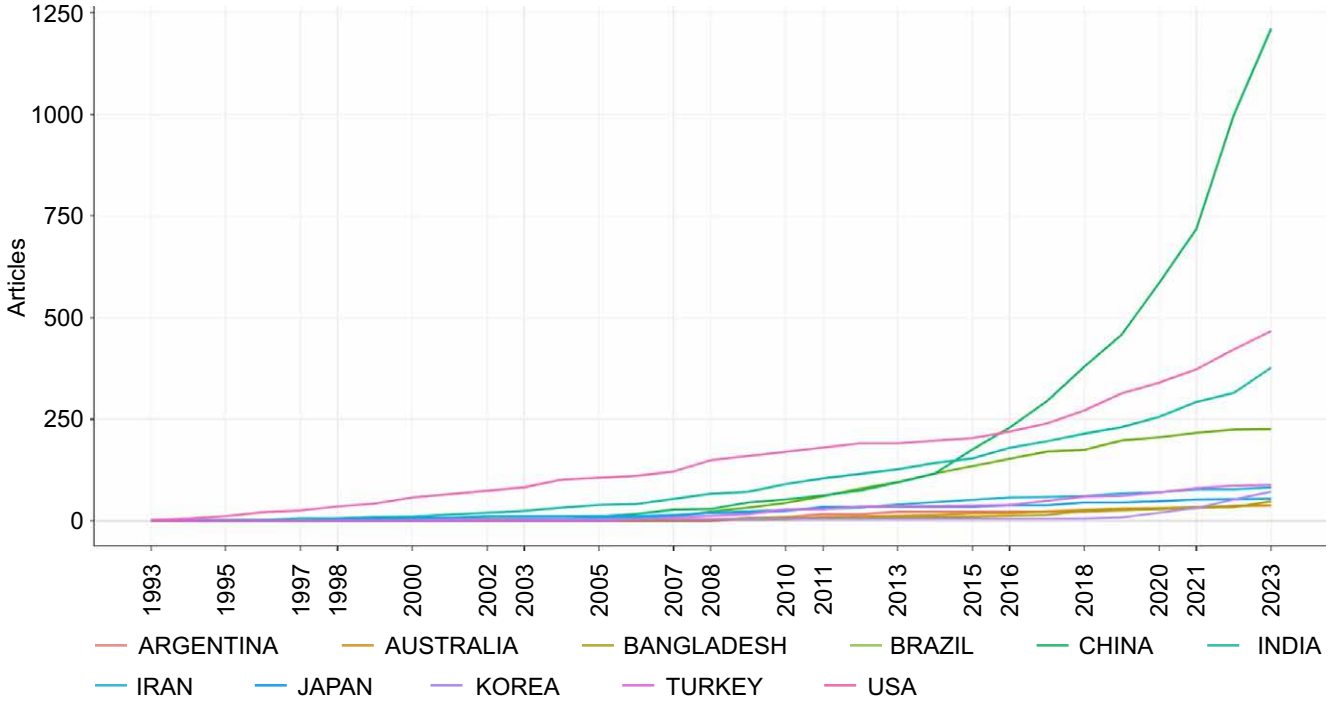

89 publications in the same year of 2023. These countries are leaders in agricultural production [6] and in the publication of scientific articles related to improvements in planting equipment, suggesting a strong correlation between academic research and agricultural production.

The analysis of the collected data revealed that the most prolific authors in research on improvements in agricultural planting machinery are predominantly Chinese, highlighting China's leadership in this field. The most productive author is LI H, with 57 publications and an H-index of 17, followed by Zhang X, with 51 articles and an H-index of 14. In third place, Wang X has 36 publications and an H-index of 11, while Wang Q, with 34 publications, also has an H-index of 17,

demonstrating the high quality of their research. Zhang Y completes the list of five authors with 33 articles and an H-index of 9 (Figure 3). These 5 authors with the most publications illustrate the trend that China, the country with the most publications, also has the authors with the most individual publications globally on improvements in agricultural planting machinery. These data not only indicate the significant amount of research carried out in China but also the high quality and impact of the same, as evidenced by the high H-indices of these authors.

Continuing with the study, the surveys indicate that the author, Taylor R., is the most globally cited, with 46 citations related to the theme of this study (Figure 4). An interesting point is to mention that this author has an H-index of 6 and 9 articles published in the period analyzed here. Another relevant aspect is the predominance of citations from Indian authors and the absence of Chinese authors, which can be indicative that agricultural machinery development in China is based on Indian information; also, it could be related to the similarity in the crop productions, such as rice and wheat and corn [7], at the top of the ranking of most cited authors (possibly due to the recent ramp up in Chinese publications).

Regarding the number of publications by affiliations, China Agricultural University leads with 138 articles, demonstrating China's predominance in this research field. Zhejiang Sci-Tech University, Jilin University, Nanjing Institute

Figure 3. Most relevant authors and index H.

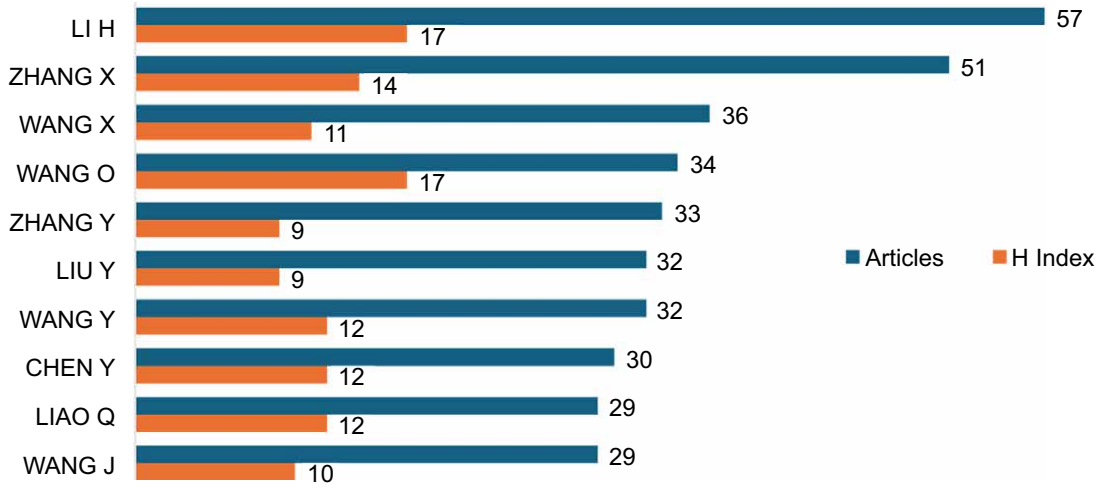

Figure 4. Most cited authors.

of Agricultural Mechanization, and Northeast Agricultural University are major contributors. The predominance of Chinese institutes and universities reflects China's substantial investment and focus on agricultural technological advances. An interesting point is that Brazil, occupying the fourth place in the ranking of publications by countries (Figure 1), has the affiliation Universidade Federal Santa Maria with the highest number of published articles (46) after the Chinese affiliations (Figure 5).

The evaluation of the most cited documents points in the first position the 2008 publication "No-Tillage Crop Production: A Revolution in Agriculture!" by author Triplett Jr [8], has 400 citations related to the theme of this study (Figure 6), shows a direct connection between the publication, innovation, and sustainability-driven by techniques improvements in agriculture such as no-tillage (NT), enabled by better planters, modern herbicides, and accumulated experience has revolutionized agriculture by allowing more efficient land management with less energy, labor, and machinery. NT improves erosion control and water and fertilizer use efficiency, often yielding better crops than tilled systems. Despite its sustainability, challenges remain for broader adoption and crop variety [8].

Figure 5. Most relevant affiliations.

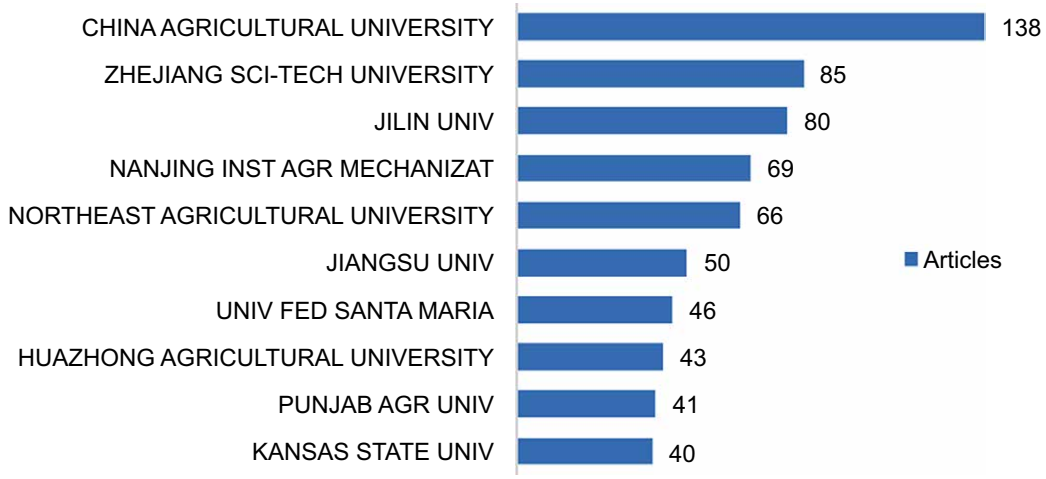

Figure 6. Most global cited documents.

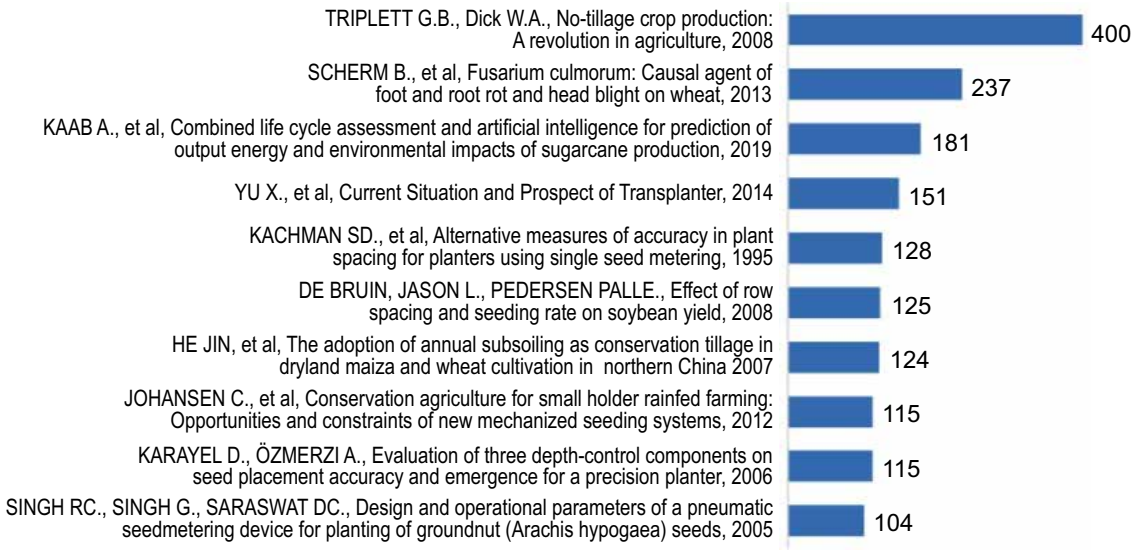

Continuing the relevant article's quick review, "Alternative measures of accuracy in plant spacing for planters using single seed metering," by Kachman [9], that examines the performance of planters using single seed metering mechanisms by evaluating the accuracy of seed placement. It discusses factors affecting seed spacing and compares various accuracy measures, including mean, standard deviation, quality of feed index, multiples index, miss index, and precision. The study concludes that mean and standard deviation are not suitable measures of accuracy [9]. Another remarkable article with significant citations, "Current Situation and Prospect of Transplanter—2014" by author Yu [10] and colleagues discuss the importance of transplanting agronomy for China's agriculture, emphasizing the role of potted-seeding transplanting machines in boosting grain yields. It reviews the evolution of transplanting machinery, analyzes current development levels, and forecasts future trends, stressing the need for advanced knowledge and skills to progress in this field [10].

Regarding the most frequent author's Keywords, the 15 most frequent (Figure 7), The result points to a particular relevance for the term agricultural machinery with 147 mentions, followed by design, planter, transplanter, and mechanization as the 5 most cited. One point that stands out is that the crops of corn and rice appear approximately 30 times, which makes it possible to conclude that they must be the cultivars with the most research and publications related to technological advances linked to improvements in yield, performance, and efficiency in planting equipment. Also, rice cultivation in Asia is related to a flooded technique, which requires modifications in standard machinery to work in those conditions.

Conclusion

This bibliometric review highlights the significant advancements in agricultural planting machinery over the past three decades. The analysis reveals a substantial increase in scientific publications, particularly precision equipment and sustainable technologies. China and the USA lead research output, with notable contributions from India and Brazil.

The findings show the rapid evolution of planting equipment technology, driven by the global need for increased agricultural efficiency and sustainability. Adopting new techniques and integrating automation, sensors, and renewable energy sources has enhanced the performance and precision of these machines, contributing to higher crop yields and reduced resource usage. This review also emphasizes the importance of international and interdisciplinary collaboration in advancing agricultural technologies.

Figure 7. Most frequent words (author's keywords).

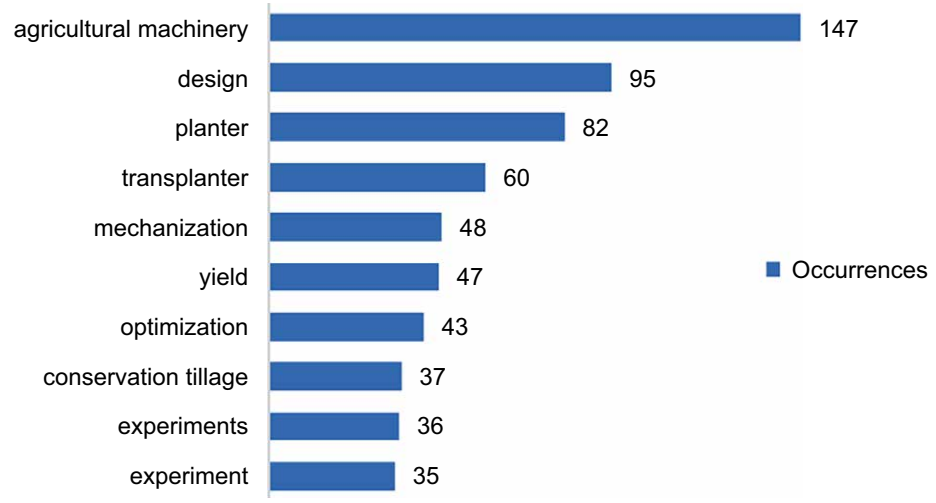

Overall, the research landscape for agricultural planting machinery is dynamic and growing, with significant contributions from leading institutions and prolific authors. Future research should continue to focus on emerging technologies and sustainable practices to address global challenges in food security and environmental sustainability.

Acknowledgments

The authors would like to acknowledge Shell Brasil and ANP (Agência Nacional do Petróleo, Gás Natural e Biocombustíveis) for the strategic support provided through regulatory incentives for Research, Development, and innovation. We also acknowledge EMBRAPII and SENAI CIMATEC for their encouragement and funding.

References

1. van Dijk M, Morley T, Rau ML et al. A meta-analysis of projected global food demand and population at risk of hunger for the period 2010–2050. Nat Food 2021;2:494-501.
2. Scopus database Available at: <https://www.scopus.com/search/form.uri?display=basic#basic>. Accessed on: June 5, 2024.
3. Web of Science. Available database at: <https://www.webofscience.com/wos/woscc basic-search>. Accessed on: June 5, 2024.
4. RStudio Team. RStudio: Integrated Development for R. RStudio, PBC, Boston, MA,2024.
5. Aria M, Cuccurullo C. Bibliometrix: An R-tool for comprehensive science mapping analysis, Journal of Informetrics 2017;11(4):959-975, Elsevier.
6. Food and Agriculture Organization of the United Nations – FAOSTAT Available database at: <https://www.fao.org/faostat/en/#data/QCL>. Accessed on: July 25, 2024.
7. Ministry of Agriculture & Farmers Welfare - India Available at: <https://pib.gov.in/PressReleasePage.aspx?PRID=1968931#:~:text=As%20per%20F inal%20Estimates%2C%20the,Wheat%20%E2%80%93%201105.54%20Lakh%20to nnes>. Accessed on: June 5, 2024.
8. Triplett, Jr, GB, Warren A. Dick. No-Tillage Crop Production: A Revolution in Agriculture! Celebrate the Centennial [A Supplement to Agronomy Journal] 2008:153-165.
9. Kachman SD, Smith JA. Alternative measures of accuracy in plant spacing for planters using single seed metering. Transactions of the ASAE 1995;38(2):379-387.
10. Yu X et al. Current situation and prospect of transplanter, transactions of the chinese society for agricultural machinery. 2014;45:44-53.

The Role of Enzymes in an Efficient Ethanol Production: A Review and Technological Prospection

Leandro Freitas Sales[1*], Douglas José Faria[1], Lilian Lefol Nani Guarieiro[1], Ana Lucia Barbosa de Souza[1], Sabrina Teixeira Martinez[1], Tatiana Oliveira do Vale[1]

[1]SENAI CIMATEC University; Salvador, Bahia, Brazil

This work reviews the literature on the use of enzymes in ethanol production. The bibliographic survey was carried out using the Web of Science (WoS) database, where advanced search techniques were applied with relevant keywords and Boolean operators. Articles published between 2015 and 2024 were selected, focusing on "Biotechnology Applied Microbiology" and "Energy Fuels". In total, 182 articles were analyzed using the Vosviewer software to build bibliometric networks. The results highlight the importance of enzymes as biocatalysts that increase the efficiency of ethanol production and explore technologies that can be implemented in industries to increase efficiency and reduce costs.

Keywords: Bioethanol. Enzymes. Lignocellulosic Biomass. Fermentation. Technological Prospecting.

The increasing demand for sustainable energy sources and the urgent need to mitigate climate change have driven biofuel research and development [1,2]. Among these, ethanol stands out as a promising alternative to fossil fuels [1-8]. Ethanol offers several advantages, including reducing greenhouse gas (GHG) emissions and potentially decreasing dependence on fossil fuels [3,9,10]. It is key in transitioning to a cleaner and more sustainable energy matrix.

Ethanol production can be classified into first-generation (1G), using sources such as corn and sugarcane juice, and second-generation (2G), employing lignocellulosic biomass [2,4,7]. While 1G ethanol is already widely commercialized, 2G ethanol faces significant technical and economic challenges. In this context, enzymes play a fundamental role in ethanol production, acting as biocatalysts that improve the efficiency of converting biomass into fermentable sugars and subsequently into ethanol.

Enzymes, as biocatalysts, can accelerate specific chemical reactions, such as the hydrolysis of polysaccharides into fermentable sugars and the subsequent fermentation into ethanol [8]. This catalytic ability increases process efficiency by reducing time and allows using renewable and abundant raw materials, such as lignocellulosic biomass, to produce second-generation (2G) ethanol. Furthermore, developing more robust and efficient enzymes through enzyme engineering can overcome biomass resistance and byproduct inhibition challenges, resulting in a more sustainable and economically viable process [8]. The use of enzymatic cocktails in the ethanol production process is still very costly [3].

Therefore, research and enhancement of enzymes are essential to advancing the commercial viability of ethanol as a clean and renewable energy alternative.

Technological prospecting can utilize bibliometric analysis to explore and assess large datasets, identifying emerging trends, research components, and collaboration patterns in a specific scientific field. This method uses quantitative techniques to analyze publication and citation metrics, providing a robust foundation for evaluating scientific and technological development. This study aimed to conduct a bibliometric analysis of the technical and economic feasibility of using enzymes in ethanol production, investigating related research topics and highlighting recent advances and challenges in this field.

Received on 13 September 2024; revised 21 December 2024.
Address for correspondence: Leandro Freitas Sales. Avenida Orlando Gomes, 1845, Piatã. Salvador, Bahia, Brazil. Zipcode: 41650-010. E-mail: leandrofreitassales@gmail.com.

J Bioeng. Tech. Health 2025;8(1):81-88

Materials and Methods

This research is a bibliographic review with a qualitative-quantitative character, as it includes a bibliometric analysis of articles published in the field of study and technological prospecting. Figure 1 provides an overview of how the research methodology for this study was established.

We used the Web of Science (WoS) academic database for this bibliographic review. This platform was chosen due to its comprehensiveness and relevance as a scientific database. The search for articles was conducted in April 2024, using the advanced search mode of WoS to achieve more terrific refinement in the research. We defined the most relevant keywords for the study topic and then included similar terms to capture more articles within the theme. Boolean operators combine the terms (AND to include all specified terms, OR to include any terms, NOT to exclude terms). In WoS, to search for terms exactly as written, they must be placed in double quotes, and to group terms and control the search order, they must be placed in parentheses. Table 1 shows how the search for articles was defined in this research.

After an initial search, we refined the study by focusing on articles from 2015 to 2024 and setting the research areas to "Biotechnology Applied Microbiology" and "Energy Fuels." This yielded 182 articles. We then began data processing, examining the relationship between years and publication numbers, identifying the most cited publications, and linking articles to the SDGs. Using Vosviewer software, we constructed bibliometric networks to analyze authors' most frequently used keywords (minimum of 5 occurrences, resulting in 25 keywords) and the most frequently occurring words in the texts (minimum of 10 occurrences, resulting in 34 keywords).

Literature Review

This section presents the most discussed concepts in publications regarding first-generation ethanol (1G), second-generation ethanol (2G), the role of enzymes in ethanol production, and emerging technologies for increasing efficiency and reducing costs in their use in industrial ethanol production processes.

First Generation Ethanol Production (1G)

First-generation bioethanol production uses food raw materials, mainly starchy materials such as corn, wheat, barley, cassava, and potatoes, as well as sucrose-containing raw materials such

Figure 1. Flowchart of method used.

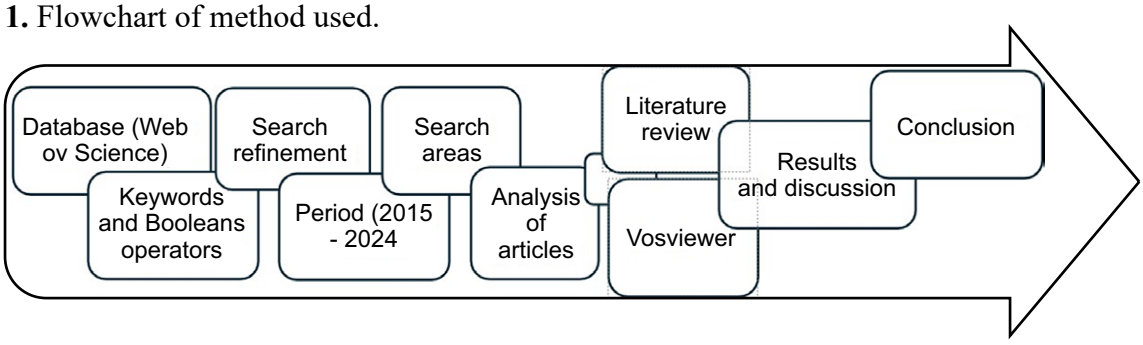

Table 1. Search parameters used in Web of Science.

(Keywords 1)	Boolean Operator	(Keywords 2)
(ethanol OR bioethanol)	AND	(1G OR first-generation OR 2G OR second-generation)
(Keywords 3)		**(Keywords 4)**
(enzymes OR enzyme)		(fermentation OR fermentacion)

as sugar cane, sugar beet, and sweet sorghum [1,3]. *Saccharomyces cerevisiae* is the most used microorganism in the bioethanol industry, having advantages such as high fermentative capacity, tolerance to ethanol, low demand for nutrients, and less formation of byproducts [9].

However, producing first-generation bioethanol from food crops, such as corn and sugarcane, raises the food *versus* fuel debate, raising concerns about food security and rising food prices [1,2]. This competition with food has brought about the need to find more sustainable ways of producing ethanol, leading to the development of second-generation (2G) ethanol.

Although 1G ethanol is well-established industrially, searching for alternatives that do not compete with food production has become essential. Using agricultural residues and lignocellulosic biomass in 2G ethanol production emerges as a promising solution, reducing the impact on food security and offering a more sustainable pathway for biofuel production.

Second Generation Ethanol Production (2G)

Second-generation (2G) bioethanol is typically produced from lignocellulosic biomass, but it is also possible to use industrial byproducts, such as whey or crude glycerol, as feedstock [1]. The conversion of lignocellulose into reducing sugars is more complex than that of starch used in first-generation (1G) ethanol production [1]. However, 2G bioethanol, produced from lignocellulosic biomass such as agricultural residues, offers an alternative that does not compete with food production and uses materials that would otherwise be wasted [5].

The yeast *Saccharomyces cerevisiae*, widely used in the ethanol industry, quickly ferments hexoses present in 1G substrates. However, it has a low capacity to ferment pentoses, which are predominant in 2G substrates [9]. Converting lignocellulosic biomass into ethanol is challenging due to the recalcitrant nature of cellulose and hemicellulose, which require pretreatment and enzymatic hydrolysis [1].

Researchers worldwide are focused on finding routes that make 2G ethanol production viable. Key areas of research include the development of efficient pretreatment methods and the engineering of microbial strains to improve pentose fermentation. These innovations are essential to overcoming the technical and economic obstacles associated with 2G ethanol production.

Enzymes and Their Applications

Enzymes are biocatalysts that directly hydrolyze polysaccharides into fermentable sugars. Compared to other industrial techniques, enzymatic hydrolysis has the main advantage of being sustainable and environmentally friendly. Unlike acids, enzymatic hydrolysis reacts only with specific substrates, generating significantly lower inhibitors [2].

The enzymatic hydrolysis of lignocellulosic biomass primarily involves cellulases and hemicellulases. Cellulases break cellulose into glucose, while hemicellulases break down hemicellulose into a mixture of pentoses and hexoses [3]. This synergistic action of the enzymes is essential for efficiently converting biomass into fermentable sugars.

The cost of enzymes is a significant component of the production cost of 2G ethanol, representing about 65% of the total cost in the short term [7]. However, these costs are expected to decrease significantly with technological advances in 2G ethanol production. Local enzyme production, genetic engineering of microorganisms to increase enzyme production, and the use of enzymatic cocktails are strategies that can potentially reduce these costs.

Technical-Economic Viability

Among the challenges in establishing efficient 2G ethanol production, the technical and economic feasibility of implementing enzymes in the process stands out. Researchers have been striving to identify efficient ways to reduce enzyme usage

costs and enhance technical feasibility. Cripwell and colleagues (2020) conducted a study that concludes that integrating first—and second-generation technologies can consolidate the advantages of both by utilizing starch-rich and lignocellulosic raw materials in a single plant, significantly increasing ethanol production efficiency and reducing greenhouse gas (GHG) emissions [11].

The articles found in the literature present various processes for saccharification and fermentation of lignocellulosic substrates. Dahnum and colleagues (2015) analyze the methods of separate hydrolysis and fermentation (SHF) and simultaneous saccharification and fermentation (SSF) [3], concluding that the SSF method has superior performance in final ethanol production since this process combines enzymatic hydrolysis and fermentation in a single reactor, increasing efficiency and reducing operational costs. This process is also corroborated by Choudhary and colleagues (2016) [6].

One way to significantly reduce enzyme costs is to produce these strains within the industry. Siqueira and colleagues (2020) [4] conducted a comparative study that demonstrates a significant cost reduction compared to the purchase and transportation of enzymes. The life cycle assessment (LCA) presented by Olofsson and colleagues (2017) reveals that integrated enzyme production can reduce greenhouse gas emissions compared to off-site enzyme production, highlighting the potential environmental benefits of integrated processes [10].

An important highlight in enzyme use is the implementation of enzymatic cocktails since each enzyme acts on a specific substrate. The use of enzymatic cocktails with different enzymes increases saccharification efficiency. Pandiyan. et al. (2019) highlight that combining cellulase and hemicellulase resulted in a 30% higher yield than isolated cellulases [5].

The studies also found a strong emphasis on genetic engineering. Choudhary and colleagues (2016) explain that developing thermotolerant yeasts through genetic and metabolic engineering can significantly improve lignocellulosic ethanol production efficiency and economic viability [6].

Rocha-Martin and colleagues (2017) show that adding additives such as PEG4000 significantly increased glucose yields by enhancing the activity of beta-glucosidase and endoglucanase without affecting their thermal stability [8]. This result demonstrates that enzymatic supplementation further enhances their hydrolytic power.

Results and Discussion

This section presents the results of the bibliometric review conducted. It explains the types of publications on the topic over the years, the most cited works, the relationship of these articles with the SDGs, the most frequently used keywords by the authors, and the most frequent keywords in the texts.

Relationship of Years with Number of Publications

Between 2015 and 2024, publications on sustainability and clean energy increased significantly. The number of publications grew exponentially from 2015 to 2017, driven by the adoption of the Sustainable Development Goals (SDGs) by United Nations member countries, peaking in 2017 as researchers rushed to present experimental results. However, there was a decline in 2019, likely due to the COVID-19 pandemic.

From 2015 to 2019, most publications were experimental with practical results. After 2019, bibliographic review articles increased, reflecting lockdown restrictions that limited laboratory access. Figure 2 shows the growth of publications and citations over the years in WoS.

In reviewing articles on the role of enzymes in ethanol production, there was a strong emphasis on the Sustainable Development Goals (SDGs). Most articles related to SDG 7 (Affordable and Clean Energy) and SDG 12 (Responsible Consumption and Production) highlight the importance of these themes for sustainability.

Figure 2. Several publications and citations *vs*. years.

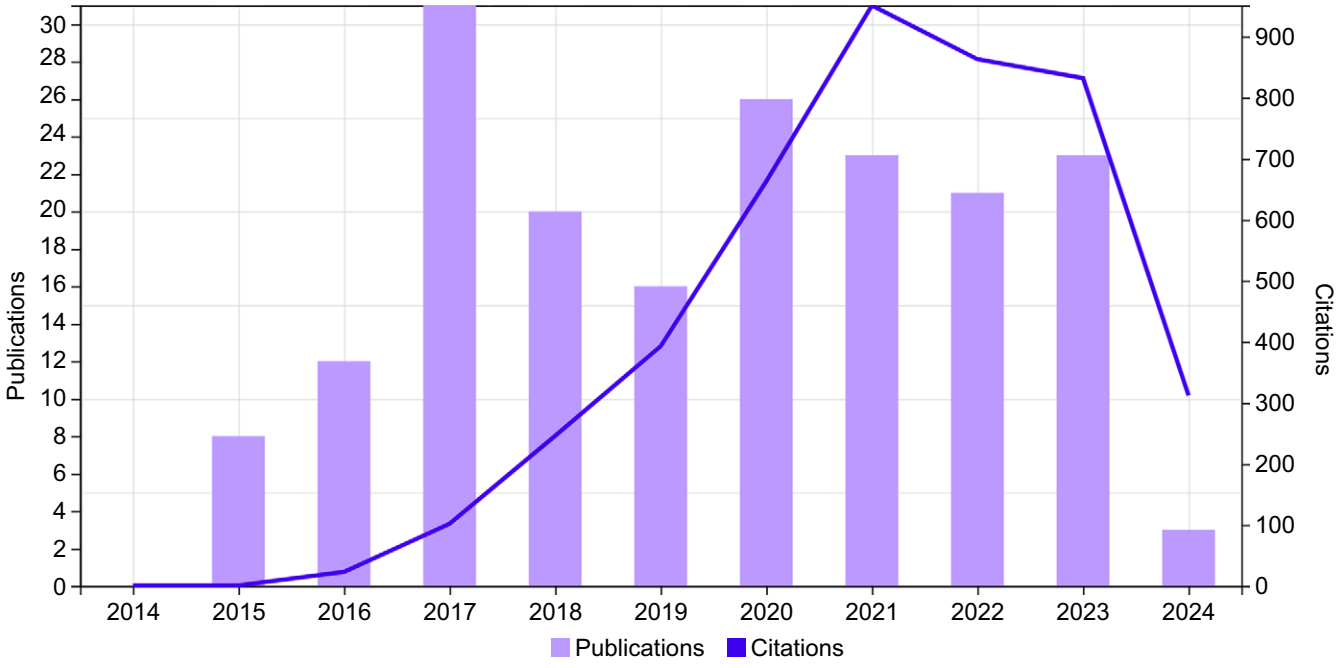

SDG 3 (Good Health and Well-being) and SDG 15 (Life on Land) were noted, emphasizing biofuels' environmental and public health benefits and their positive impact on terrestrial ecosystems. Among the countries publishing during this period, Brazil led with 53 publications, attributed to its leadership in first-generation ethanol production from sugarcane and efforts to develop second-generation ethanol from sugarcane bagasse. India ranked second with 31 publications, focusing on efficient biofuel alternatives due to food scarcity challenges. Second-generation ethanol, which doesn't compete with food production, is seen as viable. The United States was third with 16 publications, being the largest ethanol producer, mainly using corn and exploring biofuels from lignocellulosic crops for more efficient production.

Keywords Most Used by Authors and the Most Frequent in Texts

The selected publications created two bibliometric networks, as shown in Figure 3. In Figure 3A, we have the sets of the authors' most used keywords; in Figure 3B, we have the most frequently found keywords in the body of the texts. Words with the same colors indicate a higher co-occurrence in the articles, while the circle size represents the most frequent keywords. The connections between words indicate interactions among them, regardless of the group. Figure 3A, 25 high-occurrence keywords were selected and divided into five groups. Key terms include "bioethanol", "fermentation", "enzymatic hydrolysis", "ethanol", "lignocellulosic biomass" and "pretreatment". In Figure 3B, 34 high-occurrence keywords were chosen and organized into four distinct groups, identifying "fermentation," "bioethanol," "enzymatic hydrolysis," and "saccharification" as the most frequent words in each group. The analysis of bibliometric networks allows the selection of the most significant articles for reading by identifying the most relevant keywords for the search. This methodology was used to determine the references of this work among the 182 articles identified in WoS.

The reviewed studies demonstrate that implementing enzymes in the 2G ethanol production process can significantly increase process efficiency. Additionally, local enzyme

Figure 3. Bibliometric network of authors' keywords.

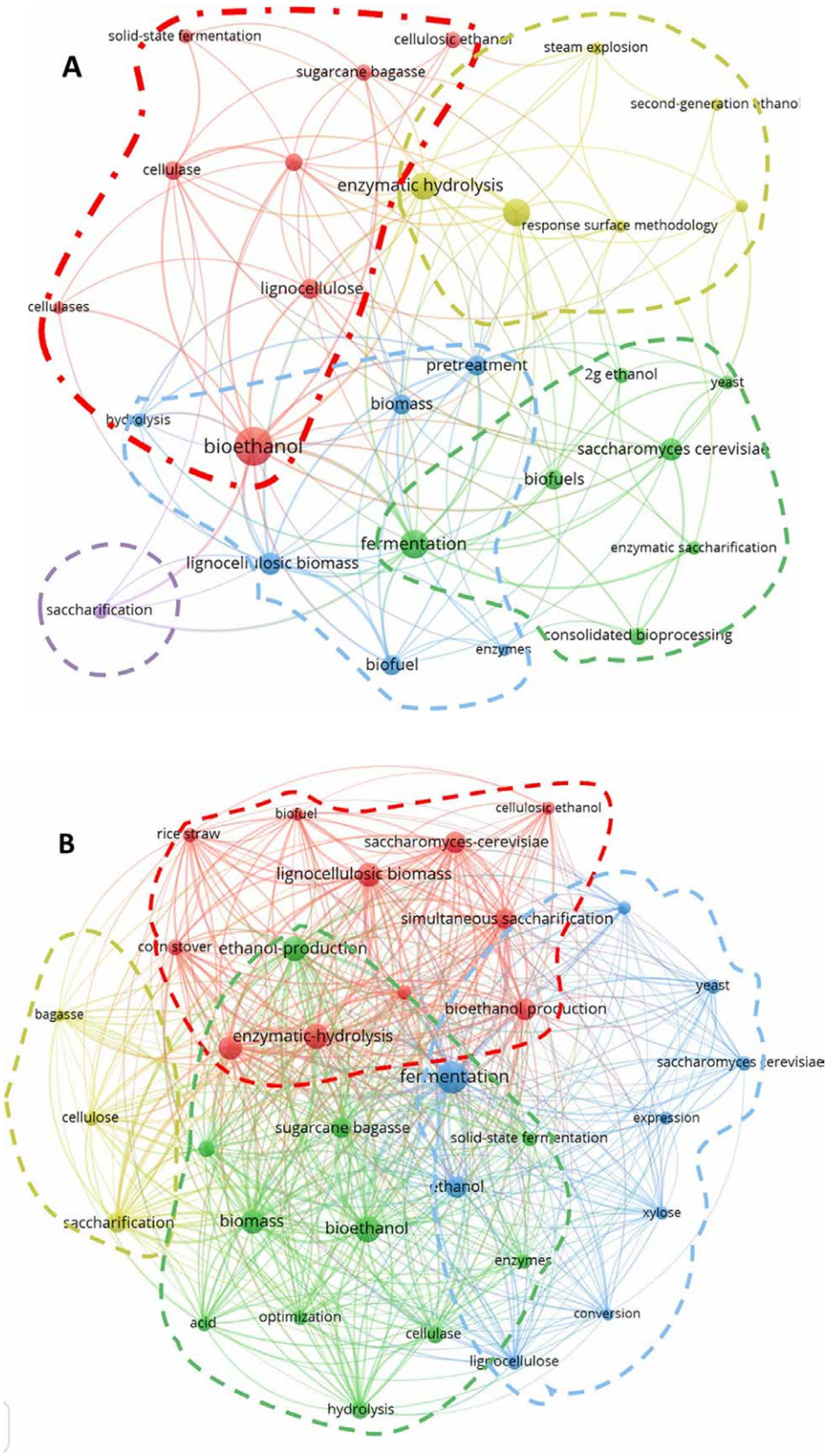

production can reduce production costs by up to 40%, as evidenced by Siqueira and colleagues (2020) [4]. Integrating first and second-generation technologies can increase profits by up to 25% due to economies of scale and resource optimization [11]. The life cycle assessment (LCA) presented by Olofsson and colleagues (2017) reveals that integrated enzyme production can reduce greenhouse gas emissions by up to 15% [10]. These data confirm that second-generation ethanol production using enzymatic processes is a viable and sustainable alternative with significant potential to contribute to the biofuel industry.

Conclusion

This study employed technological foresight and bibliometric analysis to thoroughly explore and evaluate large data sets, identifying emerging trends, research components, and collaboration patterns in ethanol production. The analysis highlighted the growing importance of enzymes as biocatalysts in efficient ethanol production, emphasizing their critical role in both first- and second-generation biofuels. Enzymes are essential to efficiently convert lignocellulosic biomass into fermentable sugars, reducing the presence of inhibitors. Additionally, integrating first- and second-generation technologies into a single factory can increase efficiency and reduce greenhouse gas emissions.

The study also demonstrated the superiority of the simultaneous saccharification and fermentation (SSF) process over other methods. Promising strategies to reduce enzyme-related costs include local production of enzymes, genetic engineering of microorganisms, and enzyme cocktails. These strategies make the second-generation (2G) ethanol production process more economically viable. In conclusion, this study affirms that using enzymes in the production of second-generation ethanol is a viable and sustainable alternative with significant potential to assist in the transition to a cleaner and more efficient energy matrix. Investment in research and development is essential to overcome technical and economic challenges, promote the commercial strategy for 2G ethanol, and promote scientific and technological progress in this field.

Acknowledgments

The authors would like to acknowledge Shell Brasil and ANP (Agência Nacional do Petróleo, Gás Natural e Biocombustíveis) for the strategic support provided through regulatory incentives for Research, Development, and innovation. We also acknowledge EMBRAPII and Senai CIMATEC for the encouragement and funding.

References

1. Robak K, Balcerek M. Review of second generation bioethanol production from residual biomass. Food technology and biotechnology 2018;56(2):174.
2. Rastogi M, Shrivastava S. Recent advances in second generation bioethanol production: An insight to pretreatment, saccharification and fermentation processes. Renewable and Sustainable Energy Reviews 2017;80:330-340.
3. Dahnum D et al. Comparison of SHF and SSF processes using enzyme and dry yeast for optimization of bioethanol production from empty fruit bunch. Energy Procedia 2015;68:107-116.
4. Siqueira JGW et al. Current advances in on-site cellulase production and application on lignocellulosic biomass conversion to biofuels: a review. Biomass and Bioenergy 2020;132:105419.
5. Pandiyan K et al. Technological interventions for utilization of crop residues and weedy biomass for second generation bio-ethanol production. Renewable Energy 2019;132:723-741.
6. Choudhary J, Singh S, Nain L. Thermotolerant fermenting yeasts for simultaneous saccharification fermentation of lignocellulosic biomass. Electronic Journal of Biotechnology 2916;21:82-92.
7. Junqueira TL et al. Techno-economic analysis and climate change impacts of sugarcane biorefineries considering different time horizons. Biotechnology for Biofuels 2017;10:1-12.
8. Rocha-Martín J et al. Additives enhancing enzymatic hydrolysis of lignocellulosic biomass. Bioresource Technology 2017;244:48-56.
9. Roukas T, Kotzekidou P. From food industry wastes to second generation bioethanol: a review. Reviews in Environmental Science and Bio/Technology 2022;21(1):299-329.

10. Olofsson J et al. Integrating enzyme fermentation in lignocellulosic ethanol production: life-cycle assessment and techno-economic analysis. Biotechnology for biofuels 2017;10:1-14.

11. Cripwell R A. et al. Consolidated bioprocessing of raw starch to ethanol by *Saccharomyces cerevisiae*: Achievements and challenges. Biotechnology Advances 2020;42:107579.

Review of Techniques for Measuring and Monitoring Seabed Subsidence

Matheus Anselmo da Silva[1*], Miguel Barbosa de Argolo[1], Rodrigo Fonseca Carneiro[1]
[1]SENAI CIMATEC University; Salvador, Bahia, Brazil

Underwater subsidence is an event present in several petroleum exploration areas. Early detection of these events minimizes environmental consequences and improves the exploration region's geomechanical model. This material reviews works that present solutions for monitoring and measuring underwater subsidence. It was identified that most techniques use pressure data to monitor the subsidence occurrences, and some use inclination data. The identified techniques include data treatment: for pressure data, a 14 data average, and using a local measurement as a reference, and for inclination data, Kalman filter and integration of angles. It was concluded that using pressure data with a local reference offers the best accuracy.
Keywords: Seabed Subsidence. Subsidence Monitoring. Pressure Sensing. Angle Sensing.

In offshore production, especially in the oil and gas industry, monitoring structures like pipelines and Christmas trees is essential to ensure the safety and integrity of these installations. In addition to these structures, the marine environment is typically monitored by measuring factors such as temperature, acidity, salinity, and the dynamics and characteristics of the underwater soil. Data on seabed depth is also important for environmental monitoring and helps acquire geomechanical models. Depth data and inclination measurements can be used to identify potential deformations in the seabed.

A common deformation in offshore production is seabed subsidence, which is the vertical displacement of soil. Various factors, including the extraction of oil, can cause it. Due to the depth, external influences, and the difficulty of accessing deep regions, obtaining high-accuracy data about vertical displacement is challenging. In addition to direct measurements, in this case, depth measurement, other measurements, and strategies can be employed to detect and monitor vertical deformations in the seabed.

This material reviews leading research, articles, and other scientific materials related to monitoring submarine subsidence. The research provides the latest methods and strategies for measuring vertical displacement to achieve high-accuracy data in monitoring and measurement of seabed subsidence.

Received on 26 September 2024; revised 20 November 2024.
Address for correspondence: Matheus Anselmo da Silva. Avenida Orlando Gomes, 1845, Piatã. Salvador, Bahia, Brazil. Zipcode: 41650-010. E-mail: matheus.anselmo@fieb.org.br.

J Bioeng. Tech. Health 2025;8(1):89-93

Materials and Methods

The selection of papers followed specific criteria. The materials selected needed to include contents directly related to the development of seabed monitoring and pressure and depth measurement in deep-sea environments.

Keywords such as "submarine subsidence," "seabed deformations," and "subsidence sensing" were used to search for materials in the Scopus bibliographic database. The review included each material if its abstract indicated relevant content about seabed monitoring.

The publications from 2012 to 2024 were obtained from Earthdoc, SEG Library, ScienceDirect, and MDPI. After selecting the materials, analyses were conducted to identify current strategies for monitoring and identifying submarine subsidence.

Results and Discussion

There are many strategies for identifying and monitoring seabed subsidence. Some involve collecting data to measure vertical displacement and modeling the exploration field. Thomas

and colleagues [1] presented various strategies for monitoring subsidence were reviewed and presented, including air gap measurements, bathymetry, tiltmeters, and bottom pressure recorders.

As noted by Hatchell and colleagues [2], many strategies use pressure data to monitor subsidence, the most widely used technique for measuring seafloor subsidence. They recommended three strategies for monitoring and measuring subsidence: a self-calibrating system, the placement of a weight collar on PMTS, and pressure measurements with a reference at the seabed.

Aimed to acquire high-quality data on pressure measurement, Sasagawa and Zumberge [3] developed a tool, the SCPR, a self-calibrate pressure recorder. This sphere-shaped tool, with a diameter of 41.6 cm, contains two recording pressure gauges to measure ambient seawater pressure. For every ten days, for 20 minutes, the gauges are hydraulically connected to a piston gauge that provides a reference pressure to determine their drift and account for it on the pressure measurement. The result pressure data accuracy is 5 cm.

Also, intending to obtain high-quality pressure data, Vries and colleagues [4] applied a 14-day average to data collected by various pressure monitoring transducers (PMTs) instruments across the Gulf of Mexico. The 14-day average reduced the effect of tides and other external effects. Beyond this smooth method, a weight collard and tripod base were also placed on PMTs to reduce external influences. Figure 1 shows the influence on the data after the weight collar was placed with the tripod; each line on the graph is from a distinct PMT.

Another strategy was developed by Eiken and colleagues [5], using high-precision pressure sensors, concrete monuments, and ROVs. This technique involves moving sensor tools between concrete monuments, some expected to subside and others not. The monuments expected not to subside serve as references to other ones; in other words, it is necessary to assume that some regions of the monitoring target will not suffer from subsidence. Figure 2 shows the results of this technique applied in the Ormen Lange field. The main advantage of this technique is its accuracy, which is less than 1 cm. However, it requires that some areas not suffer vertical displacement and involve high costs due to the need for skilled ROV operators on vessels. Dutta and colleagues [6] also applied the strategy of measuring reference to others. Figure 3 shows the difference in subsidence data after the reference data is considered for all measurements. After the correction, the subsidence data appears more homogeneous and continuous with smoother gradation. This application's resulting accuracy was 3 cm.

Other sensors may also be employed to aid in monitoring and identifying subsidence.

Figure 1. Pressure data before and after the installation of the weight collar.

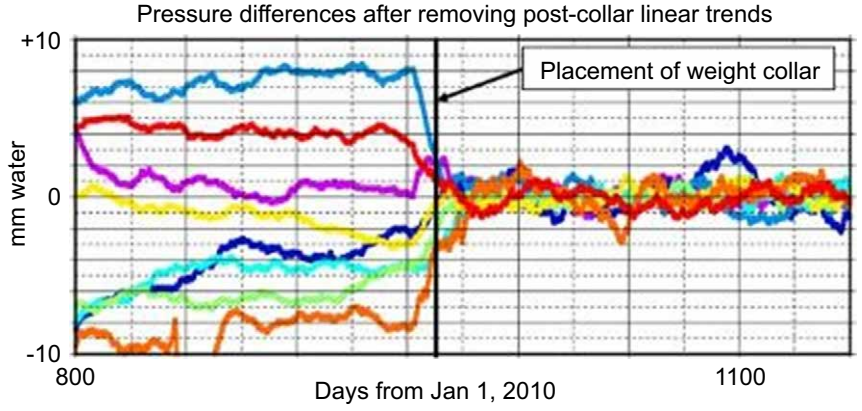

Source: Hatchell and colleagues [2].

Figure 2. Subsidence monitoring on Ormen Lange.

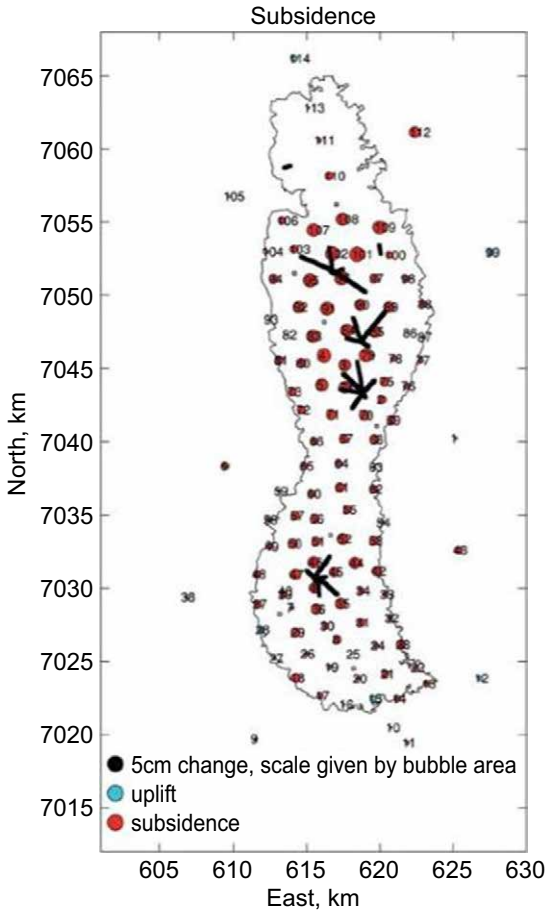

Source: Hatchell and colleagues [2].

Inclinometer and accelerometer sensors were used to track ground behavior on top of a tunnel section to monitor ground subsidence [7]. In addition to the data collected by the sensors, filtering was applied to lessen noise in the signal. The filtering process was executed by applying a Kalman Filter to the original signal. Figure 4 presents the graph of the original and the treated data.

The data from two sensors, the inclinometer and the accelerometer, and the result of the Kalman Filter application are shown. As expected, the data from the Kalman filter had a small noise presence. A significant variation in filtered signal may indicate the occurrence of ground subsidence in the tunnel. The same principle can be used to accuse or identify subsidence at the seabed.

Aimed directly at seabed subsidence, Miandro and colleagues [8] show a system that uses tiltmeters to monitor subsidence. The system's principle is to allocate tiltmeters in an array over the field to measure the inclination of the soil at specific points. Integration over distance is used to obtain data about subsidence. Each node of the array is separated by 300 m.

Figure 5 shows the layout of this system. Beyond the array of tiltmeters, a GPS station is presented as central for acquiring data from the sensors. Another strategy for monitoring subsidence is deploying fiber cables, according to Measures [9].

The cable-based subsidence monitoring system was presented in three ways of measurement: strain, cable inclination, and pressure measurement.

Figure 3. Measured relative subsidence before (left) and after (right) corrections.

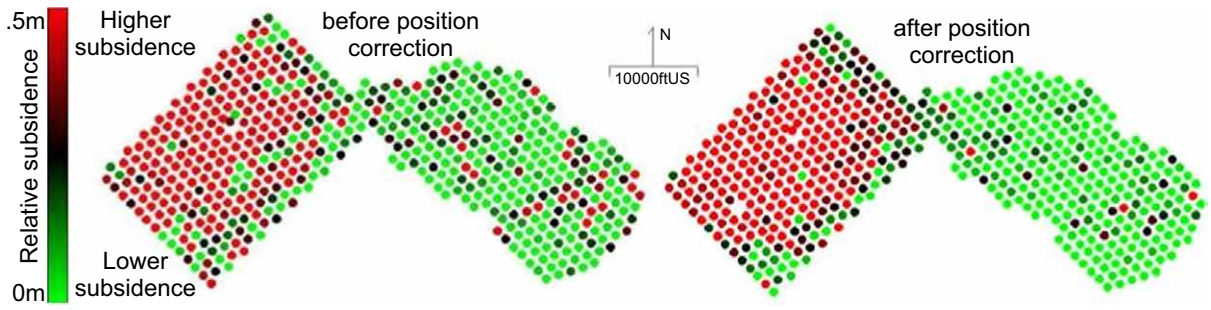

Source: Dutta and colleagues [6].

Figure 4. Data from the accelerometer and inclinometer of two nodes.

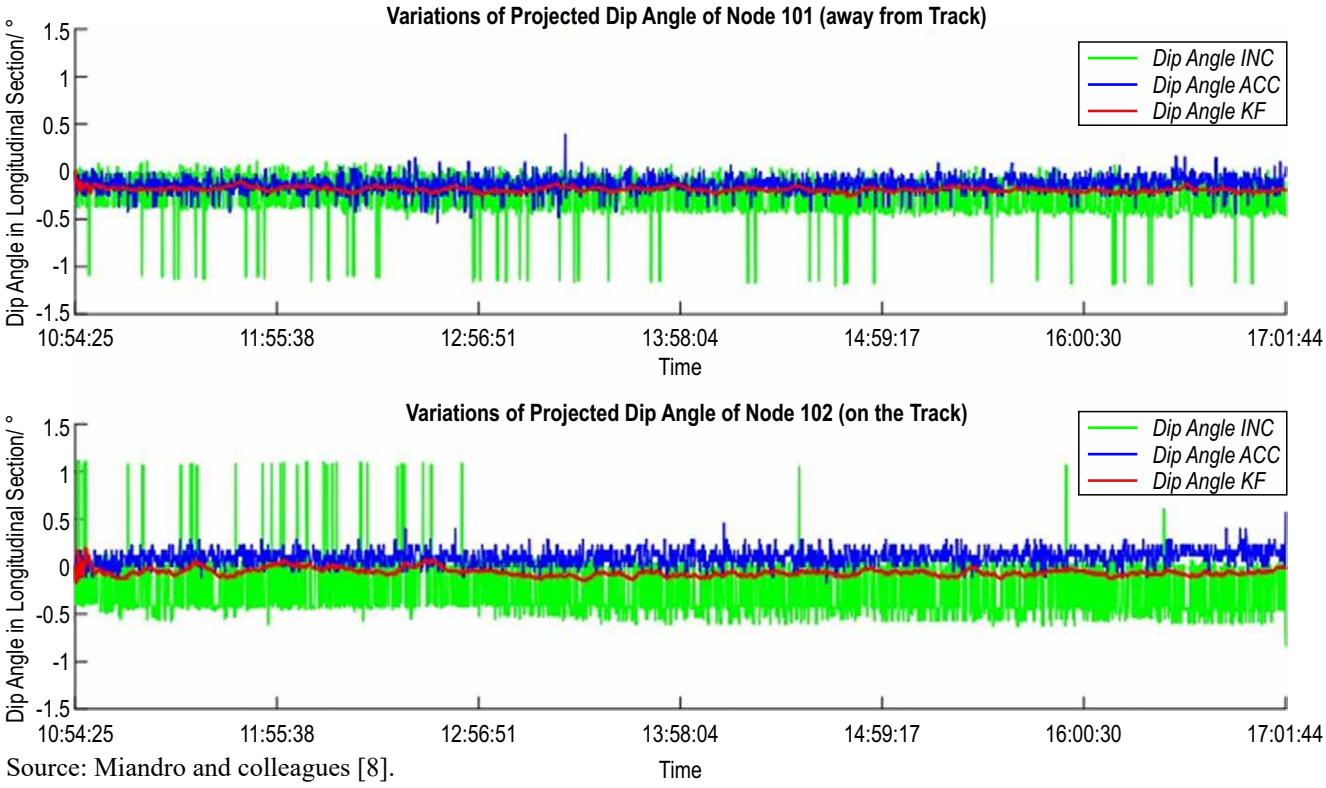

Source: Miandro and colleagues [8].

Figure 5. Array of depth sensor.

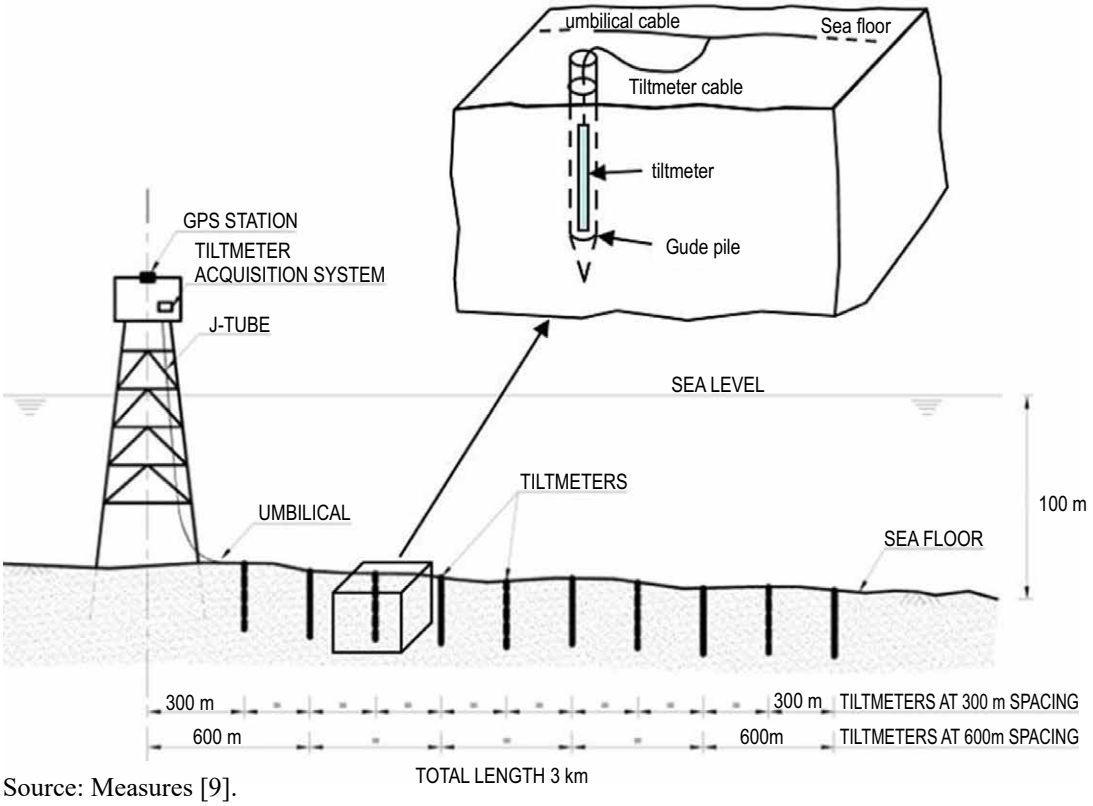

Source: Measures [9].

The strain measurement considers that the shape of the cable can be obtained through data from optic sensors that consider a certain distance of a neutral line. So, the occurrence of strain on the cable may indicate the occurrence of subsidence. The inclinations measurement considers that an inclination of a part of the cable can result in the vertical displacement of the other part, which can be viewed as a subsidence occurrence. Pressure measurement detects pressure changes across the cable when the cable moves vertically.

Conclusion

There are many strategies for monitoring and measuring subsidence. Most of them use pressure to infer the possible vertical displacement, but sensors that can collect the inclination and angle of soil can also aid in motoring. Beyond the raw measurements, the data treatment also plays an important role in monitoring. The Kalman filter method used on sensors that measure angles and inclination provided a signal with a small presence of noise, which is suitable for monitoring.

Additionally, it was noted that a 14-day average is a good strategy to reduce noise on PMTs, which can result in pressure sensors. As with anyone, pressure data on the seabed suffer from noise and external effects. Using a reference measurement that will not suffer from subsidence to others is a good strategy because it reduces most external effects and has accuracy below 1 cm over 2000 m of depth.

References

1. Thomas F, Livio FA, Ferrario MF, Pizza M. A review of subsidence monitoring techniques in offshore environments. Sensors 2024;4164.
2. Hatchell P, Vries RD, Gee V, Cousson H. Seafloor deformation monitoring: Past, present, and future. SEGAM 2017:5233-5238.
3. Sasagawa G, Zumberge MA. A self-calibrating pressure recorder for detecting seafloor. IEEE Journal of Oceanic Engineering 2013:447-454, 2013.
4. Vries RD, Noble T, Hatchell P, Dunn S. Along-term seafloor deformation monitoring campaign at ormen lange gas field. First EAGE Workshop on Practical Reservoir Monitoring 2017.
5. Eiken O, Zumberge M, Stenvold T, Sagasawa G, Nooner S. Gravimetric monitoring of gas production from the Troll field. Geophysics 2008.
6. Dutta P, Kiyashenko D, Wang K, Libak A. Subsidence measurement and improved statics solutions through accurate node depth determination during time-lapse deepwater OBN surveys. International Meeting for Applied Geoscience & Energy, 2023.
7. Li C, Azzam R, Steeger-Fernandez TM. Kalman filters in geotechnical monitoring of ground subsidence using data from MEMS sensors. Sensors 2016.
8. Miandro R, Dacome C, Mosconi A, Roncari G. Subsidence monitoring system for offshore applications: technology scouting and feasibility studies. PIAHS 2015:323-330.
9. Measures RM. Structural monitoring with fiber optic technology. Academic Press Inc, San Diego, cap. 5, 6, 7, 716 pp., 2001.

Detection Methods in CV-QKD System: A Systematic Literature Review

Maria Heloísa Fraga da Silva[1*], William Emanuel Viana[1], Seyed Saman Mahjour[1], Valéria Loureiro da Silva[1]
[1]QuIIN - Quantum Industrial Innovation, EMBRAPII CIMATEC Competence Center in Quantum Technologies, SENAI CIMATEC SENAI CIMATEC University: Salvador, Bahia, Brazil

Continuous Variable Quantum Key Distribution (CV-QKD) aims to strengthen communications security by using quantum mechanics to protect encryption against eavesdropping. In this context, the effective detection of quantum states is a crucial factor for the performance and security of CV-QKD systems. In order to provide a current and concise overview of the detection methods used in experimental CV-QKD setups, 42 articles published between 2019 and 2024 were selected and analyzed. As a result, trends were identified, such as the temporal evolution of publications and the predominant detection method. In summary, CV-KD detection studies have shown an upward trend over the last five years and are promising for the future of communications security.
Keywords: Systematic Literature Review. Quantum Key Distribution. Continuous Variable. Detection.

Security is crucial in a digital environment increasingly threatened by sophisticated attacks [1]. In this context, Continuous Variable Quantum Key Distribution (CV-QKD) emerges as a technology that promises to shape the future of communication, guaranteeing the protection of cryptographic keys through the principles of quantum mechanics [2]. Using the unique properties of quantum states, CV-QKD offers cryptography theoretically immune to interception, surpassing traditional methods [3]. Considering the growing complexity of cyber threats, CV-QKD represents an advanced solution for ensuring secure communication.

Although CV-QKD systems have been extensively studied [4], there is a gap in the literature regarding reviews that focus specifically on detection methods. Efficiently detecting quantum states is crucial to the efficacy of CV-QKD systems, where homodyne and heterodyne detection methods are particularly highlighted [5]. While homodyne detection is recognized for its sensitivity and precision, heterodyne detection is known for its speed and robustness [6]. This study aims to fill the gap in the literature by reviewing detection methods in detail, offering a critical analysis intended to provide an overview of this topic for future studies.

This paper is structured as follows: Section 2 details the research methodology. Section 3 presents the results. Section 4 summarizes the conclusion of our study.

Materials and Methods

Review Method

The method used is a systematic literature review (SLR), which is defined as a protocol-driven comprehensive review and synthesis of data focusing on a topic or related key questions [7]. Hereinafter, the essential aspects of an SLR are defined, such as the research questions that will guide the study, the search strategy adopted, and the exclusion criteria that will delimit the selection of articles [8,9].

Research Questions

The five research questions presented in Table 1 will guide this study. Therefore, the answers presented later will satisfy the objective of this review.

Search Strategy

The search strategy involves an automated search utilizing a search string to ensure a systematic approach, as recommended by previous

Received on 28 September 2024; revised 22 November 2024.
Address for correspondence: Maria Heloísa Fraga da Silva. Avenida Orlando Gomes, 1845, Piatã. Salvador, Bahia, Brazil. Zipcode: 41650-010. E-mail: maria.fraga@fbter.org.br.

J Bioeng. Tech. Health 2025;8(1):94-100

research. Four digital libraries are used here: IEEE Xplore, Scopus, arXiv, and Google Scholar. A comprehensive search string incorporates Quantum Key Distribution, Continuous Variable, and Detection. Variations of "CV" and equivalent terms used for methods are included, along with specifications for Detection in Homodyne or Heterodyne. The final search string is: "QKD" AND ("CV" OR "Continuous Variable" OR "Continuous-Variable") AND "Detection" AND ("Homodyne" OR "Heterodyne") AND ("Method" OR "Technique" OR "Implementation" OR "Design"). Adapted search strings for each database are provided in Table 2.

Study Selection

The four exclusion criteria used to select the primary studies are shown in Table 3.

Selection Process

Figure 1 shows a workflow of the selection process, from selecting the digital libraries to extracting the data needed to answer the research questions. The blue hexagons indicate the number of articles filtered after each of the five stages shown in the image.

Threats to Validity

This review aims to analyze studies on detection methods used in experimental setups of CV-QKD systems. It is worth noting that potential biases were not considered in the selection of studies and that the search was not conducted through a manual analysis of all journal article titles. Consequently, some relevant articles on

Table 1. Research questions on literature review.

ID	Research Question
RQ1	Which journal is the most significant concerning publications on QKD detection methods?
RQ2	Which kind of detection methods are the most used in CV-QKD systems?
RQ3	What are the advantages of the detection method(s) discussed in the article?
RQ4	What methods of Digital Signal Processing (DSP) are researchers selecting?
RQ5	Which model of the interferometer is most often used in experimental CV-QKD setups?

Table 2. Search string according to the database.

Database	Search String
IEEE Xplore	"All Metadata": "QKD") AND ("All Metadata": "CV" OR "All Metadata": "Continuous Variable" OR "All Metadata": "Continuous-Variable") AND ("All Metadata": "Detection") AND ("All Metadata": "Homodyne" OR "All Metadata": "Heterodyne") AND ("All Metadata": "Method" OR "All Metadata": "Technique" OR "All Metadata": "Implementation" OR "All Metadata": "Design"
Scopus	"QKD" AND ("CV" OR "Continuous Variable" OR "Continuous-Variable") AND "Detection" AND ("Homodyne" OR "Heterodyne") AND ("Method" OR "Technique" OR "Implementation" OR "Design")
arXiv	AND all= "QKD"; AND all= "CV" OR "Continuous Variable" OR "Continuous-Variable"; AND all= "Detection"; AND all= "Homodyne" OR "Heterodyne"; AND all= "Method" OR "Technique" OR "Implementation" OR "Design"
Google Scholar	"QKD" AND ("CV" OR "Continuous Variable" OR "Continuous-Variable") AND "Detection" AND ("Homodyne" OR "Heterodyne") AND ("Method" OR "Technique" OR "Implementation" OR "Design")

Table 3. Exclusion criteria on literature review.

ID	Exclusion Criteria
EC1	Article not written in English
EC2	Article published before 2019 (5 years ago)
EC3	Article does not cover CV-QKD systems only
EC4	Article does not cover a detection method in detail

Figure 1. Workflow of the selection process.

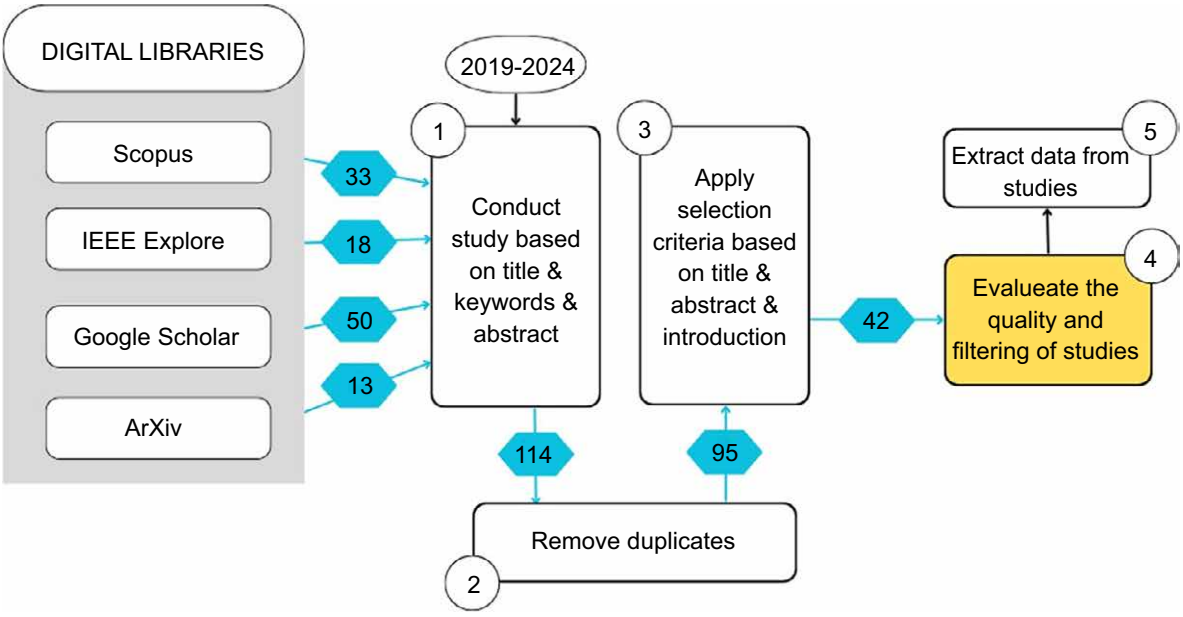

detection from conference proceedings or journals may have been missed. In addition, the analysis includes studies from conference proceedings, as experience reports are often published in these.

Results and Discussion

Research Question 1

This literature review includes 42 primary studies on CV-QKD systems detection methods. Question 1 is "Which journal is the most significant in terms of publications on QKD detection methods?". Figure 2 (a) presents a distribution of these studies across different years to illustrate the emerging interest in this topic over time, while Figure 2 (b) displays the most significant detection methods journals. It is noted that, although the number of publications is still in its early stages, the number of studies focused specifically on detection methods for CV-QKD systems has shown an increasing trend over the last five years.

Research Question 2

Question 2 is, "Which detection methods are the most used in CV-QKD systems?" As illustrated in Figure 3, the most used method in the selected studies was homodyne detection (42.9%), followed by heterodyne detection (35.7%), studies covering both (19%) and dual-threshold/ heterodyne detection (DT/HD) (2.4%). As a result, the percentage of the two main detection methods used was closely aligned, differing by just 7.2%.

Figure 2. Distribution of selected studies over (a) the years and (b) journal publications.

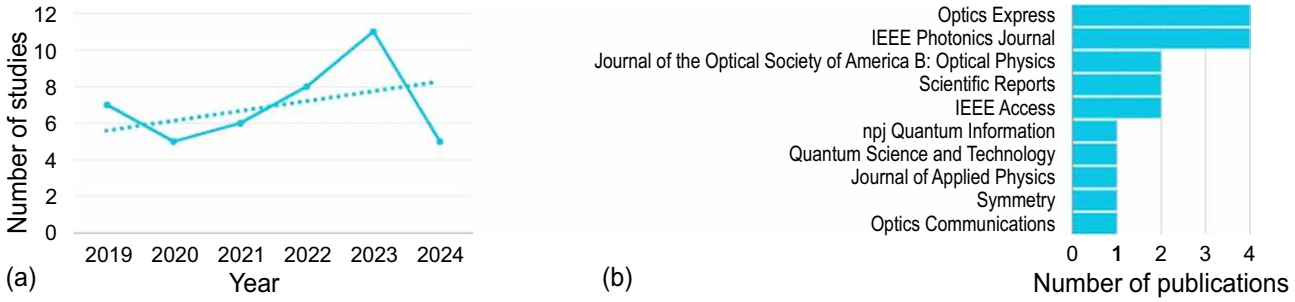

Figure 3. Distribution of detection methods of selected studies.

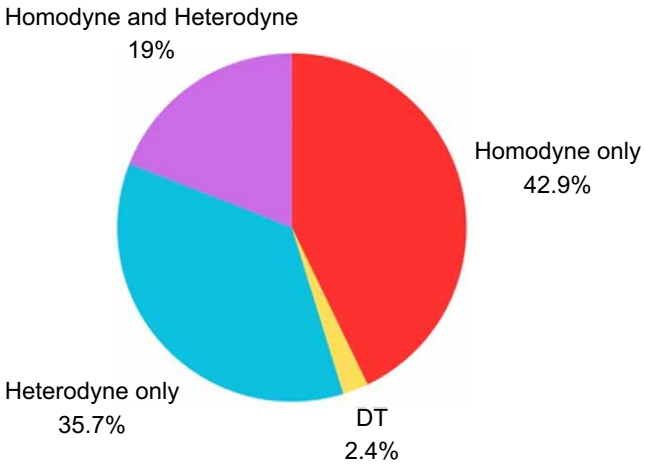

Research Question 3

Question 3 is "What are the advantages of the detection method(s) discussed in the article?". The selected studies agreed that the CV-QKD systems primarily utilize homodyne and heterodyne detection methods. The main advantages described by the selected studies for each of these methods are summarized by homodyne detection, heterodyne detection and Dual-threshold/ heterodyne detection (DT/HD).

Homodyne Detection

Thismethodismorestraightforwardtoimplement and more efficient, allowing the measurement of one quadrature component at a time by randomly selecting phase shift of $\theta = 0$ or $\theta = \pi 2$ for each incoming mode [4]. It facilitates straightforward extraction of phase information from the quantum states transmitted between Alice and Bob [10], and it uses standard optical components, making it practical for real-world applications [11]. It effectively manages noise, crucial for maintaining key distribution integrity over long distances and in fluctuating environments [12]. The method enables higher key rates than discrete-variable systems by extracting more information from quantum states. Its high sensitivity and ability to achieve a high signal-to-noise ratio (SNR) benefit long-distance communication. Also in this category, variations such as balanced homodyne detection [13,14], parametric homodyne detection [15], and time-division dual-quadrature homodyne detection (TDDQHD) [16] have been adopted by the selected studies.

Heterodyne Detection

This method enables the simultaneous measurement of both quadratures [4], enhancing the amount of information extracted and improving the key generation rate [10,11,17,18]. It offers better noise resilience and increased robustness against specific eavesdropping attacks [4]. Heterodyne detection also avoids security risks related to local local oscillator (LLO) manipulation, which can concern homodyne setups [19]. Furthermore, it is compatible with existing coherent optical telecommunications infrastructure, facilitating easier integration into current systems [20].

Dual-Threshold/Heterodyne Detection (DT/HD)

Implementing a DT/HD receiver improves the receiver's sensitivity compared to dual-threshold/ direct detection (DT/DD), thereby offering the advantage of reducing quantum bit errors. In the selected study, this detection method was used to strengthen the reliability and viability of satellite EB/CV-QKD/FSO systems, which utilizes the continuous-variable (CV) method for quantum state representation and the entanglement-based (EB) scheme for QKD implementation. Furthermore, these systems are expected to contribute to global security in the upcoming sixth-generation (6G) wireless communications [21].

Research Question 4

Question 4 is "What methods of Digital Signal Processing (DSP) are being selected by researchers?". According to the selected studies, the DSP methods being used by researchers include real-time polarization calibration, phase compensation, data synchronization [22], clock synchronization, static and dynamic equalization, frame synchronization, pulse shaping [4], error correction, privacy amplification [17], real-time phase feedback and quadrature remapping [13]. Besides, improvements in algorithms and numerical methods are being explored to enhance the proposed protocol's performance, including using neural network models to predict secure key rates quickly and accurately [23]. It also adopted the use of optimized high-pass filters (HPFs) to manage noise and intersymbol interference (ISI), as well as machine learning frameworks for phase carrier recovery [24]. Lastly, a pilot-tone-assisted frequency locking algorithm was used to ensure phase and frequency coherence between the transmitter and receiver's laser signals, thereby enhancing the reliability of the CV-QKD system [25].

Research Question 5

Question 5 is "Which interferometer model is most often used in experimental CV-QKD setups?". Figure 4 shows the distribution of the three interferometer models used in the CV-QKD experimental setups. As shown in the figure, most articles did not explicitly specify the interferometer model used (66.7%). Among the models specified, the most used was Mach-Zehnder (28.6%), followed by Faraday-Michelson (2.4%) [16] and SU(1,1) (2.4%) [15]. Accordingly, some potential reasons for the Mach-Zehnder interferometer being the most widely used in CV-QKD systems may include its high sensitivity, flexibility in configuration, ability to measure specific changes, and lower sensitivity to external disturbances. Besides, its ability to effectively manipulate and measure the quantum states allows the necessary phase and polarization adjustments required for secure key distribution [22].

Conclusion

In summary, this systematic literature review analyzed 42 articles based on exclusion criteria to fill the gap of review articles focusing specifically on detection methods in CV-QKD experimental setups. The results, guided by the research questions, revealed a growing trend in publications in the area over the last five years. Among the detection methods adopted in the selected studies, the homodyne emerged as the most widely used,

Figure 4. Distribution of interferometer models of selected studies.

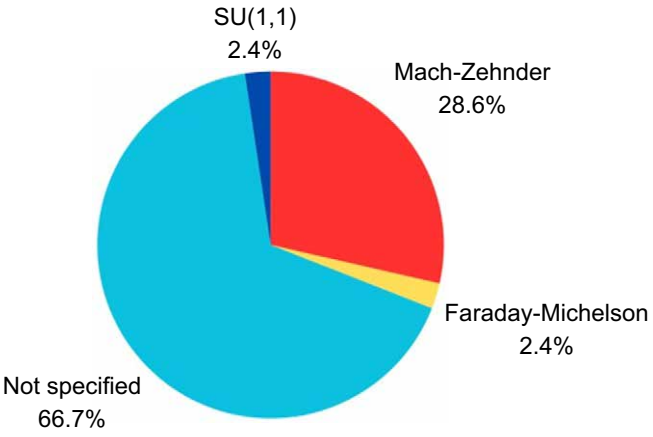

while the Mach-Zehnder interferometer was the most common in experimental implementations. In addition, the digital signal processing (DSP) methods used by researchers and the advantages associated with each detection technique were identified. Future research should focus on integrating these detection methods into real communication scenarios to improve the safety and effectiveness of CV-QKD systems.

Acknowledgments

This work has been fully funded by the project "Flexible testbed for evaluating CV-QKD systems" supported by QuIIN - EMBRAPII CIMATEC Competence Center in Quantum Technologies, with financial resources from the PPI IoT/ Manufatura 4.0 / PPI HardwareBR of the MCTI grant number 053/2023, signed with EMBRAPII.

References

1. Aslan O.et al. A comprehensive review of cyber security vulnerabilities, threats, attacks, and solutions. Electronics 2023;12(6):1333.
2. Zhao H et al. Simple continuous-variable quantum key distribution scheme using a Sagnac- based Gaussian modulator. Optics Letters 2022;47(12):2939-2942.
3. Zhang G et al. An integrated silicon photonic chip platform for continuous-variable quantum key distribution. Nature Photonics 2019;13(12):839-842.
4. Zhang Y et al. Continuous-variable quantum key distribution system: Past, present, and future. Applied Physics Reviews 2024;11(1).
5. Silva NA et al. Practical imperfections affecting the performance of CV-QKD based on coherent detection. In: 2020 22nd international conference on transparent optical networks (ICTON). IEEE 2020:1-4.
6. Liu W-B et al. Homodyne detection quadrature phase shift keying continuous-variable quantum key distribution with high excess noise tolerance. PRX Quantum 2021;2(4):040334.
7. García-Holgado A, Marcos-Pablos S. García-Peñalvo F. Guidelines for performing systematic research projects reviews. 2020.
8. Keele Staffs et al. Guidelines for performing systematic literature reviews in software engineering. Technical Report 2007.
9. Wahono RS. A systematic literature review of software defect prediction. Journal of Software Engineering 2015;1(1):1-16.
10. Ghorai S, Diamanti E, Leverrier A. Composable security of two-way continuous-variable quantum key distribution without active symmetrization. Physical Review A 2019;99(1):012311.
11. Kish SP et al. Feasibility assessment for practical continuous variable quantum key distribution over the satellite-to-Earth channel. Quantum Engineering 2020;2(3):e50.
12. Kovalenko O et al. Frequency-multiplexed entanglement for continuous-variable quantum key distribution. Photonics Research 2021;9(12):2351-2359.
13. Tian Y et al. Experimental demonstration of continuous-variable measurement-device- independent quantum key distribution over optical fiber. Optica 2022;9(5):492-500.
14. Qi D et al. High-performance intermediate-frequency balanced homodyne detector for local local oscillator continuous-variable quantum key distribution. Symmetry 2023;15(7):1314.
15. Eldan A et al. Multiplexed processing of quantum information across an ultra-wide pptical bandwidth. arXiv preprint arXiv:2310.17819, 2023.
16. Oh J, Cho J, Kevin Rhee J-K. Continuous-variable quantum key distribution with time-division dual-quadrature homodyne detection. Optics Express 2023;31(19):30669-30681.
17. Mountogiannakis AG, Papanastasiou P, Pirandola S. Data postprocessing for the one-way heterodyne protocol under composable finite-size security. Physical Review A 2022;106(4):042606.
18. Shen T et al. Experimental demonstration of LLO continuous-variable quantum key distribution with polarization loss compensation. IEEE Photonics Journal 2023;15(2):1-9.
19. Yamano S et al. Finite-size security proof of binary-modulation continuous-variable quantum key distribution using only heterodyne measurement. Physica Scripta 2024;99(2):025115.
20. Hajomer AAE et al. Long-distance continuous-variable quantum key distribution over 100- km fiber with local local oscillator. Science Advances 2024;10(1):eadi9474.
21. Nguyen TV et al. Enhancing design and performance analysis of satellite en tanglement- based CV-QKD/ FSO systems. IEEE Access 2023.
22. Zhang Y et al. Continuous-variable QKD over 50 km commercial fiber. Quantum Science and Technology 2019;4(3):035006.
23. Liu W-B et al. Homodyne detection quadrature phase shift keying continuous-variable quantum key distribution with high excess noise tolerance. PRX Quantum 2021;2(4):040334.

24. Hajomer AAE et al. Modulation leakage-free continuous-variable quantum key distribution. npj Quantum Information 2022;8(1):136.
25. Ruiz-Chamorro A, Garcia-Callejo A, Fernandez V. Low-complexity continuous-variable quantum key distribution with true local oscillator using pilot-assisted frequency locking. Scientific Reports 2024;14(1):10770.

Instructions for Authors

The Authors must indicate in a cover letter the address, telephone number and e-mail of the corresponding author. The corresponding author will be asked to make a statement confirming that the content of the manuscript represents the views of the co-authors, that neither the corresponding author nor the co-authors have submitted duplicate or overlapping manuscripts elsewhere, and that the items indicated as personal communications in the text are supported by the referenced person. Also, the protocol letter with the number should be included in the submission article, as well as the name of sponsors (if applicable).

Manuscripts may be submitted within designated categories of communication, including:

- Original basic or clinical investigation (original articles on topics of broad interest in the field of bioengineering and biotechnology applied to health). We particularly welcome papers that discuss epidemiological aspects of international health, clinical reports, clinical trials and reports of laboratory investigations.
- Case presentation and discussion (case reports must be carefully documented and must be of importance because they illustrate or describe unusual features or have important practice implications).
- Brief reports of new methods or observations (short communications brief reports of unusual or preliminary findings).
- State-of-the-art presentations (reviews on protocols of importance to readers in diverse geographic areas. These should be comprehensive and fully referenced).
- Review articles (reviews on topics of importance with a new approach in the discussion). However, review articles only will be accepted after an invitation of the Editors.
- Letters to the editor or editorials concerning previous publications (correspondence relating to papers recently published in the Journal, or containing brief reports of unusual or preliminary findings).
- Editor's corner, containing ideas, hypotheses and comments (papers that advance a hypothesis or represent an opinion relating to a topic of current interest).
- Innovative medical products (description of new biotechnology and innovative products applied to health).
- Health innovation initiatives articles (innovative articles of technological production in Brazil and worldwide, national policies and directives related to technology applied to health in our country and abroad).

The authors should checklist comparing the text with the template of the Journal.

Supplements to the JBTH include articles under a unifying theme, such as those summarizing presentations of symposia or focusing on a specific subject. These will be added to the regular publication of the Journal as appropriate, and will be peer reviewed in the same manner as submitted manuscripts.

Statement of Editorial Policy

The editors of the Journal reserve the right to edit manuscripts for clarity, grammar and style. Authors will have an opportunity to review these changes prior to creation of galley proofs. Changes in content after galley proofs will be sent for reviewing and could be required charges to the author. The JBTH does not accept articles which duplicate or overlap publications elsewhere.

Peer-Review Process

All manuscripts are assigned to an Associate Editor by the Editor-in-Chief and Deputy Editor, and sent to outside experts for peer review. The Associate Editor, aided by the reviewers' comments, makes a recommendation to the Editor-in-Chief regarding the merits of the manuscript. The Editor-in-Chief makes a final decision to accept, reject, or request revision of the manuscript. A request for revision does not guarantee ultimate acceptance of the revised manuscript.

Manuscripts may also be sent out for statistical review ou *ad hoc* reviewers. The average time from submission to first decision is three weeks.

Revisions

Manuscripts that are sent back to authors for revision must be returned to the editorial office by 15 days after the date of the revision request. Unless the decision letter specifically indicates otherwise, it is important not to increase the text length of the manuscript in responding to the comments. The cover letter must include a point-by-point response to the reviewers and Editors comments, and should indicate any additional changes made. Any alteration in authorship, including a change in order of authors, must be agreed upon by all authors, and a statement signed by all authors must be submitted to the editorial office.

Style

Manuscripts may be submitted only in electronic form by www.jbth.com.br. Each manuscript will be assigned a registration number, and the author notified that the manuscript is complete and appropriate to begin the review process. The submission file is in OpenOffice, Microsoft Word, or RTF document file format for texts and JPG (300dpi) for figures.

Authors must indicate in a cover letter the address, telephone number, fax number, and e-mail of the corresponding author. The corresponding author will be asked to make a statement confirming that the content of the manuscript represents the views of the co-authors, that neither the corresponding author nor the co-authors have submitted duplicate or overlapping manuscripts elsewhere, and that the items indicated as personal communications in the text are supported by the referenced person.

Manuscripts are to be typed as indicated in Guide for Authors, as well as text, tables, references, legends. All pages are to be numbered with the order of presentation as follows: title page, abstract, text, acknowledgements, references, tables, figure legends and figures. A running title of not more than 40 characters should be at the top of each page. References should be listed consecutively in the text and recorded as follows in the reference list, and must follow the format of the National Library of Medicine as in Index Medicus and "Uniform Requirements for Manuscripts Submitted to Biomedical Journals" or in "Vancouver Citation Style". Titles of journals not listed in Index Medicus should be spelled out in full.

Manuscript style will follow accepted standards. Please refer to the JBTH for guidance. The final style will be determined by the Editor-in-Chief as reviewed and accepted by the manuscript's corresponding author.

Approval of the Ethics Committee

The JBTH will only accept articles that are approved by the ethics committees of the respective institutions (protocol number and/or approval certification should be sent after the references). The protocol number should be included in the end of the Introduction section of the article.

Publication Ethics

Authors should observe high standards with respect to publication ethics as set out by the International Committee of Medical Journal Editors (ICMJE). Falsification or fabrication of data, plagiarism, including duplicate publication of the authors' own work without proper citation, and misappropriation of the work are all unacceptable practices. Any cases of ethical misconduct are treated very seriously and will be dealt with in accordance with the JBTH guidelines.

Conflicts of Interest

At the point of submission, each author should reveal any financial interests or connections, direct or indirect, or other situations that might raise the question of bias in the work reported or the conclusions, implications, or opinions stated - including pertinent commercial or other sources of funding for the individual author(s) or for the associated department(s) or organizations(s), and personal relationships. There is a potential conflict of interest when anyone involved in the publication process has a financial or other beneficial interest in

the products or concepts mentioned in a submitted manuscript or in competing products that might bias his or her judgment.

Material Disclaimer

The opinions expressed in JBTH are those of the authors and contributors, and do not necessarily reflect those of the SENAI CIMATEC, the editors, the editorial board, or the organization with which the authors are affiliated.

Privacy Statement

The names and email addresses entered in this Journal site will be used exclusively for the stated purposes of this journal and will not be made available for any other purpose or to any other party.

Brief Policies of Style

Manuscript	Original	Review	Birief Comunication	Case Report	Editorial ; Letter to the Editor; Editor' s Corner	Innovative Medical Products	State-of-the-Art	Health Innovation Initiatives
Font Type	Times or Arial	Times or Arial	Times or Arial	Times or Arial	Times or Arial	Times or Arial	Times or Arial	Times or Arial
Number of Words – Title	120	90	95	85	70	60	120	90
Font Size/Space-Title	12; double space	12; double space	12; double space	12; double space	12; double space	12; double space	12; double space	12; double space
Font Size/Space-Abstracts/Key Words and Abbreviations	10; single space	10; single space	10; single space	10; single space	-	-	10; single space	10; single space
Number of Words – Abstracts/Key Words	300/5	300/5	200/5	250/5	-	-	300/5	300/5
Font Size/Space-Text	12; Double space	12; Double space	12; Double space	12; Double space	12; Double space	12; Double space	12; Double space	12; Double space
Number of Words – Text	5,000 including spaces	5,500 including spaces	2,500 including spaces	1,000 including spaces	1,000 including spaces	550 including spaces	5,000 including spaces	5,500 including spaces
Number of Figures	8 (title font size 12, double space)	3 (title font size 12, double space)	2 (title font size 12, double space)	2 (title font size 12, double space)	-	2 (title font size 12, double space)	8 (title font size 12, double space)	8 (title font size 12, double space)
Number of Tables/Graphic	7 title font size 12, double space	2 title font size 12, double space	2(title font size 12, double space)	1(title font size 12, double space)	-	-	7 title font size 12, double space	4 title font size 12, double space
Number of Authors and Co-authors*	15	10	5	10	3	3	15	10
References	20 (font size 10,single space	30(font size 10,single space	15 (font size 10,single space)	10 (font size 10,single space)	10 (font size 10,single space	5(font size 10,single space	20 (font size 10,single space	20

*First and last name with a sequencing overwritten number. Corresponding author(s) should be identified with an asterisk; Type 10, Times or Arial, single space. Running title of not more than 40 characters should be at the top of each page. References should be listed consecutively in the text. References must be cited on (not above) the line of text and in brackets instead of parentheses, e.g., [7,8]. References must be numbered in the order in which they appear in the text. References not cited in the text cannot appear in the reference section. References only or first cited in a table or figures are numbered according to where the table or figure is cited in the text. For instance, if a table is placed after reference 8, a new reference cited in table 1 would be reference 9.1 would be reference 9.

Checklist for Submitted Manuscripts

❑1. Please provide a cover letter with your submission specifying the corresponding author as well as an address, telephone number and e-mail.

❑2. Submit your paper using our website www.jbth.com.br. Use Word Perfect/Word for Windows, each with a complete set of original illustrations.

❑3. The entire manuscript (including tables and references) must be typed according to the guidelines instructions.

❑4. The order of appearance of material in all manuscripts should be as follows: title page, abstract, text, acknowledgements, references, tables, figures/graphics/diagrams with the respective legends.

❑5. The title page must include a title of not more than three printed lines (please check the guidelines of each specific manuscript), authors (no titles or degrees), institutional affiliations, a running headline of not more than 40 letters with spaces.

❑6. Acknowledgements of persons who assisted the authors should be included on the page preceding the references.

❑7. References must begin on a separate page.

❑8. References must be cited on (not above) the line of text and in brackets instead of parentheses, e.g., [7,8].

❑9. References must be numbered in the order in which they appear in the text. References not cited in the text cannot appear in the reference section. References only or first cited in a table or figures are numbered according to where the table or figure is cited in the text. For instance, if a table is placed after reference 8, a new reference cited in table 1 would be reference 9.

❑10. Reference citations must follow the format established by the "Uniform Requirements for Manuscripts Submitted to Biomedical Journals" or in "Vancouver Citation Style".

❑11. If you reference your own unpublished work (i.e., an "in press" article) in the manuscript that you are submitting, you must attach a file of the "in press" article and an acceptance letter from the journal.

❑12. If you cite unpublished data that are not your own, you must provide a letter of permission from the author of that publication.

❑13. Please provide each figure in high quality (minimum 300 dpi: JPG or TIF). Figure must be on a separate file.

❑14. If the study received a financial support, the name of the sponsors must be included in the cover letter and in the text, after the author's affiliations.

❑15. Provide the number of the Ethics Committees (please check the guidelines for authors).